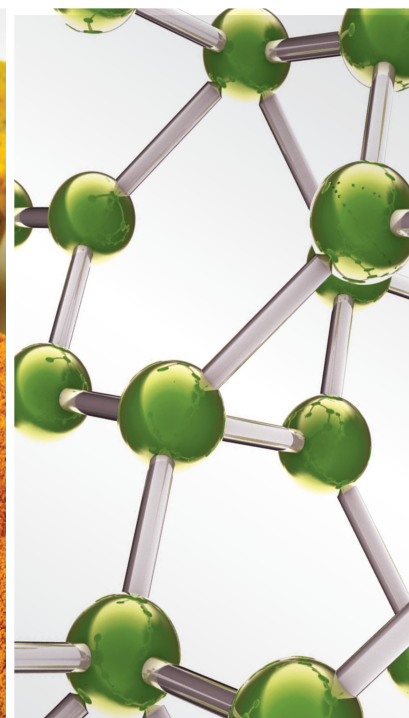# Regulation of Redox Signaling in Tumor Immunology, and the Role of Antioxidants

Lead Guest Editor: Muhammad Farrukh Nisar
Guest Editors: Shiva Gholizadeh- Ghaleh Aziz, Ahmad Ud Din, Anser Ali, and Amjad Islam Aqib

# Regulation of Redox Signaling in Tumor Immunology, and the Role of Antioxidants
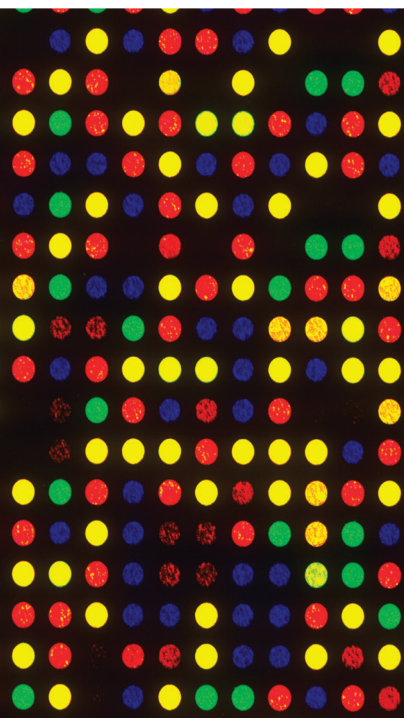
# Regulation of Redox Signaling in Tumor Immunology, and the Role of Antioxidants

Lead Guest Editor: Muhammad Farrukh Nisar
Guest Editors: Shiva Gholizadeh- Ghaleh Aziz, Ahmad Ud Din, Anser Ali, and Amjad Islam Aqib

# Chief Editor

Jian-Li Gao (iD), China

Arthur De Sá Ferreira (iD), Brazil
Nunziatina De Tommasi (iD), Italy
Marinella De leo (iD), Italy
Gourav Dey (iD), India
Dinesh Dhamecha, USA
Claudia Di Giacomo (iD), Italy
Antonella Di Sotto (iD), Italy
Mario Dioguardi, Italy
Jeng-Ren Duann (iD), USA
Thomas Efferth (iD), Germany
Abir El-Alfy, USA
Mohamed Ahmed El-Esawi (iD), Egypt
Mohd Ramli Elvy Suhana, Malaysia
Talha Bin Emran, Japan
Roger Engel (iD), Australia
Karim Ennouri (iD), Tunisia
Giuseppe Esposito (iD), Italy
Tahereh Eteraf-Oskouei, Iran
Robson Xavier Faria (iD), Brazil
Mohammad Fattahi (iD), Iran
Keturah R. Faurot (iD), USA
Piergiorgio Fedeli (iD), Italy
Laura Ferraro (iD), Italy
Antonella Fioravanti (iD), Italy
Carmen Formisano (iD), Italy
Hua-Lin Fu (iD), China
Liz G Müller (iD), Brazil
Gabino Garrido (iD), Chile
Safoora Gharibzadeh, Iran
Muhammad N. Ghayur (iD), USA
Angelica Gomes (iD), Brazil
Elena González-Burgos, Spain
Susana Gorzalczany (iD), Argentina
Jiangyong Gu (iD), China
Maruti Ram Gudavalli (iD), USA
Jian-You Guo (iD), China
Shanshan Guo, China
Narcís Gusi (iD), Spain
Svein Haavik, Norway
Fernando Hallwass, Brazil
Gajin Han (iD), Republic of Korea
Ihsan Ul Haq, Pakistan
Hicham Harhar (iD), Morocco
Mohammad Hashem Hashempur (iD), Iran
Muhammad Ali Hashmi (iD), Pakistan

Waseem Hassan (iD), Pakistan
Sandrina A. Heleno (iD), Portugal
Pablo Herrero (iD), Spain
Soon S. Hong (iD), Republic of Korea
Md. Akil Hossain (iD), Republic of Korea
Muhammad Jahangir Hossen (iD), Bangladesh
Shih-Min Hsia (iD), Taiwan
Changmin Hu (iD), China
Tao Hu (iD), China
Weicheng Hu (iD), China
Wen-Long Hu, Taiwan
Xiao-Yang (Mio) Hu, United Kingdom
Sheng-Teng Huang (iD), Taiwan
Ciara Hughes (iD), Ireland
Attila Hunyadi (iD), Hungary
Liaqat Hussain (iD), Pakistan
Maria-Carmen Iglesias-Osma (iD), Spain
Amjad Iqbal (iD), Pakistan
Chie Ishikawa (iD), Japan
Angelo A. Izzo, Italy
Satveer Jagwani (iD), USA
Rana Jamous (iD), Palestinian Authority
Muhammad Saeed Jan (iD), Pakistan
G. K. Jayaprakasha, USA
Kyu Shik Jeong, Republic of Korea
Leopold Jirovetz (iD), Austria
Jeeyoun Jung (iD), Republic of Korea
Nurkhalida Kamal (iD), Saint Vincent and the
Grenadines
Atsushi Kameyama (iD), Japan
Kyungsu Kang, Republic of Korea
Wenyi Kang (iD), China
Shao-Hsuan Kao (iD), Taiwan
Nasiara Karim (iD), Pakistan
Morimasa Kato (iD), Japan
Kumar Katragunta (iD), USA
Deborah A. Kennedy (iD), Canada
Washim Khan, USA
Bonglee Kim (iD), Republic of Korea
Dong Hyun Kim (iD), Republic of Korea
Junghyun Kim (iD), Republic of Korea
Kyungho Kim, Republic of Korea
Yun Jin Kim (iD), Malaysia
Yoshiyuki Kimura (iD), Japan

Nebojša Kladar, Serbia
Mi Mi Ko, Republic of Korea
Toshiaki Kogure, Japan
Malcolm Koo, Taiwan
Yu-Hsiang Kuan, Taiwan
Robert Kubina, Poland
Chan-Yen Kuo, Taiwan
Kuang C. Lai, Taiwan
King Hei Stanley Lam, Hong Kong
Fanuel Lampiao, Malawi
Ilaria Lampronti, Italy
Mario Ledda, Italy
Harry Lee, China
Jeong-Sang Lee, Republic of Korea
Ju Ah Lee, Republic of Korea
Kyu Pil Lee, Republic of Korea
Namhun Lee, Republic of Korea
Sang Yeoup Lee, Republic of Korea
Ankita Leekha, USA
Christian Lehmann, Canada
George B. Lenon, Australia
Marco Leonti, Italy
Hua Li, China
Min Li, China
Xing Li, China
Xuqi Li, China
Yi-Rong Li, Taiwan
Vuanghao Lim, Malaysia
Bi-Fong Lin, Taiwan
Ho Lin, Taiwan
Shuibin Lin, China
Kuo-Tong Liou, Taiwan
I-Min Liu, Taiwan
Suhuan Liu, China
Xiaosong Liu, Australia
Yujun Liu, China
Emilio Lizarraga, Argentina
Monica Loizzo, Italy
Nguyen Phuoc Long, Republic of Korea
Zaira López, Mexico
Chunhua Lu, China
Ângelo Luís, Portugal
Anderson Luiz-Ferreira, Brazil
Ivan Luzardo Luzardo-Ocampo, Mexico

Michel Mansur Machado, Brazil
Filippo Maggi, Italy
Juraj Majtan, Slovakia
Toshiaki Makino, Japan
Nicola Malafronte, Italy
Giuseppe Malfa, Italy
Francesca Mancianti, Italy
Carmen Mannucci, Italy
Juan M. Manzaneque, Spain
Fatima Martel, Portugal
Carlos H. G. Martins, Brazil
Maulidiani Maulidiani, Malaysia
Andrea Maxia, Italy
Avijit Mazumder, India
Isac Medeiros, Brazil
Ahmed Mediani, Malaysia
Lewis Mehl-Madrona, USA
Ayikoé Guy Mensah-Nyagan, France
Oliver Micke, Germany
Maria G. Miguel, Portugal
Luigi Milella, Italy
Roberto Miniero, Italy
Letteria Minutoli, Italy
Prashant Modi, India
Daniel Kam-Wah Mok, Hong Kong
Changjong Moon, Republic of Korea
Albert Moraska, USA
Mark Moss, United Kingdom
Yoshiharu Motoo, Japan
Yoshiki Mukudai, Japan
Sakthivel Muniyan, USA
Saima Muzammil, Pakistan
Benoit Banga N'guessan, Ghana
Massimo Nabissi, Italy
Siddavaram Nagini, India
Takao Namiki, Japan
Srinivas Nammi, Australia
Krishnadas Nandakumar, India
Vitaly Napadow, USA
Edoardo Napoli, Italy
Jorddy Neves Cruz, Brazil
Marcello Nicoletti, Italy
Eliud Nyaga Mwaniki Njagi, Kenya
Cristina Nogueira, Brazil

Sakineh Kazemi Noureini, Iran
Rômulo Dias Novaes, Brazil
Martin Offenbaecher, Germany
Oluwafemi Adeleke Ojo, Nigeria
Olufunmiso Olusola Olajuyigbe, Nigeria
Luís Flávio Oliveira, Brazil
Mozaniel Oliveira, Brazil
Atolani Olubunmi, Nigeria
Abimbola Peter Oluyori, Nigeria
Timothy Omara, Austria
Chiagoziem Anariochi Otuechere, Nigeria
Sokcheon Pak, Australia
Antônio Palumbo Jr, Brazil
Zongfu Pan, China
Siyaram Pandey, Canada
Niranjan Parajuli, Nepal
Gunhyuk Park, Republic of Korea
Wansu Park, Republic of Korea
Rodolfo Parreira, Brazil
Mohammad Mahdi Parvizi, Iran
Luiz Felipe Passero, Brazil
Mitesh Patel, India
Claudia Helena Pellizzon, Brazil
Cheng Peng, Australia
Weijun Peng, China
Sonia Piacente, Italy
Andrea Pieroni, Italy
Haifa Qiao, USA
Cláudia Quintino Rocha, Brazil
DANIELA RUSSO, Italy
Muralidharan Arumugam Ramachandran,
Singapore
Manzoor Rather, India
Miguel Rebollo-Hernanz, Spain
Gauhar Rehman, Pakistan
Daniela Rigano, Italy
José L. Rios, Spain
Francisca Rius Diaz, Spain
Eliana Rodrigues, Brazil
Maan Bahadur Rokaya, Czech Republic
Mariangela Rondanelli, Italy
Antonietta Rossi, Italy
Mi Heon Ryu, Republic of Korea
Bashar Saad, Palestinian Authority
Sabiu Saheed, South Africa

Mohamed Z.M. Salem, Egypt
Avni Sali, Australia
Andreas Sandner-Kiesling, Austria
Manel Santafe, Spain
José Roberto Santin, Brazil
Tadaaki Satou, Japan
Roland Schoop, Switzerland
Sindy Seara-Paz, Spain
Veronique Seidel, United Kingdom
Vijayakumar Sekar, China
Terry Selfe, USA
Arham Shabbir, Pakistan
Suzana Shahar, Malaysia
Wen-Bin Shang, China
Xiaofei Shang, China
Ali Sharif, Pakistan
Karen J. Sherman, USA
San-Jun Shi, China
Insop Shim, Republic of Korea
Maria Im Hee Shin, China
Yukihiro Shoyama, Japan
Morry Silberstein, Australia
Samuel Martins Silvestre, Portugal
Preet Amol Singh, India
Rajeev K Singla, China
Kuttulebbai N. S. Sirajudeen, Malaysia
Slim Smaoui, Tunisia
Eun Jung Sohn, Republic of Korea
Maxim A. Solovchuk, Taiwan
Young-Jin Son, Republic of Korea
Chengwu Song, China
Vanessa Steenkamp, South Africa
Annarita Stringaro, Italy
Keiichiro Sugimoto, Japan
Valeria Sulsen, Argentina
Zewei Sun, China
Sharifah S. Syed Alwi, United Kingdom
Orazio Taglialatela-Scafati, Italy
Takashi Takeda, Japan
Gianluca Tamagno, Ireland
Hongxun Tao, China
Jun-Yan Tao, China
Lay Kek Teh, Malaysia
Norman Temple, Canada

Kamani H. Tennekoon (iD), Sri Lanka
Seong Lin Teoh, Malaysia
Menaka Thounaojam (iD), USA
Jinhui Tian, China
Zipora Tietel, Israel
Loren Toussaint (iD), USA
Riaz Ullah (iD), Saudi Arabia
Philip F. Uzor (iD), Nigeria
Luca Vanella (iD), Italy
Antonio Vassallo (iD), Italy
Cristian Vergallo, Italy
Miguel Vilas-Boas (iD), Portugal
Aristo Vojdani (iD), USA
Yun WANG (iD), China
QIBIAO WU (iD), Macau
Abraham Wall-Medrano (iD), Mexico
Chong-Zhi Wang (iD), USA
Guang-Jun Wang (iD), China
Jinan Wang (iD), China
Qi-Rui Wang (iD), China
Ru-Feng Wang (iD), China
Shu-Ming Wang (iD), USA
Ting-Yu Wang (iD), China
Xue-Rui Wang (iD), China
Youhua Wang (iD), China
Kenji Watanabe (iD), Japan
Jintanaporn Wattanathorn (iD), Thailand
Silvia Wein (iD), Germany
Katarzyna Winska (iD), Poland
Sok Kuan Wong (iD), Malaysia
Christopher Worsnop, Australia
Jih-Huah Wu (iD), Taiwan
Sijin Wu (iD), China
Xian Wu, USA
Zuoqi Xiao (iD), China
Rafael M. Ximenes (iD), Brazil
Guoqiang Xing (iD), USA
JiaTuo Xu (iD), China
Mei Xue (iD), China
Yong-Bo Xue (iD), China
Haruki Yamada (iD), Japan
Nobuo Yamaguchi, Japan
Junqing Yang, China
Longfei Yang (iD), China

Mingxiao Yang (iD), Hong Kong
Qin Yang (iD), China
Wei-Hsiung Yang, USA
Swee Keong Yeap (iD), Malaysia
Albert S. Yeung (iD), USA
Ebrahim M. Yimer (iD), Ethiopia
Yoke Keong Yong (iD), Malaysia
Fadia S. Youssef (iD), Egypt
Zhilong Yu, Canada
RONGJIE ZHAO (iD), China
Sultan Zahiruddin (iD), USA
Armando Zarrelli (iD), Italy
Xiaobin Zeng (iD), China
Y Zeng (iD), China
Fangbo Zhang (iD), China
Jianliang Zhang (iD), China
Jiu-Liang Zhang (iD), China
Mingbo Zhang (iD), China
Jing Zhao (iD), China
Zhangfeng Zhong (iD), Macau
Guoqi Zhu (iD), China
Yan Zhu (iD), USA
Suzanna M. Zick (iD), USA
Stephane Zingue (iD), Cameroon

# Contents

*Retraction*

# Retracted: Research on the Correlation of Peripheral Blood Inflammatory Markers with PCT, CRP, and PCIS in Infants with Community-Acquired Pneumonia

## Evidence-Based Complementary and Alternative Medicine

This article has been retracted by Hindawi following an investigation undertaken by the publisher [1]. This investigation has uncovered evidence of one or more of the following indicators of systematic manipulation of the publication process:

(1) Discrepancies in scope

(2) Discrepancies in the description of the research reported

(3) Discrepancies between the availability of data and the research described

(4) Inappropriate citations

(5) Incoherent, meaningless and/or irrelevant content included in the article

(6) Peer-review manipulation

The presence of these indicators undermines our confidence in the integrity of the article's content and we cannot, therefore, vouch for its reliability. Please note that this notice is intended solely to alert readers that the content of this article is unreliable. We have not investigated whether authors were aware of or involved in the systematic manipulation of the publication process.

Wiley and Hindawi regrets that the usual quality checks did not identify these issues before publication and have since put additional measures in place to safeguard research integrity.

We wish to credit our own Research Integrity and Research Publishing teams and anonymous and named external researchers and research integrity experts for contributing to this investigation.

The corresponding author, as the representative of all authors, has been given the opportunity to register their agreement or disagreement to this retraction. We have kept a record of any response received.

## References

[1] L. Li, H. Miao, X. Chen, S. Yang, and X. Yan, "Research on the Correlation of Peripheral Blood Inflammatory Markers with PCT, CRP, and PCIS in Infants with Community-Acquired Pneumonia," *Evidence-Based Complementary and Alternative Medicine*, vol. 2022, Article ID 9024969, 6 pages, 2022.

*Retraction*

# Retracted: Meta-Analysis of Different Acupuncture Points in the Treatment of Ankylosing Spondylitis with Supervised Moxibustion

## Evidence-Based Complementary and Alternative Medicine

This article has been retracted by Hindawi following an investigation undertaken by the publisher [1]. This investigation has uncovered evidence of one or more of the following indicators of systematic manipulation of the publication process:

(1) Discrepancies in scope

(2) Discrepancies in the description of the research reported

(3) Discrepancies between the availability of data and the research described

(4) Inappropriate citations

(5) Incoherent, meaningless and/or irrelevant content included in the article

(6) Peer-review manipulation

The presence of these indicators undermines our confidence in the integrity of the article's content and we cannot, therefore, vouch for its reliability. Please note that this notice is intended solely to alert readers that the content of this article is unreliable. We have not investigated whether authors were aware of or involved in the systematic manipulation of the publication process.

In addition, our investigation has also shown that one or more of the following human-subject reporting requirements has not been met in this article: ethical approval by an Institutional Review Board (IRB) committee or equivalent, patient/participant consent to participate, and/or agreement to publish patient/participant details (where relevant).

Wiley and Hindawi regrets that the usual quality checks did not identify these issues before publication and have since put additional measures in place to safeguard research integrity.

We wish to credit our own Research Integrity and Research Publishing teams and anonymous and named external researchers and research integrity experts for contributing to this investigation.

The corresponding author, as the representative of all authors, has been given the opportunity to register their agreement or disagreement to this retraction. We have kept a record of any response received.

## References

[1] J. Cheng, X. Wang, L. Wang et al., "Meta-Analysis of Different Acupuncture Points in the Treatment of Ankylosing Spondylitis with Supervised Moxibustion," *Evidence-Based Complementary and Alternative Medicine*, vol. 2022, Article ID 4688689, 7 pages, 2022.

*Research Article*

# Association of Kinase-Insert-Domain-Containing Receptor Polymorphisms with Glioma Susceptibility in a Chinese Population: A Hospital-Based Case-Control Study

**Zhi-Fa Huang** [ID],[1] **Wei Zhu**,[2] **Chen Wang**,[3] **Li-Dong Mo**,[3] **Hui-Ling Huang** [ID],[3] **and Xiao-Guang Tong** [ID][2]

[1]*Clinical College of Neurology, Neurosurgery and Neurorehabilitation, Tianjin Medical University, Tianjin, China*
[2]*Department of Neurosurgery, Tianjin Huanhu Hospital, Tianjin, China*
[3]*Tianjin Key Laboratory of Cerebral Vascular and Neurodegenerative Diseases, Tianjin Neurosurgical Institute, Tianjin Huanhu Hospital, Tianjin, China*

Correspondence should be addressed to Hui-Ling Huang; huanghuiling@126.com and Xiao-Guang Tong; tongxiaoguang2021@163.com

*Background.* Gliomas are the most common malignant tumors of the central nervous system. However, the inherited genetic variation in gliomas is presently unclear. Therefore, this study investigated the association of the rs2071559 and rs2239702 gene polymorphisms with glioma susceptibility in Chinese patients. *Methods.* In this study, a case-control approach was used to compare and analyze whether two genes, rs2071559 and rs2239702, were associated with the risk of glioma formation. *Results.* The cases and controls were matched for sex, smoking status, and family history of cancer using single nucleotide polymorphisms. Specific rs2071559 and rs2239702 alleles were found much more frequently in the glioma group than in the control group ($P < 0.001$ and $P = 0.014$, respectively). *Conclusions.* These findings suggest that specific rs2071559 and rs2239702 polymorphisms are associated with a higher risk of glioma development; the risk allele is C in rs2071559 or A in rs2239702. Moreover, the kinase-insert-domain-containing receptor may act as a suppressor of tumor progression.

## 1. Introduction

Cancer is a major global health issue, and its worldwide incidence and mortality continue to increase rapidly; in China, cancer is the leading cause of death [1, 2]. China is the most populous country in the world, with an estimated population of 1.42 billion; in 2020, there were 4.5 million cancer patients and over 3 million cancer-related deaths. In addition, cancer accounts for over 67 million disability-adjusted life years in China [3]. Although primary brain tumors account for only an estimated 1.8% of malignancies, worldwide, they account for a disproportionate burden of cancer mortalities because of their high fatality rate [4].

Gliomas (including astrocytomas, oligodendrogliomas, ependymomas, and a variety of rare histologies [5]) are the most common malignant tumors of the central nervous system, accounting for up to 80% of all malignant brain tumors. According to the World Health Organization (WHO) classification, gliomas are graded from 1 (slow-growing tumors) to 4 (fast-growing tumors) [6, 7]. These tumors can have profound effects on physical, neurocognitive, and social functioning, beginning at an early stage in patients with high-grade, fast-growing tumors [8]. The neurocognitive effects of the disease, accompanied by the increased dependency and social isolation, can result in an enormous burden on patient relationships with family members/care providers [9]. The main reason for this tragic situation is a lack of understanding of the etiology of this disease. To date, exposure to ionizing radiation is the only exogenous factor that has been established as contributing to

glioma formation [10]. However, the role of inherited genetic variation in gliomas is presently unclear.

Gliomas are rich in blood vessels, and angiogenesis is a prerequisite for tumor growth [11]. Vascular endothelial growth factor (VEGF) and VEGF receptor (VEGFR) are thought to play major roles in tumor angiogenesis [11]. VEGFR is a typical transmembrane integral protein divided into VEGFR-1 (Flk-1), VEGFR-2 (Flt-1/kinase-insert-domain-containing receptor (KDR)), and VEGFR-4 (Flt-3) [12]. VEGFR-2 is generally known to play a principal role in mediating VEGF-induced responses [13, 14]. Importantly, VEGFR-2 is the most important receptor for angiogenesis during tumor invasion [15]. KDR overexpression has been studied in relation to several different types of cancer, including lung [16], colon [17], uterine and ovarian [18], and breast [19] cancers. Moreover, there is a significant correlation between KDR expression and vasculogenesis and angiogenesis in gliomas [20]. However, little is known regarding the association between KDR single nucleotide polymorphisms (SNPs) and glioma susceptibility. Both the rs2071559 and rs2239702 polymorphisms are located in the promoter region of KDR, and certain studies have found that this polymorphism affects mRNA and protein expression [21].

Thus, we aimed to determine if there was an association between the rs2071559 and rs2239702 polymorphisms and susceptibility to glioma development using a case-control study in a Chinese population.

## 2. Methods

### 2.1. Study Population.
Patients with pathologically confirmed gliomas and of Han Chinese origin were consecutively recruited from October 2009 to February 2011 in the Department of Neurosurgery at the Huashan Hospital of Fudan University (Shanghai, China). Although there were no restrictions on age, sex, or histology, the exclusion criteria included previous chemotherapy and radiotherapy for unknown disease conditions and a self-reported history of cancer. The controls, trauma patients from the Tianjin Huanhu Hospital and Huashan Hospital, had no self-reported history of cancer, central nervous system-related disease, or history of radiotherapy/chemotherapy.

To obtain detailed information on demographic factors, smoking status, family history of cancer (fhc), and health characteristics, each consenting patient was interviewed using a structured questionnaire. The epidemiological questionnaire was designed with reference to the Brain Tumor Epidemic Questionnaire (MD Anderson Cancer Center; Houston, TX, USA). After strict training, the investigators conducted face-to-face inquiries and investigations on the basis of the informed consent of the respondents and accurately recorded them. The contents of the epidemiological investigation included general demographic characteristics (age, sex, and place of origin), occupation, history of major diseases, family history of tumors in first-degree relatives, smoking status, and dietary nutritional status, and clinical data (including diagnoses and treatments). Participants were classified as nonsmokers,

former smokers, and current smokers according to their smoking status. In this study, smokers were defined as those who smoked at least one cigarette per day for more than one year. At the time of the survey, those who had quit smoking for more than one year were defined as former smokers. The glioma types were roughly divided into three types according to their pathological origin: glioblastoma, astrocytoma other than glioblastoma (mainly diffuse and anaplastic astrocytoma and diffuse and anaplastic astrocytomas), and other types of gliomas (including oligodendroglioma, anaplastic oligodendroglioma, ependymoma, medulloblastoma, choroid plexus papilloma, and mixed glioma) [22]. All questionnaire contents and responses were digitally archived. After checking, error correction, and conversion assignment, an information database for glioma cases and normal controls was established.

This study was approved by the Fudan University Ethics Committee for Human Subject Research and each participant provided written informed consent. For minors (individuals less than 18 years of age), signed informed consent was obtained from a guardian/parent.

### 2.2. Blood Sample Collection.
A 5 mL peripheral venous blood sample was collected from each patient and placed into a tube containing a citrate-dextrose anticoagulant. All samples were maintained at room temperature prior to analysis.

### 2.3. Gene Variant Selection and Genotyping.
Searching for functional variants in the promoter regions of a gene is important because the promoter region functions in regulating gene transcription and production. Previous studies demonstrated that VEGFR-2 promoter polymorphisms may alter susceptibility to coronary heart disease, stroke, and atopy [21, 23, 24]. rs2071559 and rs2239702 are two of the 16 SNPs in the KDR. They are located to each other in the promoter region of KDR gene. rs2071559 is located in the binding site of the promoter region of the KDR of ribonucleoprotein (a putative transcriptional factor). This SNP ($-604T > C$) is predicted to lead to a lower binding efficiency for the promoter region of KDR and its corresponding transcription factor, downregulating KDR expression, and decreasing the levels of KDR. The rs2071559 polymorphism is associated with lymphatic metastasis in patients with nasopharyngeal carcinoma (NPC) and in those with reduced susceptibility to atherothrombotic stroke [23, 25]. Therefore, these two variants of the promoter region were included in the present study.

Venous blood (2 mL) from each patient was collected in tubes containing ethylenediaminetetraacetic acid. White blood cell fractions were processed for genomic DNA extraction using the Qiagen Blood Kit (Qiagen, Chatsworth, California, USA). Then, the genomic DNA was diluted to a concentration of 15–20 ng/$\mu$L for genotyping assays. Polymerase chain reaction was used to amplify polymorphism spanning fragments, and both variants (rs2071559 and rs2239702) were genotyped using the Mass ARRAY iPLEX platform (Sequenom, San Diego, CA, USA) using an

TABLE 1: The demographical features at baseline in all patients.

| Characteristics | Case group ($n = 465$) | Control group ($n = 527$) | P |
|---|---|---|---|
| Gender, $n$ (%): | | | 0.327 |
| Men | 272 (58.5) | 292 (55.4) | |
| Women | 193 (41.5) | 235 (44.6) | |
| Age, years, means (SD) | 42.22 (15.46) | 40.20 (16.30) | 0.046 |
| Age group, $n$ (%): | | | <0.001 |
| <18 years | 33 (7.1) | 29 (5.5) | |
| 18~39 years | 156 (33.5) | 255 (48.4) | |
| 40~59 years | 208 (44.7) | 157 (29.8) | |
| ≥18 years | 68 (14.6) | 86 (16.3) | |
| Cigarette smoking[a], $n$ (%): | | | 0.572 |
| Never | 258 (55.5) | 333 (63.2) | |
| Ever | 59 (12.7) | 63 (12.0) | |
| Current | 109 (23.4) | 127 (24.1) | |
| Missing data | 39 (8.4) | 4 (0.7) | |
| Family history of cancer, $n$ (%): | | | 0.378 |
| No | 344 (74.0) | 424 (80.5) | |
| Yes | 82 (17.6) | 87 (16.5) | |
| Missing data | 39 (8.4) | 16 (3.0) | |

allele-specific matrix-assisted laser desorption/ionization time-of-flight mass spectrometry assay; the assays were conducted without the analyst having knowledge of the control or case status of the sample. MassARRAY Assay Design software, version 3.1 (Sequenom) was used to design primers for the amplification and extension reactions, and SNP genotypes were obtained according to the iPLEX protocol provided by the manufacturer. Genotyping quality was examined using a detailed quality control procedure consisting of a >95% successful call rate with duplicate calling of genotypes, internal positive control samples, and subsequent Hardy–Weinberg equilibrium testing.

*2.4. Statistical Analysis.* Deviation from the Hardy–Weinberg equilibrium was assessed using Fisher's exact test for each SNP among the controls, and $\chi^2$ tests were used to compare the differences in demographic characteristics as well as frequency distributions of alleles and genotypes between the controls and cases. The multivariate logistic regression analyses were conducted to estimate the odds ratios (ORs) and 95% confidence intervals (CIs) of SNPs, adjusted for sex and age; sex, age, and family history of cancer; and sex, age, smoking status, and family history of cancer. The reference group had the most common genotype among the controls. All statistical tests were 2-sided. For the two SNPs in the KDR, we used Haploview (Broad Institute; Cambridge, MA, USA) to estimate pairwise linkage disequilibrium in the control subjects. We used the software package HaploStats (https://www.mayo.edu/hsr/Sfunc.html) to perform the haplotype analysis. Patients with glioma were stratified into three subgroups according to the lesion histology: glioblastoma, other than the glioblastoma astrocytoma (diffuse and anaplastic astrocytomas), and other types of gliomas (including oligodendroglioma, anaplastic oligodendroglioma, ependymoma, medulloblastoma, choroid plexus papilloma, and mixed glioma). Subgroup analyses were performed to estimate the specific ORs based on histology. For the risk alleles that were independently associated with increased glioma risk, their cumulative effect was assessed by counting the number of risk alleles per person from the two SNPs of the KDR (categories were 0–1, 2, 3, and 4). SPSS software (Version 17.0; SPSS; Chicago, IL, USA) was used to perform all statistical analyses unless otherwise indicated.

## 3. Results

*3.1. Baseline Characteristics.* In total, 465 glioma patients and 527 cancer-free control patients were enrolled in the study. The characteristics of the included patients are summarized in Table 1. Overall, the cases and controls appeared to be adequately matched for sex, smoking status, and fhc ($P = 0.327$, 0.572, and 0.378, respectively). Although there was no evidence of general demographic difference between the patients with glioma and the control patients, there was a statistically significant difference in age between the groups ($P = 0.046$). The mean (± standard deviation) age of the patients with gliomas was $42.22 \pm 15.46$ years and $40.20 \pm 16.30$ years in the control patients; males accounted for 58.5% of the patients with gliomas and 55.4% of the control patients.

Among the 465 patients with gliomas, the tumors were classified as astrocytic gliomas (173, 37.2%), glioblastomas (159, 34.2%), ependymomas (67, 14.4%), oligodendrogliomas (47, 10.1%), and mixed gliomas (19, 4.1%). Moreover, 210 patients demonstrated low-grade, slow-growing tumors, and 255 demonstrated high-grade, fast-growing tumors, according to the WHO classification (Table 2).

*3.2. Hardy–Weinberg Equilibrium.* The observed allele frequencies are presented in Table 3 using SNP information. In the control population, both polymorphisms demonstrated Hardy–Weinberg equilibrium ($P > 0.05$) (Table 3).

TABLE 2: The clinical features at baseline in all patients.

|  | $n$ | Percentage (%) |
|---|---|---|
| *Histologic-type, n (%)*: | | |
| Astrocytic glioma | 173 | 37.2 |
| Glioblastoma | 159 | 34.2 |
| Oligodendroglioma | 47 | 10.1 |
| Ependymoma | 67 | 14.4 |
| Mixed glioma | 19 | 4.1 |
| *WHO classification, n (%)*: | | |
| I | 49 | 10.5 |
| II | 161 | 34.6 |
| III | 91 | 19.6 |
| IV | 164 | 35.3 |

TABLE 3: The observed allele frequencies by using SNP information.

|  | rs2071559 | rs2239702 |
|---|---|---|
| Chromosome | 4 | 4 |
| Location on chromosome | 53,494,277 | 53,494,050 |
| $P_1$ | 0.4244 | 0.7115 |
| Risk allele | C | A |
| *MAF*: | | |
| Case group | 0.386 | 0.189 |
| Control group | 0.302 | 0.1448 |
| Database | 0.300 | 0.116 |
| $P_2$ | <0.001 | 0.014 |

MAF: minor allele frequency; Database: MAF for Chinese from HapMap databases; $P_1$: $P$ value for Hardy–Weinberg Equilibrium; $P_2$: $P$ value for difference in allele frequency distributions between cases and controls.

### 3.3. SNP Genotyping Results.

The minor allele frequencies among the controls were in the range of the published allele frequencies for the Han Chinese population (Table 3). The cases and controls were matched for sex, smoking status, and fhc for each SNP. There were differences in the distribution of the rs2071559 and rs2239702 alleles ($P < 0.001$ and 0.014, respectively) between the cases and controls.

The genotypic distributions of rs2071559 and rs2239702 in the case and control patients are summarized in Table 4. The C allele of rs2071559 was present in 38.6% of cases and in 32.2% of the controls, whereas the A allele of rs2239702 was present in 18.9% of cases and in 14.8% of the controls. The frequencies of the rs2071559 T/T, C/T, and C/C genotypes were 38.7%, 45.4%, and 15.9% in controls and 49.5%, 40.6%, and 9.9% in the cases, respectively. The frequencies of the rs2239702 G/G, G/A, and A/A genotypes were 67.7%, 26.7%, and 5.6% in the controls and 72.9%, 24.6%, and 2.5% in the cases, respectively (Table 4).

### 3.4. Association between Individual SNP and Glioma Risk in the Univariable Analysis.

Overall, Table 4 shows that the C allele of rs2071559 was associated with an increased risk of glioma compared with the T allele (OR = 1.46; 95% CI, 1.21–1.75; $P < 0.001$), and the A allele of rs2239702 was associated with an increased risk of glioma compared with the G allele (OR = 1.34; 95% CI, 1.06–1.70; $P = 0.014$). For rs2071559, the C/T and C/C genotypes were both associated with an increased risk of glioma development (OR = 1.43;

95% CI, 1.09–1.87 and OR = 2.06; 95% CI, 1.38–3.09, respectively), using the T/T genotype as a reference. For rs2239702, the A/A genotype was associated with an increased risk of glioma development (OR = 2.44; 95% CI, 1.23–4.82), using the G/G genotype as a reference. For rs2071559, the dominant genetic model showed that T/T was significantly associated with glioma risk in the univariate analysis (OR = 1.55, 95% CI, 1.21–2.00, $P = 0.001$). A recessive genetic model also showed that C/C was associated with glioma risk in the univariate analysis (OR = 1.73, 95% CI, 1.18–2.53, $P = 0.004$). For rs2239702, a recessive genetic model showed that A/A was associated with glioma risk in the univariate analysis (OR = 2.34; 95% CI, 1.19–4.61, $P = 0.012$).

### 3.5. Association between Individual SNP and Glioma Risk in the Multivariate Analysis.

For rs2071559, the C/T and C/C genotypes were both associated with an increased risk of glioma formation (adjusted OR = 1.45; 95% CI, 1.10–1.92 and adjusted OR = 2.04; 95% CI, 1.35–3.09, respectively), using the T/T genotype as a reference. For rs2239702, the A/A genotype was associated with an increased risk of glioma development (adjusted OR = 2.50; 95% CI, 1.25–5.01), using the G/G genotype as a reference. For rs2071559, the dominant genetic model showed that T/T was significantly associated with glioma risk in the multivariate model (adjusted OR = 1.57; 95% CI, 1.20–2.04, $P = 0.001$). A recessive genetic model showed that C/C was associated with glioma risk in the multivariate model (adjusted OR = 1.69; 95% CI, 1.15–2.50; $P = 0.008$). For rs2239702, a recessive genetic model showed that A/A was associated with glioma risk in the multivariate model (adjusted OR = 2.63; 95% CI, 1.34–5.35; $P = 0.011$) (Table 5).

## 4. Discussion

In this study, we assessed the contribution of two potentially functional variants of the KDR gene to the risk of glioma in the Han Chinese population. We found that both variants in the promoter region were associated with glioma risk. In the present study, a haplotype analysis revealed that the haplotype containing the risk allele (C in rs2071559 or A in rs2239702) is associated with increased glioma risk. In addition, we showed that the CC and CT genotypes of rs2071559 and the AA homozygote of rs2239702 showed a significantly increased association with the risk of glioma. The positive association of variants rs2071559 and rs2239702 with glioma risk remained significant after adjusting for both sex and age or adjusting for sex, age, smoking status, and fhc. These findings suggest that genetic variants of VEGFR-2 may be associated with glioma development in the Chinese population.

The study of inherited susceptibility to gliomas has been one of the most important areas of research during the past decade. We can better understand the biological mechanism of glioma development and identify potential targets for therapeutic interventions if susceptibility genes can be identified. The development of new capillary networks is

TABLE 4: The univariate analysis: results of gene frequency comparison between two groups.

| | Frequency | | | Unadjusted | |
| | Case | Control | P | OR (95% CI) | P |
| --- | --- | --- | --- | --- | --- |
| *1559* | | | | | |
| Genotype, *n* (%) | | | 0.001 | | |
| TT | 180 (38.7) | 261 (49.5) | | 1.00 | |
| CT | 211 (45.4) | 214 (40.6) | | 1.43 (1.09, 1.87) | 0.009 |
| CC | 74 (15.9) | 52 (9.9) | | 2.06 (1.38, 3.09) | <0.001 |
| Allele, *n* (%) | | | <0.001 | | |
| T | 571 (61.4) | 736 (69.8) | | 1.00 | |
| C | 359 (38.6) | 318 (32.2) | | 1.46 (1.21, 1.75) | <0.001 |
| Dominant, *n* (%) | | | 0.001 | | |
| CC + CT | 285 (61.3) | 266 (50.5) | | 1.00 | |
| TT | 180 (38.7) | 261 (49.5) | | 1.55 (1.21, 2.00) | 0.001 |
| Recessive, *n* (%) | | | 0.005 | | |
| CT + TT | 391 (84.1) | 475 (90.1) | | 1.00 | |
| CC | 74 (15.9) | 52 (9.9) | | 1.73 (1.18, 2.53) | 0.004 |
| *9702* | | | | | |
| Genotype, *n* (%) | | | 0.024 | | |
| GG | 315 (67.7) | 384 (72.9) | | 1.00 | |
| GA | 124 (26.7) | 130 (24.7) | | 1.16 (0.87, 1.55) | 0.304 |
| AA | 26 (5.6) | 13 (2.5) | | 2.44 (1.23, 4.82) | 0.008 |
| Allele, *n* (%) | | | 0.014 | | |
| G | 754 (81.1) | 898 (85.2) | | 1.00 | |
| A | 176 (18.9) | 156 (14.8) | | 1.34 (1.06, 1.70) | 0.014 |
| Dominant, *n* (%) | | | 0.075 | | |
| GG | 315 (67.7) | 384 (72.9) | | 1.00 | |
| GA + AA | 150 (32.3) | 143 (27.1) | | 1.28 (0.97, 1.68) | 0.078 |
| Recessive, *n* (%) | | | 0.014 | | |
| GG + GA | 439 (94.4) | 514 (97.5) | | 1.00 | |
| AA | 26 (5.6) | 13 (2.5) | | 2.34 (1.19, 4.61) | 0.012 |

necessary for glioma growth and tumor angiogenesis is thought to be mediated by soluble factors released from tumor cells. These factors act on the endothelial cells in a paracrine manner. VEGF is a prime regulator of tumor angiogenesis and vasculogenesis, and KDR is a receptor for various VEGF isoforms. Previous studies have shown that VEGF and the high-affinity VEGF receptor KDR are key regulators of tumor angiogenesis. Strategies to block VEGF/ KDR signaling have been successfully used to inhibit experimental tumor growth and indicate that KDR is the prime signaling VEGF receptor involved in the proliferating tumor endothelium [26].

Some reports on the relationship between KDR and glioma susceptibility have been published. Coexpression of VEGF and KDR commonly occurs in astrocytoma and glioblastoma cells [27]. KDR is upregulated in the tumor vasculature of anaplastic oligodendrogliomas, glioblastoma multiforme, and ependymomas with necrosis, whereas oligodendroglioma, grade II astrocytomas, and anaplastic astrocytomas tend to express weak-to-nondetectable signals [28]. Moreover, significantly elevated levels of KDR mRNA have been reported in malignant tumor endothelia [29]. These previous studies suggest that overexpression of KDR may influence cell activity in brain tissues and consequently contribute to glioma formation.

Although there are few reports on the relationship between KDR SNPs and glioma susceptibility, some studies have investigated the predisposing role of rs2071559 in other diseases, with conflicting results. Millauer et al. demonstrated that KDR is generally involved in the growth of many solid tumors, such as mammary, ovarian, and lung carcinomas, as well as glioblastomas [30]. The T/T genotype of rs2071559 was reported to be associated with an increased risk of age-related macular degeneration and coronary heart disease [21, 31]. Compared with the homozygous wild-type genotype, variant-containing genotypes exhibited a borderline increased relapse rate in patients with colorectal cancer [32]. For rs2071559, Sjostrom et al. found an association between the major allele and survival time, with shorter survival in heterozygote patients compared with homozygote patients [33]. Chen et al. found that the C/C homozygote of rs2071559 is associated with an increased risk of the glioma development [34].

Therefore, we studied the association of the rs2071559 and rs2239702 polymorphisms with glioma susceptibility in a relatively large sample size from a hospital population of people sharing a common ethnicity (465 cases and 527 controls). However, our study has several limitations, including selection bias, effects of multiple environmental factors on genes, and the representativeness of the studied SNPs in VEGFR-2. Although the controls and cases were matched by sex, smoking status, and fhc to limit potential selection bias, other selection biases cannot be ruled out. At present, owing to the lack of data on many environmental

Table 5: The multivariate analysis.

| | Model 1 | | Model 2 | |
|---|---|---|---|---|
| | OR (95% CI) | P | OR (95% CI) | P |
| *KDR-rs2071559*: | | | | |
| Genotype, *n* (%) | | | | |
| TT | 1.00 | | 1.00 | |
| CT | 1.44 (1.10, 1.88) | 0.008 | 1.45 (1.10, 1.92) | 0.009 |
| CC | 2.09 (1.40, 3.13) | <0.001 | 2.04 (1.35, 3.09) | 0.001 |
| Dominant, *n* (%) | | | | |
| TT | 1.00 | | 1.00 | |
| CC + CT | 1.56 (1.21, 2.02) | 0.001 | 1.57 (1.20, 2.04) | 0.001 |
| Recessive, *n* (%) | | | | |
| CT + TT | 1.00 | | 1.00 | |
| CC | 1.75 (1.19, 2.56) | 0.004 | 1.69 (1.15, 2.50) | 0.008 |
| *KDR-rs2239702*: | | | | |
| Genotype, *n* (%) | | | | |
| GG | 1.00 | | 1.00 | |
| GA | 1.16 (0.87, 1.55) | 0.303 | 1.12 (0.83, 1.51) | 0.447 |
| AA | 2.54 (1.28, 5.05) | 0.008 | 2.50 (1.25, 5.01) | 0.010 |
| Dominant, *n* (%) | | | | |
| GG | 1.00 | | 1.00 | |
| GA + AA | 1.29 (0.98, 1.69) | 0.072 | 1.26 (0.95, 1.66) | 0.116 |
| Recessive, *n* (%) | | | | |
| GG + GA | 1.00 | | 1.00 | |
| AA | 2.44 (1.24, 4.83) | 0.010 | 2.63 (1.34, 5.35) | 0.011 |

carcinogenic factors in the sample, we cannot clarify the relationship between environmental exposure and glioma susceptibility. In addition, only two functional SNPs in VEGFR-2 were examined in our study; these may not represent the complete genetic variability of the VEGFR-2 gene.

## 5. Conclusion

The present study showed that genetic variations in the KDR gene are associated with glioma formation in a Han Chinese population. In particular, rs2071559 and rs2239702 were associated with a higher risk of glioma, indicating that the KDR may act as a suppressor of tumor progression. However, other SNPs in KDR or other genes may also be important in the studied population. Genome-wide association studies of gliomas in a Chinese population are needed to discover all susceptibility loci and identify populations susceptible to gliomas. Early detection of glioma-susceptible individuals and risk factor monitoring are future research directions. In addition, more complex and systematic methods need to be established to analyze the etiological patterns of genes associated with a variety of environmental factors.

## Data Availability

The data supporting the findings of this study are available within the article.

## Conflicts of Interest

The authors declare that they have no conflicts of interest.

## Authors' Contributions

Zhi-Fa Huang and Wei Zhu contribute equally to this study.

## References

[1] M. Zhou, H. Wang, and X. Zeng, "Mortality, morbidity, and risk factors in China and its provinces, 1990-2017: a systematic analysis for the Global Burden of Disease Study 2017," *Lancet*, vol. 394, no. 10204, pp. 1145–1158, 2019.

[2] R. M. Feng, Y. N. Zong, S. M. Cao, and R. H. Xu, "Current cancer situation in China: good or bad news from the 2018 Global Cancer Statistics," *Cancer Communications*, vol. 39, no. 1, p. 22, 2019.

[3] H. Qiu, S. Cao, and R. Xu, "Cancer incidence, mortality, and burden in China: a time-trend analysis and comparison with the United States and United Kingdom based on the global epidemiological data released in 2020," *Cancer Communications*, vol. 41, no. 10, pp. 1037–1048, 2021.

[4] J. Ferlay, I. Soerjomataram, R. Dikshit et al., "Cancer incidence and mortality worldwide: sources, methods and major patterns in GLOBOCAN 2012," *International Journal of Cancer*, vol. 136, no. 5, pp. E359–E386, 2015.

[5] J. R. McFaline-Figueroa and E. Q. Lee, "Brain tumors," *The American Journal of Medicine*, vol. 131, no. 8, pp. 874–882, 2018.

[6] D. N. Louis, A. Perry, G. Reifenberger et al., "The 2016 world health organization classification of tumors of the central nervous system: a summary," *Acta Neuropathologica*, vol. 131, no. 6, pp. 803–820, 2016.

[7] R. Stupp, M. Brada, M. J. van den Bent, J. C. Tonn, and G. Pentheroudakis, "High-grade glioma: ESMO Clinical Practice Guidelines for diagnosis, treatment and follow-up," *Annals of Oncology*, vol. 25, no. 3, pp. 93–101, 2014.

[8] G. Moore, A. Collins, C. Brand et al., "Palliative and supportive care needs of patients with high-grade glioma and their carers: a systematic review of qualitative literature," *Patient Education and Counseling*, vol. 91, no. 2, pp. 141–153, 2013.

[9] E. Ford, S. Catt, A. Chalmers, and L. Fallowfield, "Systematic review of supportive care needs in patients with primary malignant brain tumors," *Neuro-Oncology*, vol. 14, no. 4, pp. 392–404, 2012.

[10] G. Prasad and D. A. Haas-Kogan, "Radiation-induced gliomas," *Expert Review of Neurotherapeutics*, vol. 9, no. 10, pp. 1511–1517, 2009.

[11] H. Huang, J. Held-Feindt, R. Buhl, H. M. Mehdorn, and R. Mentlein, "Expression of VEGF and its receptors in different brain tumors," *Neurological Research*, vol. 27, no. 4, pp. 371–377, 2005.

[12] M. Clauss, "Molecular biology of the VEGF and the VEGF receptor family," *Seminars in Thrombosis and Hemostasis*, vol. 26, no. 05, pp. 561–570, 2000.

[13] M. Meyer, M. Clauss, and A. Lepple-Wienhues, "A novel vascular endothelial growth factor encoded by Orf virus,

VEGF-E, mediates angiogenesis via signalling through VEGFR-2 (KDR) but not VEGFR-1 (Flt-1) receptor tyrosine kinases," *The EMBO Journal*, vol. 18, no. 2, pp. 363–374, 1999.

[14] H. Gille, J. Kowalski, B. Li et al., "Analysis of biological effects and signaling properties of flt-1 (VEGFR-1) and KDR (VEGFR-2)," *Journal of Biological Chemistry*, vol. 276, no. 5, pp. 3222–3230, 2001.

[15] R. M. Brenner, N. R. Nayak, O. D. Slayden, H. O. Critchley, and R. W. Kelly, "Premenstrual and menstrual changes in the macaque and human endometrium: relevance to endometriosis," *Annals of the New York Academy of Sciences*, vol. 955, no. 1, pp. 60–74, 2002.

[16] S. Tanno, Y. Ohsaki, K. Nakanishi, E. Toyoshima, and K. Kikuchi, "Human small cell lung cancer cells express functional VEGF receptors, VEGFR-2 and VEGFR-3," *Lung Cancer*, vol. 46, no. 1, pp. 11–19, 2004.

[17] A. Giatromanolaki, M. I. Koukourakis, E. Sivridis et al., "Activated VEGFR2/KDR pathway in tumour cells and tumour associated vessels of colorectal cancer," *European Journal of Clinical Investigation*, vol. 37, no. 11, pp. 878–886, 2007.

[18] W. A. Spannuth, A. M. Nick, N. B. Jennings et al., "Functional significance of VEGFR-2 on ovarian cancer cells," *International Journal of Cancer*, vol. 124, no. 5, pp. 1045–1053, 2009.

[19] S. Guo, L. S. Colbert, M. Fuller, Y. Zhang, and R. R. Gonzalez-Perez, "Vascular endothelial growth factor receptor-2 in breast cancer," *Biochimica et Biophysica Acta (BBA) - Reviews on Cancer*, vol. 1806, no. 1, pp. 108–121, 2010.

[20] Q. G. Alessandris and M. Martini, "VEGF isoforms as outcome biomarker for anti-angiogenic therapy in recurrent glioblastoma," *Neurology*, vol. 84, no. 18, pp. 1906–19608, 2015.

[21] Y. Wang, Y. Zheng, W. Zhang et al., "Polymorphisms of KDR gene are associated with coronary heart disease," *Journal of the American College of Cardiology*, vol. 50, no. 8, pp. 760–767, 2007.

[22] D. N. Louis, H. Ohgaki, O. D. Wiestler et al., "The 2007 WHO classification of tumours of the central nervous system," *Acta Neuropathologica*, vol. 114, no. 5, pp. 547–109, 2007.

[23] W. Zhang, K. Sun, Y. Zhen et al., "VEGF receptor-2 variants are associated with susceptibility to stroke and recurrence," *Stroke*, vol. 40, no. 8, pp. 2720–2726, 2009.

[24] H. W. Park, J. E. Lee, E. S. Shin et al., "Association between genetic variations of vascular endothelial growth factor receptor 2 and atopy in the Korean population," *Journal of Allergy and Clinical Immunology*, vol. 117, no. 4, pp. 774–779, 2006.

[25] K. Hu, X. Xie, R. Wang, F. Wu, and Y. Zhang, "Association of the rs2071559 (T/C) polymorphism with lymphatic metastasis in patients with nasopharyngeal carcinoma," *Oncology Letters*, vol. 14, no. 6, pp. 7681–7686, 2017.

[26] Z. Zhu, K. Hattori, H. Zhang et al., "Inhibition of human leukemia in an animal model with human antibodies directed against vascular endothelial growth factor receptor 2. Correlation between antibody affinity and biological activity," *Leukemia*, vol. 17, no. 3, pp. 604–611, 2003.

[27] P. Knizetova, J. Ehrmann, A. Hlobilkova et al., "Autocrine regulation of glioblastoma cell cycle progression, viability and radioresistance through the VEGF-VEGFR2 (KDR) interplay," *Cell Cycle*, vol. 7, no. 16, pp. 2553–2561, 2008.

[28] A. S. Chan, S. Y. Leung, M. P. Wong et al., "Expression of vascular endothelial growth factor and its receptors in the anaplastic progression of astrocytoma, oligodendroglioma, and ependymoma," *The American Journal of Surgical Pathology*, vol. 22, no. 7, pp. 816–826, 1998.

[29] E. Hatva, A. Kaipainen, P. Mentula et al., "Expression of endothelial cell-specific receptor tyrosine kinases and growth factors in human brain tumors," *American Journal Of Pathology*, vol. 146, no. 2, pp. 368–378, 1995.

[30] B. Millauer, M. P. Longhi, K. H. Plate et al., "Dominant-negative inhibition of Flk-1 suppresses the growth of many tumor types in vivo," *Cancer Research*, vol. 56, no. 7, pp. 1615–1620, 1996.

[31] A. Galan, A. Ferlin, L. Caretti et al., "Association of age-related macular degeneration with polymorphisms in vascular endothelial growth factor and its receptor," *Ophthalmology*, vol. 117, no. 9, pp. 1769–1774, 2010.

[32] G. Dong, X. Guo, X. Fu et al., "Potentially functional genetic variants in KDR gene as prognostic markers in patients with resected colorectal cancer," *Cancer Science*, vol. 103, no. 3, pp. 561–568, 2012.

[33] S. Sjöström, C. Wibom, U. Andersson et al., "Genetic variations in VEGF and VEGFR2 and glioblastoma outcome," *Journal of Neuro-Oncology*, vol. 104, no. 2, pp. 523–527, 2011.

[34] H. Chen, W. Wang, Z. Xingjie et al., "Association between genetic variations of vascular endothelial growth factor receptor 2 and glioma in the Chinese Han population," *Journal of Molecular Neuroscience*, vol. 47, no. 3, pp. 448–457, 2012.

*Research Article*

# Krüppel-Like Factor 2 Is a Gastric Cancer Suppressor and Prognostic Biomarker

**Xi-mei Li,[1,2] Sheng-juan Hu,[2] Jian-fang Liu,[2] Mei-juan Ma,[2] Li-meng Du,[1] and Fei-hu Bai [3]**

[1]*School of Clinical Medicine, Ningxia Medical University, Yinchuan, Ningxia 750004, China*
[2]*Department of Gastroenterology, People's Hospital of Ningxia Hui Autonomous Region, Yinchuan, Ningxia 750002, China*
[3]*Department of Gastroenterology, The Second Affiliated Hospital of Hainan Medical University,*
 *The Gastroenterology Clinical Medical Center of Hainan Province, Haikou 570216, China*

Correspondence should be addressed to Fei-hu Bai; baifeihu1963@163.com

Gastric cancer (GC) is a common digestive tract tumor. Due to its complex pathogenesis, current diagnostic and therapeutic effects remain unsatisfactory. Studies have shown that KLF2, as a tumor suppressor, is downregulated in many human cancers, but its relationship and role with GC remain unclear. In the present study, KLF2 mRNA levels were significantly lower in GC compared to adjacent normal tissues, as analyzed by bioinformatics and RT-qPCR, and correlated with gene mutations. Tissue microarrays combined with immunohistochemical techniques showed downregulation of KLF2 protein expression in GC tissue, which was negatively correlated with patient age, T stage, and overall survival. Further functional experiments showed that knockdown of KLF2 significantly promoted the growth, proliferation, migration, and invasion of HGC-27 and AGS GC cells. In conclusion, low KLF2 expression in GC is associated with poor patient prognosis and contributes to the malignant biological behavior of GC cells. Therefore, KLF2 may serve as a prognostic biomarker and therapeutic target in GC.

## 1. Introduction

Gastric cancer (GC) ranks fifth among common cancers and third among cancer-related causes of death [1]. China is a high-incidence area for GC [2]. Despite great improvements in medical equipment and treatment, overall survival remains low in GC patients, and many patients are in advanced stages once diagnosed [3, 4]. Increasing evidence suggests that *H. pylori* infection is a major risk factor for the development of GC, but the incidence of *H. pylori*-related GC is significantly reduced due to vaccination of patients or taking drugs to treat *H. pylori* infection, while the number of GC patients due to genetic variants is increasing [5]. Pereira et al. showed that transcriptional alterations and copy number variations (CNV) of GSDMC in GC are associated with stronger tumor aggressiveness [6]. In addition, an increasing number of studies have found that abnormal genomic expression in GC patients is associated with poor patient prognosis [7–9]. However, due to genetic

heterogeneity and complex patterns of genetic span across different tumor stages, so far, no specific biomarker has been able to accurately diagnose or predict the prognosis of GC [10]. Many patients lack specific diagnostic biomarkers and targeted therapies, resulting in significantly reduced survival times. Therefore, it is important to explore new diagnostic and prognostic biomarkers as well as to develop targeted therapeutics for the diagnosis and treatment of GC.

Krüppel-like factor2 (KLF2) is an important member of the Krüppel-like factor (KLF) family, which plays an anti-tumor role in many cancers [11]. KLF family members are involved in cell differentiation, proliferation, migration, and pluripotency as transcriptional regulators [12–14]. KLF has been reported to be prone to genomic changes. Yin et al. showed that the downregulation of KLF2 expression in nonsmall cell lung cancer is associated with a poor prognosis for patients [15]. In GC, KLF2 is inhibited by the regulation and expression of long chain noncoding RNA (lncRNA) and microRNA (miRNA), thus promoting the progress of GC

[16, 17]. A recent study showed that downregulation of KLF2 expression in human cancers is caused by epigenetic silencing of histone methyltransferase EZH2 [11]. These studies suggest that KLF2 as a tumor suppressor gene is closely related to tumor development. However, the relationship between KLF2 and GC and its effect on GC has not been fully elucidated. Therefore, it is worth further revealing the relationship between KLF2 and GC, its clinical characteristics, and its role.

In recent years, bioinformatics analysis of large sample data combined with clinical studies and molecular experiments to identify reliable genetic biomarkers is another important means to study tumor pathogenesis and discover new therapeutic targets. Wei et al. demonstrated that miR-486-5p is a tumor suppressor of GC and inhibits gastric cancer cell growth and migration by downregulating fibroblast growth factor 9, through the TCGA database and cell experiments [18]. In addition, Chu et al. used bioinformatics techniques combined with clinical data to analyze the expression of thrombospondin-2 (TSP2) in GC tissues and its correlation with clinicopathological features and clinical prognosis of GC patients, indicating that TSP2 is a potential marker and therapeutic target for the prognosis of GC patients. In vitro experiments further demonstrated that TSP2 promoted the proliferation and migration of HGC-27 and AGS GC cell lines by inhibiting the VEGF/PI3K/AKT signaling pathway [19]. Therefore, the aim of this study was to investigate the mechanism of KLF2 expression in GC, the correlation of clinical features, and the effect on the biological function of GC cells by using bioinformatics techniques and molecular biology experiments.

## 2. Materials and Methods

### 2.1. Data Collection and Different Expression Analysis.
Tumor Immune Estimation Resource 2.0 (TIMER2.0) (https://timer.cistrome.org/) database was used to analyze differential expression of KLF2 mRNA levels in different human tumors [20] and focused on KLF2 expression in GC. Next, The Cancer Genome Atlas (TCGA) program (https://www.cancer.gov/tcga) [21] and The Gene Expression Profiling Interactive Analysis 2 (GEPIA2, https://gepia2.cancer-pku.cn/) [22] were used to compare KLF2 expression levels in gastric cancer and adjacent normal tissues. Then, the Cancer Cell Line Encyclopedia (CCLE) database (https://portals.broadinstitute.org/ccle) was used to assess KLF2 expression levels in different cancer cell lines [23].

### 2.2. Genetic Changes and Prognostic Value Analysis.
Using the cBio Cancer Genomics Portal (cBioPortal) online software (https://cbioportal.org), genomic alterations of KLF2 in GC were analyzed, including mutations in KLF2 and the proportion of data distribution and the frequency of changes (mutations and amplifications) of KLF1 gene in gastric cancer subtypes [24]. Also, the association between KLF2 gene alterations and overall survival, disease-free survival, and progression-free survival in GC patients was investigated to assess the prognostic value. Subsequently, we

also analyzed copy number variation (CNV) of KLF2. In addition, the CNV module of Gene Set Cancer Analysis (GSCA; https://bioinfo.life.hust.edu.cn/GSCA/#/) was used to analyze the proportion of KLF2 heterozygous/homozygous and amplified/deleted in GC, the Spearman correlation between KLF2 mRNA expression and CNV, and survival differences between KLF2 CNV and wild type [25].

### 2.3. Collecting Tumor Tissue.
Thirty GC patients (median age: 61 years; age: 27–75 years) who underwent surgical resection at People's Hospital of Ningxia Hui Autonomous Region from 2019 to 2021 and their adjacent normal gastric tissues were collected and immediately stored in liquid nitrogen. No patients received chemotherapy or radiotherapy prior to sample collection. Each participant or his/her authorized representative signed an informed consent form. This study was approved by the Ethics Committee of Ningxia Hui Autonomous Hospital (Approval No.: 2017–034) and conducted according to the World Medical Association Declaration of Helsinki.

### 2.4. Tissue Microarray and Immunohistochemistry.
A chip (No.: HStmA180Su19) containing 86 adjacent noncancerous specimens and 88 gastric cancer tissues was purchased from Shanghai Biochip Limited company. The specimens were subjected to TNM pathological staging according to the 7th edition of the AJCC/UICC tumor lymph node metastasis (TNM) staging classification. The expression of KLF2 protein in the samples was detected by the immunohistochemical EnVision method. Following deparaffinization, hydration, antigen retrieval, and blocking endogenous peroxidase activity of the tissue microarray according to the kit instructions, the chip was incubated with KLF2 polyclonal antibody (PA5-40591, Invitrogen, USA) for 1 h. Afterwards, the chip was processed using the EnVision Rb Gt anti-Rb-HRP kit (K4003, Dako, Denmark) according to the manufacturer's instructions and visualized by DAB staining solution (Dako, Denmark) in the dark. Following rinsing in tap water, the chips were counterstained for chips using hematoxylin, dehydrated in a graded water-ethanol series, soaked in xylene, and finally sealed with neutral gum. Staining signals were visualized using a Nikon microscope (Tokyo, Japan) and statistically analyzed using ImageJ Pro (Media Cybernetics, Rockville, Maryland, United States). Quantitative analysis was performed independently by two pathologists who were blinded to the experimental groupings. The final score is obtained by multiplying the staining intensity and the percentage of positive tumor cells and ranges from 0 to 300. Staining intensity scores were 0 (negative), 1+ (weak), 2+ (moderate), and 3+ (strong). Percentage of positive tumor cells is 0–100%. A final score of <100% is considered low and >100% is considered high [26].

### 2.5. Cell Culture and Transfection.
GC cell lines (HGC-27 and AGS) were purchased from American Type Culture Collection and cultured in RPMI-1640 (Gibco, USA) supplemented with 10% fetal bovine serum (FBS; Gibco) and 1%

penicillin-streptomycin (Gibco) and grown at 37°C and 5% $CO_2$. Digestion and passage were performed using 0.25% trypsin (Solarbio, Beijing, China) after cells reached 80–90% confluence.

KLF2 siRNA (si-KLF2) and its control (si-control) were designed and synthesized by Invitrogen (USA). When AGS and HGC-27 cells reached 80% confluency, the above siR-NAs were transfected into GC cells using Lipofectamine® 2000 (Thermo Fisher Scientific, Inc., USA) according to the manufacturer's instructions. Six hours after transfection, the fresh serum-containing medium was replaced. The culture was continued for 48 h and cells were collected for CCK-8, colony formation, wound healing, transwell, RT-qPCR, and immunoblot analysis. The si-KLF2 sequence is as follows: si-KLF2: sense: UCAACAGCGGCUGGACUUTT, antisense: UAAGCCAGCACGCUGUGGAUTT.

*2.6. Cell Counting Kit-8 (CCK-8) Assay.* Transfected HGC-27 and AGS cells ($1 \times 10^4$ cells/well) were seeded into 96-well plates. Following incubation at 37°C and 5% $CO_2$ for 24, 48, and 72 h, 10 $\mu$l CCK-8 solution was added to each well and incubated for 2 h. Absorbance at 450 nm was measured using a microplate reader (BioTek Instruments, USA) [27].

*2.7. Colony Formation Assay.* Transfected AGS and HGC-27 cells ($5 \times 10^2$ cells/well) were seeded into 12-well plates and cultured for 14 days at 37°C in a 5% $CO_2$ incubator to form macroscopic colonies, the medium was removed, and the cells were washed three times with PBS; then, the colonies were fixed with 4% paraformaldehyde for 20 minutes at room temperature and the colonies were stained with 0.1% crystal violet for 10 minutes. Images were taken under a light microscope, and the number of cell colonies >50 cells was calculated [27].

*2.8. Wound Healing Assay.* Transfected GC cells ($3 \times 10^5$ cells/well) were seeded into 24-well plates and cultured at 37°C and 5% $CO_2$ for 24 h. When more than 90% confluent monolayers were formed, cell monolayers were scratched with a 100 $\mu$l pipette tip and washed with PBS to remove floating cells. Subsequently, fresh serum-free medium was added to each well, and after 24 h of culture, images at 0 and 24 h after scratching were collected with a light microscope (Nikon, Japan), and then, wound healing rates were measured and calculated using ImageJ software. The formula for wound healing rate is as follows: [wound width (0 h) wound width (48 h)]/wound width (0 h)×100% [27].

*2.9. Transwell Assay.* Transfected AGS and HGC-27 cells ($1 \times 10^5$ cells/ml) were suspended in serum-free RPMI-1640 medium and seeded into the upper chamber precoated with Matrigel (BD Biosciences). Then, RPMI-1640 medium containing 10% FBS was added to the lower chamber of a 24-well plate and cultured for 24 h at 37°C in an incubator with 5% $CO_2$. Remove the culture medium. Cells remaining in the upper chamber were gently removed with a cotton swab. Cells were rinsed three times with PBS, and then, cells were

fixed with 4% paraformaldehyde for 20 min at room temperature and stained with 0.1% crystal violet for 10 min at room temperature. Under a light microscope, five fields were randomly selected to observe cells, acquire images, and calculate the number of migrating or invading cells [28].

*2.10. Quantitative Real-Time Polymerase Chain Reaction (RT-qPCR).* Total RNA from tissues and cells was extracted using TRIzol reagent (Invitrogen, Carlsbad, CA, USA) and tested for concentration and purity of RNA. RNA was subsequently reverse transcribed to synthesize cDNA using the cDNA Reverse Transcription Kit (Thermo Fisher, Hudson, NH, USA). cDNA was amplified using the SYBR Green RT-qPCR kit (Thermo Fisher, Hudson, NH, USA) according to the supplier's guidelines to detect mRNA expression levels of KLF2. $\beta$-Actin was used as an internal normalization control, and relative expression levels of genes were calculated by the $2^{-\Delta\Delta CT}$ method [29]. The primer sequences were as follows: KLF2-F: 5′-CTACACCAAGAGTTCGCATCTG-3′; KLF2-R: 5′-CCG TGGCTTTCGGTAGTG-3′; human $\beta$-actin-F1: 5′-GAGAGC TACGAGCTGCCTGA-3′; human $\beta$-actin-R1: 5′-CAGACA GCACTGTTGGCG-3′.

*2.11. Western Blotting Analysis.* Total protein was extracted by lysing cells with RIPA lysis buffer containing PMSF (Beyotime Biotechnology, Shanghai, China). Then, protein concentration was detected using a BCA protein assay kit (Beyotime Biotechnology, Shanghai, China). Protein samples (30 $\mu$g) were separated with 10% SDS-PAGE. Subsequently, proteins were transferred to polyvinylidene fluoride (PVDF) membranes (Merck Millipore, Billerica, MA, USA). PVDF membranes were blocked with 5% skim milk for 1 h at room temperature. Afterwards, PVDF membranes were incubated overnight at 4°C with primary antibodies KLF2 (1 : 1000; Beyotime, China), E-cadherin (1 : 1000; Beyotime, China), N-cadherin (1 : 1000; Beyotime, China), Snail (1 : 1000; Beyotime, China), vimentin (1 : 1000; Beyotime, China), Twist (1 : 1000; Beyotime, China), and $\beta$-actin (Beyotime, China). On the following day, PVDF membranes were incubated with horseradish peroxidase-conjugatedanti-rabbit IgG secondary antibody (1 : 5000; Sigma-Aldrich, USA) and anti-mouse IgG secondary antibody (1 : 5000; Cell Signaling Technology, Inc., USA) for 1 h at room temperature. Finally, protein bands were visualized using the BeyoECL Plus kit (Beyotime Biotechnology, China) and Image Pro Plus 6.0 software (Media Control, Inc., USA) for analysis.

*2.12. Statistical Analysis.* All gene expression data were normalized by log2 transformation. Kaplan–Meier analysis and log-rank test were used for survival analysis. Cox regression models were used to analyze the relationship between KLF2 expression and clinicopathological parameters. Pearson or Spearman tests were used to assess the association between the two variables. All experiments were repeated three times. Experimental data were analyzed with GraphPad Prism 8.0 (GraphPad-La Jolla, CA, USA)

software. Experimental results are presented as mean-± standard deviation (SD). Differences between the groups were analyzed using the paired Student's $t$-test or one-way analysis of variance (ANOVA) with the multiple group Tukey's multiple comparison post hoc test. $P < 0.05$ was considered statistically significant.

## 3. Results

*3.1. KLF2 Is Lowly Expressed in GC.* Aberrant expression of KLF2 has been reported in a variety of cancers [30, 31]; however, the association and the role of KLF2 and GC have not been elucidated. In this study, we found that KLF2 mRNA levels were KLF2 expression promotes the malignant biological behavior in GC cells and accelerates GC progression. lower in various tumor tissues than in normal tissues through the TIMER2.0 database, and KLF2 mRNA expression was significantly lower in STAD tissues than in normal tissues (Figure 1(a)). CCLE database analysis showed low KLF2 expression in GC cell lines (Figure 1(b)). Data from GC tissues downloaded from the TCGA database and GEPIA database for analysis were consistent with the above results (Figures 1(c) and 1(d)). Further validation by RT-qPCR analysis revealed a significant downregulation of KLF2 mRNA levels in GC patient tissues compared to adjacent normal gastric tissues (Figure 1(e)). In addition, immunohistochemical staining showed significantly higher KLF2 protein expression in adjacent normal gastric tissues than in GC tissues (Figure 1(f)). Together, these results suggest that KLF2 is aberrantly expressed in GC tissues and may be a potential target for GC and deserves in-depth investigation.

*3.2. Association of KLF2 Genomic Alterations with Prognosis in GC.* In order to elucidate the mechanisms underlying aberrant KLF2 expression, in this study, we used the cBioPortal database to analyze the amplification frequency and mutation types of KLF2 alterations in a cohort of GC patients. The results showed that KLF2 was mutated at a frequency of 1.1% in GC, and the mutation types included mutation and amplification (Figures 2(a) and 2(b)). Further analysis of KLF2 gene mutations on the prognosis of GC patients was performed. The results showed that GC patients in the KLF2 mutant group had poorer disease-free survival (Figure 2(c)), disease-specific survival (Figure 2(d)), overall survival (Figure 2(e)), and progression-free survival (Figure 2(f)) compared with the nonmutant group, but there was no significant difference ($P > 0.05$). In addition, we analyzed the CNV distribution (including amplification and deletion) of KLF2 in GC (Figure 2(g)). In addition, further analysis by the GSCA database showed 10.66% and 26.98% CNV for total amplification and total deletion of KLF2 in STAD, with 26.76% heterozygous deletions (Figure 3(a)). The Spearman correlation between KLF2 mRNA expression and CNV was 0.2 (Figure 3(b)). Overall survival (OS) was lower in KLF2 CNV (amplifications and deletions) compared to wild type (Log-rank $P$ value = 0.38) (Figure 3(c)). These results suggest that low KLF2 expression in GC may be associated with genomic deletions.

*3.3. Correlation between KLF2 Expression and Clinicopathologic Features of GC Patients.* Subsequently, KLF2 protein expression in GC tissue microarrays was detected by IHC in this study (Figure 4(a)), and the results showed that the higher the age of patients (>75 years) and the greater the T stage (T3 and T4), the lower the KLF2 expression level (Figures 4(b) and 4(c)). In addition, GC patients with low KLF2 expression had shorter survival times and lower overall survival (Figure 4(d)). Therefore, these results suggest that low KLF2 expression promotes tumor invasion/metastasis and can be used as a diagnostic biomarker for GC with an important clinical value.

*3.4. Knockdown of KLF2 Promotes Malignant Biological Behavior of GC Cells.* To further elucidate the mechanism of KLF2's action on GC, in this study, we investigated the effect of KLF2 on GC cell growth and proliferation, migration, and invasion by knocking down KLF2 in HGC-27 and AGS cells. Western blot analysis showed that knockdown of KLF2 in GC cells resulted in higher levels of N-cadherin, Snail, vimentin, and Twist protein expression than in the si-control group, but reduced E-cadherin protein expression (Figure 5(a)). CCK-8 and colony formation assays showed that knockdown of KLF2 significantly promoted HGC-27 and AGS cell growth and proliferation compared to the si-control group (Figures 5(b)–5(e)). In addition, wound healing assay and transwell analysis showed that the wound healing rate and number of migrated and invaded cells in the si-KLF2 group were significantly higher than those in the si-control group (Figures 5(f)–5(j)). These results indicate that low KLF2 expression promotes the malignant biological behavior in GC cells and accelerates GC progression.

## 4. Discussion

GC is one of the most common gastrointestinal tumors in mammals. Due to western diets, bad living habits, and increased pressure to study and work, the incidence of GC is rising,, which will cause a huge medical burden on society. It is reported that the occurrence of GC is closely related to many factors such as *Helicobacter pylori* infection, eating habits, environment, genetics, and immunity [32–34], among which genetic factors play a crucial role [35]. At present, the treatment of GC mainly includes drug and surgical treatment, but most patients still have metastasis and recurrence after conventional radiotherapy and chemotherapy [36]. In addition, many studies have focused on the important impact of host genetic susceptibility on the development of GC. Based on this, some abnormally expressed genes have been identified as biomarkers and therapeutic targets. However, the diagnosis and prognosis of GC are still not accurate. In this study, the expression mechanism, prognostic value, and potential role of KLF2 in GC development were investigated in depth by using bioinformatics techniques combined with clinical tissue samples and cellular experiments.

Cancer-associated inflammation emerging at different stages at the time of tumorigenesis has been reported to lead

(a)



(b)



(c)



(d)



(e)



(f)
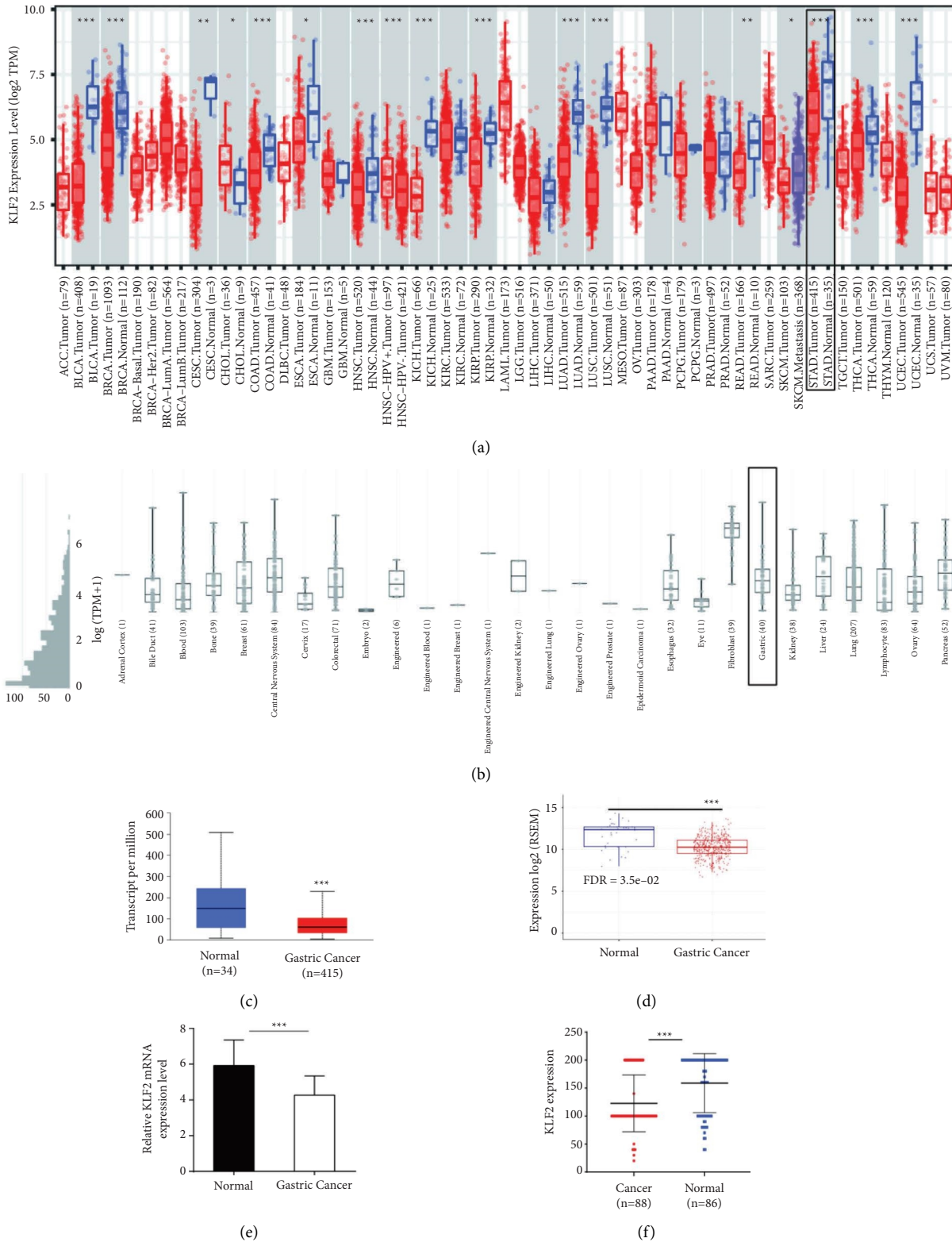
FIGURE 1: KLF2 expression is low in GC tissues. (a) TIMER2.0 database used to analyze mRNA levels of KLF2 in different tumor types. (b) KLF2 expression levels in different tumor cell lines detected by the CCLE database. (c) The TCGA database used to analyze KLF2 expression in GC tissues and paired adjacent noncancerous tissues. (d) The GEPIA database used to determine KLF2 expression in GC tissue and normal tissue data. (e) mRNA levels of KLF2 detected by RT-qPCR in GC tissues and paired adjacent noncancerous tissues ($n = 30$). (f) IHC used to analyze KLF2 protein levels in GC tissue microarrays. $P < 0.05$; $P < 0.01$; $^{***}P < 0.001$.

(a)



(b)



(c)



(d)



(e)
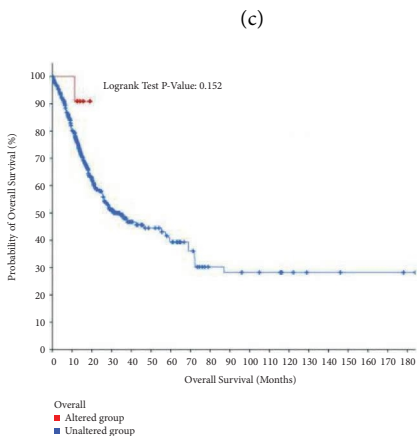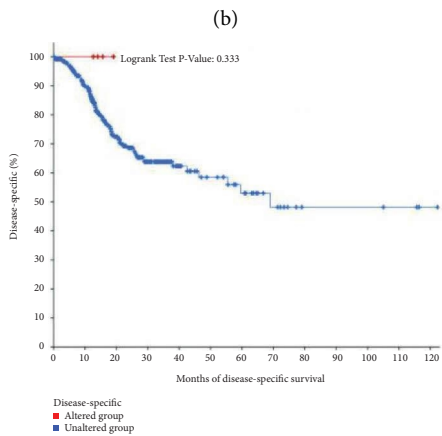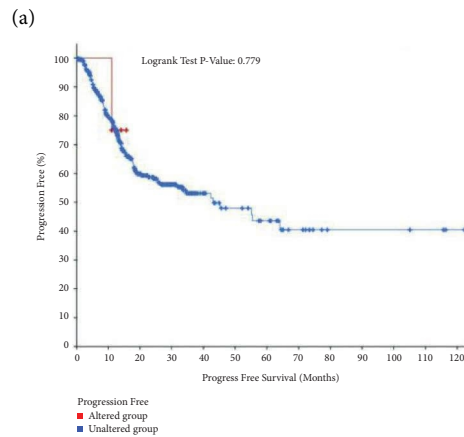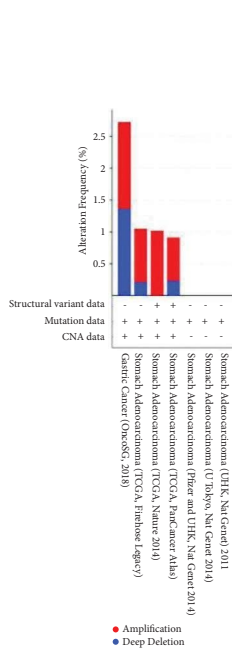
Figure 2: Continued.

(f)



(g)
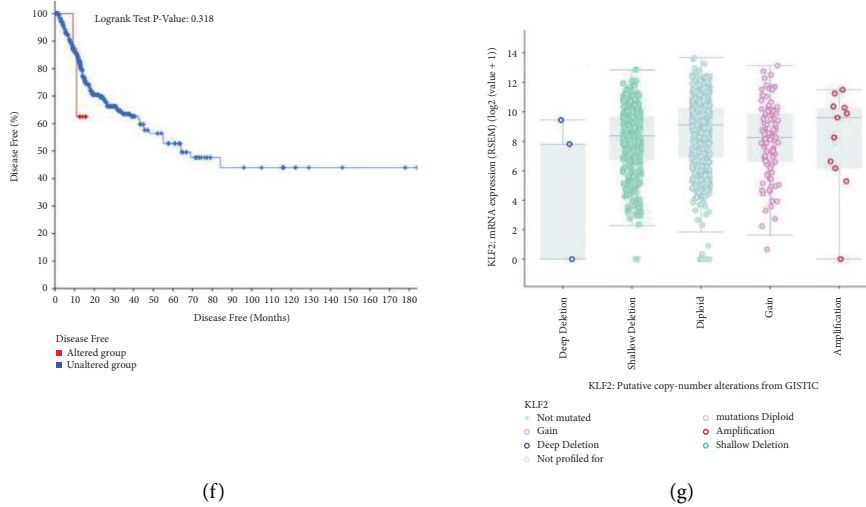
Figure 2: Association of KLF2 genomic alterations with prognosis in GC (cBioPortal). (a) OncoPrint genetically altered for KLF2 in GC cohort. (b) Cancer types summary of KLF2 genomic alterations in GC. Association of KLF2 mutations with disease-free survival (c), disease-specific survival (d), overall survival (e), and progression-free survival (f) in GC patients. (g) Box plots of KLF2 copy number changes (CNV) in GC for GISTIC. Hete., heterozygous; *Homo.*, homozygous; Amp., amplification; Dele., deletion.



(a)



(b)



(c)
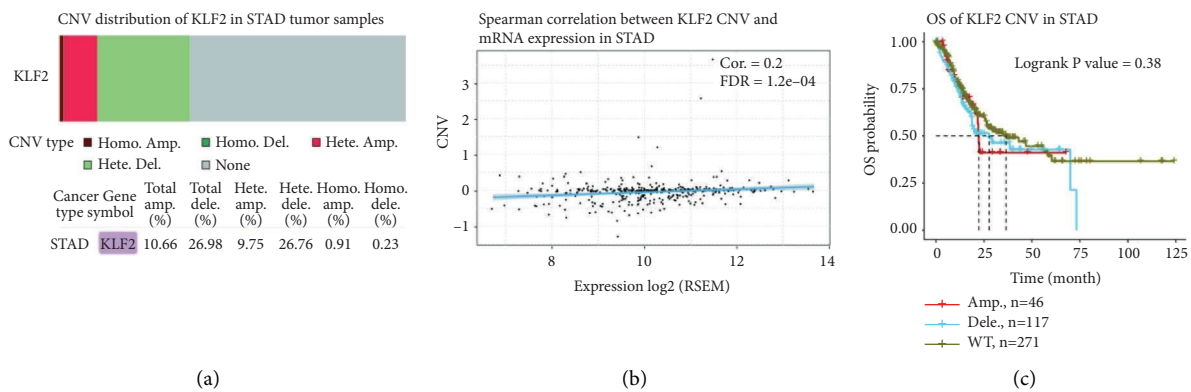
Figure 3: CNV analysis of the KLF2 gene in GC and its effect on overall survival (GSCA). (a) Proportion of KLF2 heterozygous/homozygous and amplified/deleted in STAD. (b) Spearman correlation assessment of CNV and KLF2 mRNA expression in STAD. (c) Survival difference between KLF2 CNV and wild type in STAD patients.

to genomic instability and epigenetic modifications [37]. Previous studies have shown that KLF2 is downregulated in GC and prone to genomic dysregulation [15]. In this study, KLF2 was significantly lower expressed in GC tissues and cells and may be associated with mutations in the KLF2 gene. Correlation analysis of clinical characteristics showed a negative correlation between KLF2 and age, T stage, and survival in GC patients. The knockdown of KLF2 in GC cells was further analyzed to investigate the effect of low KLF2 expression on GC function. The results showed that the knockdown of KLF2 could significantly promote the growth, proliferation, migration, and invasion of GC cells, as well as tumor development. This is in agreement with Wang et al. [38]. In addition, Li et al. showed that the long noncoding RNA DLEU1 promotes GC progression by epigenetically inhibiting KLF2 [39]. Another study showed that microRNAs promote GC cell proliferation and invasion by

targeting KLF2 [16]. MicroRNA-32-5p promotes GC development by activating the PI3K/AKT signaling pathway and targeting KLF2 expression [40]. Furthermore, a study has shown that SUZ12 may regulate proliferation and metastasis of GC, through modulating KLF2 and E-cadherin [22]. We also observed a regulatory relationship between KLF2 and E-cadherin. The knockdown of KLF2 resulted in a reduction in E-cadherin. Furthermore, the expression of epithelial-mesenchymal transition (EMT)-related proteins (N-cadherin, Snail, Vimentin, and Twist) was increased after KLF2 knockdown. These studies suggest that KLF2 may be a novel therapeutic target for GC.

In conclusion, low KLF2 expression promotes the malignant biological behavior of GC, and KLF2 acts as a tumor suppressor and may be a potential therapeutic target and prognostic biomarker for GC. Although this study provides a rationale for the role of KLF2 in GC pathogenesis, we did

(a)



(b)



(c)



(d)
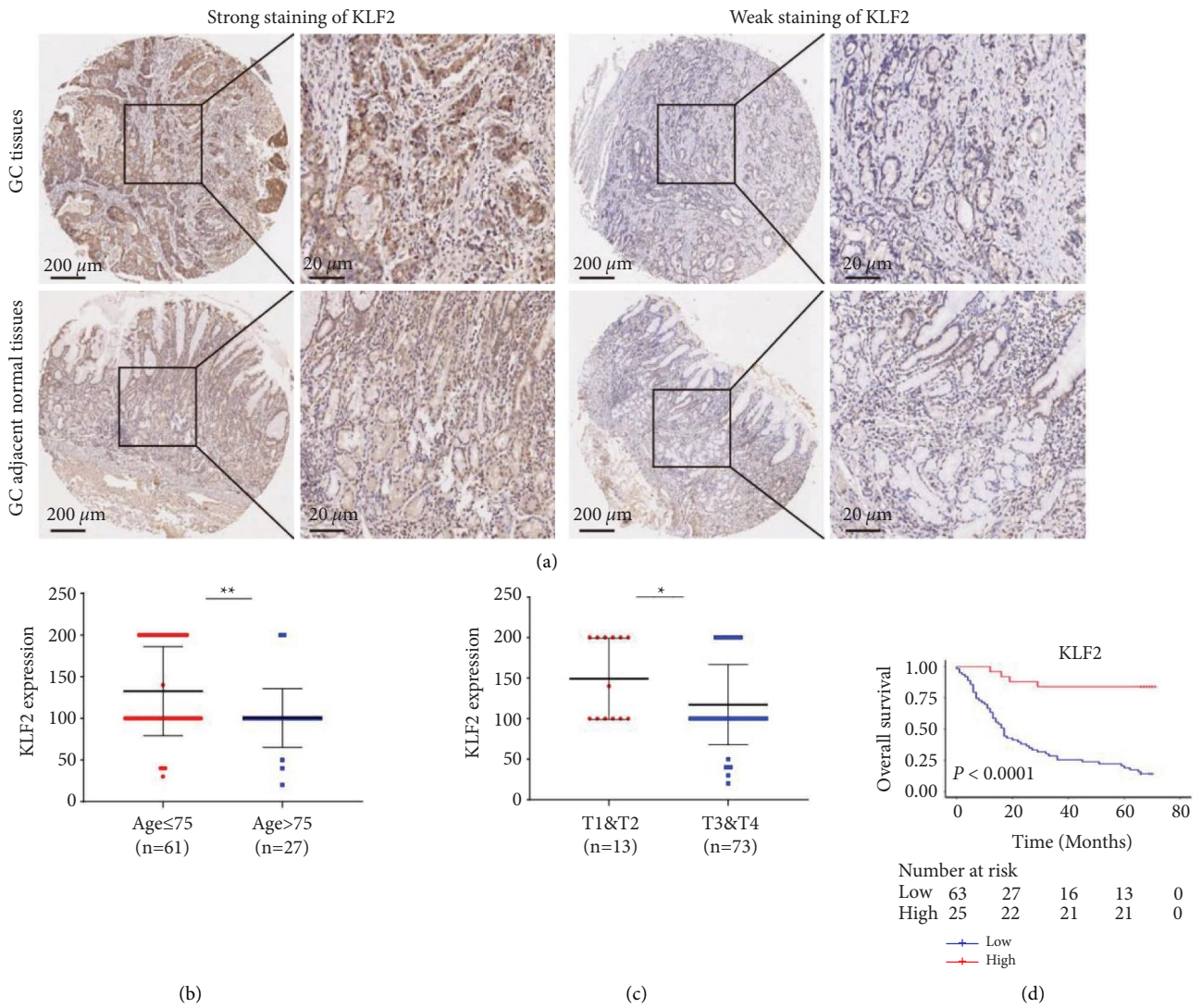
FIGURE 4: KLF2 protein expression in GC tissue microarrays (immunohistochemistry). (a) KLF2 protein expression in GC tissues ($n = 88$) and adjacent normal tissues ($n = 86$) (magnification: 200× and 400×). (b) KLF2 expression levels in GC patients of different age groups. (c) KLF2 protein expression in GC patients with different T stages. (d) Kaplan–Meier curves used to analyze KLF2 expression levels with overall survival in GC patients (log-rank test, $P < 0.0001$). *$P < 0.05$   **$P < 0.01$



(a)



(b)



(c)

FIGURE 5: Continued.

(d)

(e)

(f)

(g)

(h)

Figure 5: Continued.

(i)

(j)
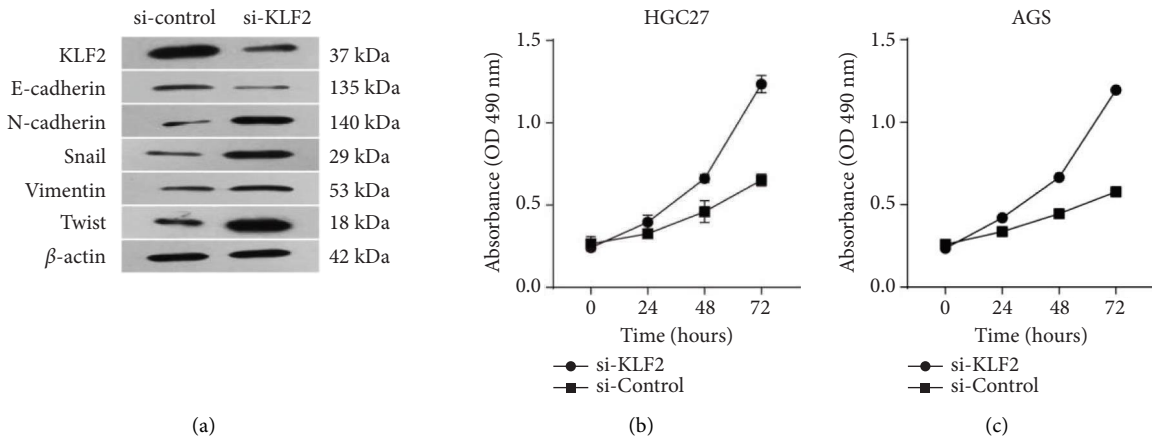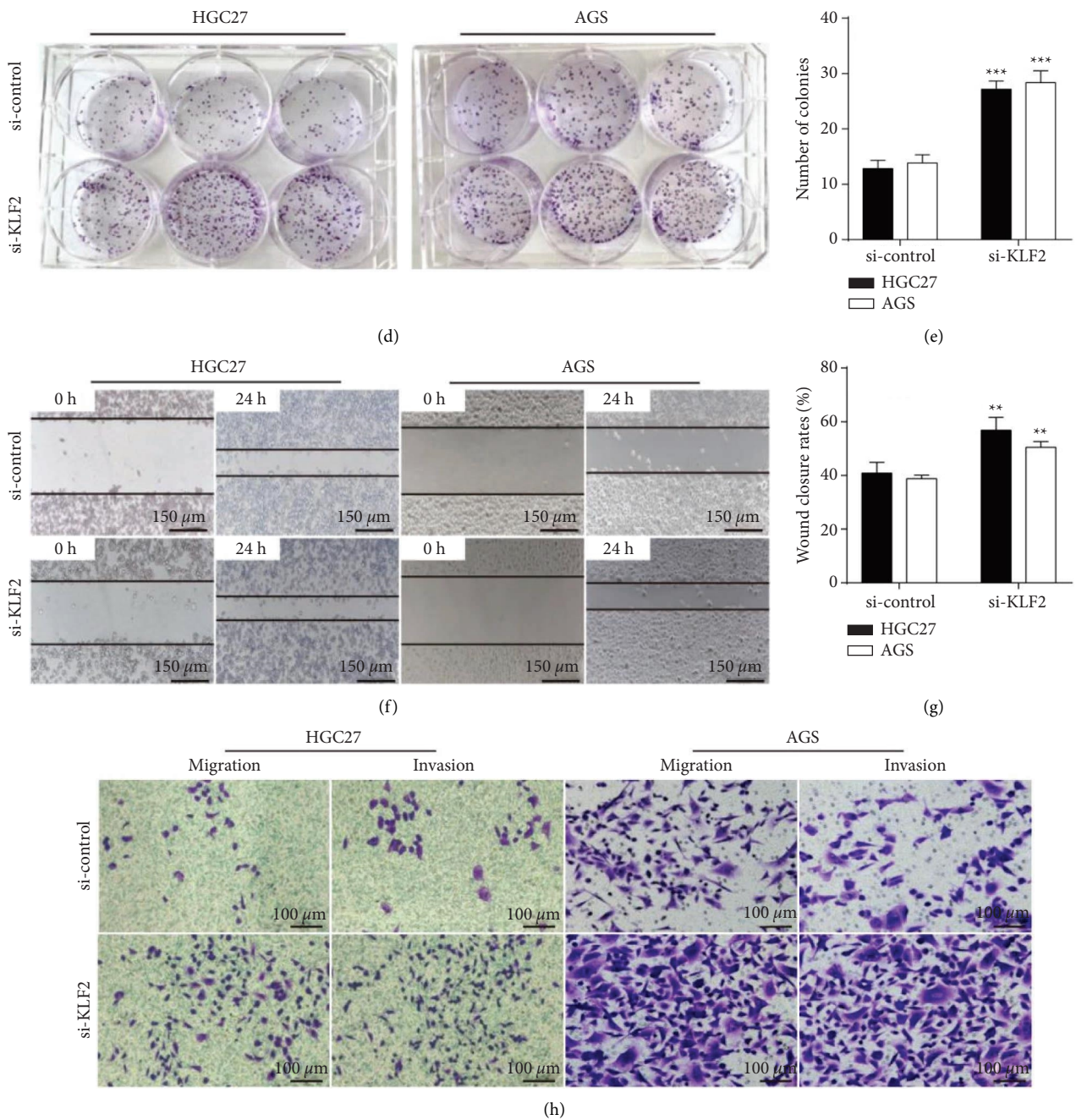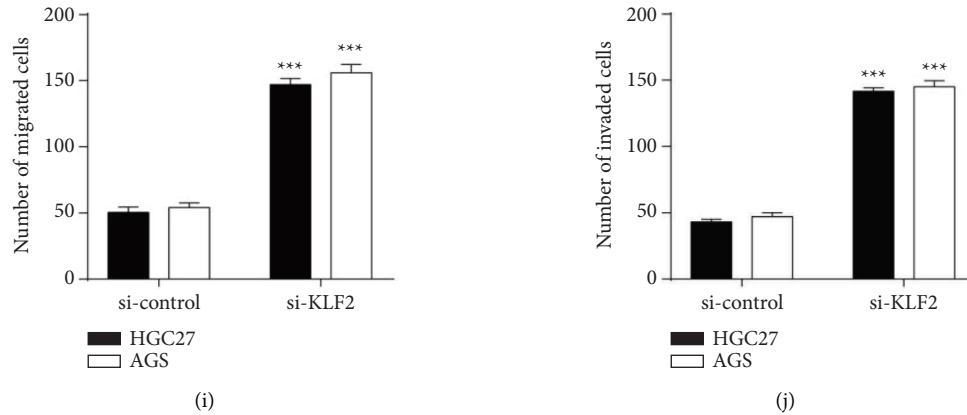
FIGURE 5: Knockdown of KLF2 promotes the growth, proliferation, migration, and invasion of GC cells. (a) Western blot used to analyze E-cadherin, N-cadherin, Snail, vimentin, and Twist protein expression levels in HGC-27 cells knocked down for KLF2, after KLF2 knockdown in HGC-27 and AGS GC cell lines. (b-c) Cell viability measured by CCK-8 assay. (d-e) A colony formation assay used to analyze GC cell proliferation ability. (f-g) Wound healing assay used to assess the migration ability of GC cells. (h–j) Transwell assay used to analyze migration and invasion of GC $^*P < 0.05$ $^{**}P < 0.01$ $^{***}P < 0.001$.

not further investigate the effect of epigenetic alterations on KLF2 underexpression in GC nor did we assess the number of patients who developed KLF2 underexpression in GC, and therefore, we will continue in-depth studies through databases and clinical trials in the future.

## Data Availability

The data used to support the findings of this study are available from the corresponding author upon request.

## Conflicts of Interest

The authors declare that they have no conflicts of interest.

## Acknowledgments

## References

[1] E. C. Smyth, M. Nilsson, H. I. Grabsch, N. C. van Grieken, and F. Lordick, "Gastric cancer," *The Lancet*, vol. 396, no. 10251, pp. 635–648, 2020.

[2] W. Chen, R. Zheng, P. D. Baade et al., "Cancer statistics in China, 2015," *CA: A Cancer Journal for Clinicians*, vol. 66, no. 2, pp. 115–132, 2016.

[3] R. L. Siegel, K. D. Miller, and A. Jemal, "Cancer statistics," *CA: A Cancer Journal for Clinicians*, vol. 69, no. 1, pp. 7–34, 2019.

[4] F. Bray, J. Ferlay, I. Soerjomataram, R. L. Siegel, L. A. Torre, and A. Jemal, "Global cancer statistics 2018: GLOBOCAN estimates of incidence and mortality worldwide for 36 cancers in 185 countries," *CA: A Cancer Journal for Clinicians*, vol. 68, no. 6, pp. 394–424, 2018.

[5] C. Schulz, K. Schütte, J. Mayerle, and P. Malfertheiner, "The role of the gastric bacterial microbiome in gastric cancer: *Helicobacter pylori* and beyond," *Therapeutic advances in gastroenterology*, vol. 12, Article ID 1756284819894062, 2019.

[6] B. S. Pereira, F. Wisnieski, D. Q. Calcagno et al., "Genetic and transcriptional analysis of 8q24.21 cluster in gastric cancer," *Anticancer Research*, vol. 42, no. 9, pp. 4381–4394, 2022.

[7] L. Li, Z. Zhu, Y. Zhao et al., "FN1, SPARC, and SERPINE1 are highly expressed and significantly related to a poor prognosis of gastric adenocarcinoma revealed by microarray and bioinformatics," *Scientific Reports*, vol. 9, no. 1, p. 7827, 2019.

[8] Z. Huang, A. He, J. Wang et al., "The circadian clock is associated with prognosis and immune infiltration in stomach adenocarcinoma," *Aging*, vol. 13, no. 12, pp. 16637–16655, 2021.

[9] J. Li, W. Zhou, J. Wei et al., "Prognostic value and biological functions of RNA binding proteins in stomach adenocarcinoma," *OncoTargets and Therapy*, vol. 14, pp. 1689–1705, 2021.

[10] F. Yicheng, L. Xin, Y. Tian, and L. Huilin, "Association of FLG mutation with tumor mutation load and clinical outcomes in patients with gastric cancer," *Frontiers in Genetics*, vol. 13, Article ID 808542, 2022.

[11] H. Taniguchi, F. V. Jacinto, A. Villanueva et al., "Silencing of Kruppel-like factor 2 by the histone methyltransferase EZH2 in human cancer," *Oncogene*, vol. 31, no. 15, pp. 1988–1994, 2012.

[12] B. B. McConnell and V. W. Yang, "Mammalian Krüppel-like factors in health and diseases," *Physiological Reviews*, vol. 90, no. 4, pp. 1337–1381, 2010.

[13] S. Yamanaka, "Strategies and new developments in the generation of patient-specific pluripotent stem cells," *Cell Stem Cell*, vol. 1, no. 1, pp. 39–49, 2007.

[14] J. Jiang, Y. S. Chan, Y. H. Loh et al., "A core Klf circuitry regulates self-renewal of embryonic stem cells," *Nature Cell Biology*, vol. 10, no. 3, pp. 353–360, 2008.

[15] L. Yin, J. p. Wang, T. p. Xu et al., "Downregulation of Kruppel-like factor 2 is associated with poor prognosis for nonsmall-cell lung cancer," *Tumor Biology*, vol. 36, no. 4, pp. 3075–3084, 2015.

[16] Q. Q. Mao, J. J. Chen, W. J. Xu, X. Z. Zhao, X. Sun, and L. Zhong, "miR-92a-3p promotes the proliferation and

invasion of gastric cancer cells by targeting KLF2," *Journal of Biological Regulators & Homeostatic Agents*, vol. 34, no. 4, pp. 1333–1341, 2020.

[17] Q. Xu, S. Qiao, L. Liu et al., "LINC00202 attenuates the progression of gastric cancer via suppressing expression level of KLF2," *Journal of BUON: Official Journal of the Balkan Union of Oncology*, vol. 26, no. 2, pp. 506–512, 2021.

[18] W. Wei, C. Liu, R. Yao, Q. Tan, Q. Wang, and H. Tian, "miR-486-5p suppresses gastric cancer cell growth and migration through downregulation of fibroblast growth factor 9," *Molecular Medicine Reports*, vol. 24, no. 5, p. 771, 2021.

[19] X. d. Chu, Z. b. Lin, T. Huang et al., "Thrombospondin-2 holds prognostic value and is associated with metastasis and the mismatch repair process in gastric cancer," *BMC Cancer*, vol. 22, no. 1, p. 250, 2022.

[20] T. Li, J. Fu, Z. Zeng et al., "TIMER2.0 for analysis of tumor-infiltrating immune cells," *Nucleic Acids Research*, vol. 48, no. W1, pp. W509–W514, 2020.

[21] J. N. Weinstein, E. A. Collisson, G. B. Mills et al., "The cancer Genome Atlas pan-cancer analysis project," *Nature Genetics*, vol. 45, no. 10, pp. 1113–1120, 2013.

[22] Z. Tang, C. Li, B. Kang, G. Gao, C. Li, and Z. Zhang, "GEPIA: a web server for cancer and normal gene expression profiling and interactive analyses," *Nucleic Acids Research*, vol. 45, no. W1, pp. W98–W102, 2017.

[23] M. Ghandi, F. W. Huang, J. Jané-Valbuena et al., "Next-generation characterization of the cancer cell line Encyclopedia," *Nature*, vol. 569, no. 7757, pp. 503–508, 2019.

[24] J. Gao, B. A. Aksoy, U. Dogrusoz et al., "Integrative analysis of complex cancer genomics and clinical profiles using the cBioPortal," *Science Signaling*, vol. 6, no. 269, p. pl1, 2013.

[25] C. J. Liu, F. F. Hu, M. X. Xia, L. Han, Q. Zhang, and A. Y. Guo, "GSCALite: a web server for gene set cancer analysis," *Bioinformatics*, vol. 34, no. 21, pp. 3771-3772, 2018.

[26] Y. Cai, Z. Chen, Y. Liang et al., "Cleavage factor Im 25 as a potential biomarker for prognosis of colorectal cancer," *Translational Cancer Research*, vol. 10, no. 12, pp. 5267–5279, 2021.

[27] A. Plaza, B. Merino, N. Del Olmo, and M. Ruiz-Gayo, "The cholecystokinin receptor agonist, CCK-8, induces adipo-nectin production in rat white adipose tissue," *British Journal of Pharmacology*, vol. 176, no. 15, pp. 2678–2690, 2019.

[28] J. Sun, X. Li, R. Yin, and X. Li, "lncRNA VIM-AS1 promotes cell proliferation, metastasis and epithelial-mesenchymal transition by activating the Wnt/β-catenin pathway in gastric cancer," *Molecular Medicine Reports*, vol. 22, no. 6, pp. 4567–4578, 2020.

[29] K. J. Livak and T. D. Schmittgen, "Analysis of relative gene expression data using real-time quantitative PCR and the 2−ΔΔCT method," *Methods (San Diego, CA, United States)*, vol. 25, no. 4, pp. 402–408, 2001.

[30] N. Wu, S. Chen, Q. Luo et al., "Kruppel-like factor 2 acts as a tumor suppressor in human retinoblastoma," *Experimental Eye Research*, vol. 216, Article ID 108955, 2022.

[31] F. Hu, Y. Ren, Z. Wang et al., "Bioinformatics analysis of KLF2 as a potential prognostic factor in ccRCC and association with epithelial-mesenchymal transition," *Experimental and Therapeutic Medicine*, vol. 24, no. 3, p. 561, 2022.

[32] P. B. Ernst, H. Takaishi, and S. E. Crowe, "*Helicobacter pylori*>, Infection as a model for gastrointestinal immunity and chronic inflammatory diseases," *Digestive Diseases*, vol. 19, no. 2, pp. 104–111, 2001.

[33] C. Ferrone and G. Dranoff, "Dual roles for immunity in gastrointestinal cancers," *Journal of Clinical Oncology*, vol. 28, no. 26, pp. 4045–4051, 2010.

[34] K. P. Haley and J. A. Gaddy, "Nutrition and *Helicobacter pylori*: host diet and nutritional immunity influence bacterial virulence and disease outcome," *Gastroenterology research and practice*, vol. 2016, Article ID 3019362, 10 pages, 2016.

[35] K. Rudnicka, S. Backert, and M. Chmiela, "Genetic poly-morphisms in inflammatory and other regulators in gastric cancer: risks and clinical consequences," *Current Topics in Microbiology and Immunology*, vol. 421, pp. 53–76, 2019.

[36] Y. Lu and X. Zhang, "Radiochemotherapy-induced DNA repair promotes the biogenesis of gastric cancer stem cells," *Stem Cell Research & Therapy*, vol. 13, no. 1, p. 481, 2022.

[37] D. Zhang, S. Guo, and S. J. Schrodi, "Mechanisms of DNA methylation in virus-host interaction in hepatitis B infection: pathogenesis and oncogenetic properties," *International Journal of Molecular Sciences*, vol. 22, no. 18, p. 9858, 2021.

[38] C. Wang, L. Li, Q. Duan, Q. Wang, and J. Chen, "Krüppel-like factor 2 suppresses human gastric tumorigenesis through inhibiting PTEN/AKT signaling," *Oncotarget*, vol. 8, no. 59, pp. 100358–100370, 2017.

[39] X. Li, Z. Li, Z. Liu, J. Xiao, S. Yu, and Y. Song, "Long non-coding RNA DLEU1 predicts poor prognosis of gastric cancer and contributes to cell proliferation by epigenetically sup-pressing KLF2," *Cancer Gene Therapy*, vol. 25, no. 3-4, pp. 58–67, 2018.

[40] Q. Wang, Y. He, W. Kan et al., "microRNA-32-5p targets KLF2 to promote gastric cancer by activating PI3K/AKT signaling pathway," *American Journal of Tourism Research*, vol. 11, no. 8, pp. 4895–4908, 2019.

*Retraction*

# Retracted: Research on the Correlation of Peripheral Blood Inflammatory Markers with PCT, CRP, and PCIS in Infants with Community-Acquired Pneumonia

## Evidence-Based Complementary and Alternative Medicine

This article has been retracted by Hindawi following an investigation undertaken by the publisher [1]. This investigation has uncovered evidence of one or more of the following indicators of systematic manipulation of the publication process:

(1) Discrepancies in scope

(2) Discrepancies in the description of the research reported

(3) Discrepancies between the availability of data and the research described

(4) Inappropriate citations

(5) Incoherent, meaningless and/or irrelevant content included in the article

(6) Peer-review manipulation

The presence of these indicators undermines our confidence in the integrity of the article's content and we cannot, therefore, vouch for its reliability. Please note that this notice is intended solely to alert readers that the content of this article is unreliable. We have not investigated whether authors were aware of or involved in the systematic manipulation of the publication process.

Wiley and Hindawi regrets that the usual quality checks did not identify these issues before publication and have since put additional measures in place to safeguard research integrity.

We wish to credit our own Research Integrity and Research Publishing teams and anonymous and named external researchers and research integrity experts for contributing to this investigation.

The corresponding author, as the representative of all authors, has been given the opportunity to register their agreement or disagreement to this retraction. We have kept a record of any response received.

## References

[1] L. Li, H. Miao, X. Chen, S. Yang, and X. Yan, "Research on the Correlation of Peripheral Blood Inflammatory Markers with PCT, CRP, and PCIS in Infants with Community-Acquired Pneumonia," *Evidence-Based Complementary and Alternative Medicine*, vol. 2022, Article ID 9024969, 6 pages, 2022.

*Research Article*

# Research on the Correlation of Peripheral Blood Inflammatory Markers with PCT, CRP, and PCIS in Infants with Community-Acquired Pneumonia

**Linwei Li,[1] Hongyun Miao,[2] Xue Chen,[1] Shengjie Yang,[1] and Xiaoyong Yan [1]**

[1]*Department of Pediatrics, Jiangjin Hospital Affiliated to Chongqing University, No. 725, Jiangzhou Avenue, Dingshan Street, Jiangjin District, Chongqing, China*
[2]*Department of Endocrinology, Jiangjin Hospital Affiliated to Chongqing University, No. 725, Jiangzhou Avenue, Dingshan Street, Jiangjin District, Chongqing, China*

Correspondence should be addressed to Xiaoyong Yan; 100280@yzpc.edu.cn

*Aims.* This study aimsto investigate the relationship between peripheral blood neutrophil/lymphocyte ratio (NLR), platelet/lymphocyte ratio (PLR), systemic immune-inflammatory index (SII), and procalcitonin (PCT), C-reactive protein (CRP), and pediatric critical illness score (PCIS) in infants with community-acquired pneumonia (CAP). *Methods.* 100 infants with bacterial CAP admitted to our hospital between January 2021 and December 2021 were selected as the infected group, and another 100 healthy infants who underwent health check-ups at the same time were selected as the control group, and the NLR, PLR, and SII of peripheral blood of infants in both groups and the serum PCT, CRP, and PCIS scores of infants in the infected group were tested. The correlation between NLR, PLR, SII, and PCT, CRP, and PCIS was analyzed by Spearman's analysis. *Results.* The peripheral blood levels of NLR, PLR, and SII were higher in the infected group than in the control infants ($P < 0.05$). The ROC results showed that the AUCs of peripheral blood NLR, PLR, and SII for the diagnosis of infants with CAP were 0.934, 0.737, and 0.882, respectively. The ROC results showed that the AUCs of peripheral blood NLR, PLR, and SII for assessing the extent of disease in infants with CAP were 0.815, 0.710, and 0.813, respectively, with best cut-off values of 2.05, 98.57, and 823.41; the joint predicted AUC was 0.862. *Conclusions.* NLR, PLR, and SII were significantly elevated in the peripheral blood of infants with CAP, positively correlated with PCT and CRP, and negatively correlated with PSIC scores, and NLR and SII also have some guiding value in early diagnosis and assessment of the extent of the disease in infants and toddlers with CAP.

## 1. Introduction

Community-acquired pneumonia (CAP) remains the most common respiratory disease in children and the leading cause of death in children under five years of age. Due to their anatomical and immunological characteristics, infants are prone to respiratory infections, and their infections spread easily, and their upper respiratory tract infections are also prone to develop into pneumonia, even severe pneumonia [1, 2]. Many factors can cause pneumonia in infants, such as pathogenic infections, poor lung development, poor environment, and care, etc. Among them, pathogenic infections (bacteria, viruses, and so on.) are the most common

and can affect the growth and development of infants in severe cases [3].

Clinical studies have shown that the key to the treatment of CAP in infants lies in the early identification of the pathogen and the targeted adoption of reasonable anti-infection treatment, which can effectively improve clinical symptoms and prognosis and has important clinical significance [4]. In recent years, with the development of serological diagnostic markers, serum indicators such as procalcitonin (PCT) and C-reactive protein (CRP) have become more clinically accepted indicators to assess the status of infection, and their elevation can reflect the severity of the disease; the PCIS score is also the most objective,

widely used, and effective score in China, which can effectively reflect the criticality of the child's condition and has a good predictive effect on the risk of death [5]. However, the above indexes and scores are difficult to apply in primary hospitals due to the difficulties of venous blood collection from small infants, long laboratory time, and poor generalizability. In this study, peripheral blood inflammatory markers: neutrophil/lymphocyte ratio (NLR), platelet/lymphocyte ratio (PLR), and systemic immune inflammatory index (SII, platelets × neutrophils/lymphocytes) were used to explore their correlation with blood CRP, PCT, and pediatric critical illness score (PCIS). To explore a quick, easy, and cost-effective way to assess the condition of pneumonia in infants, and to provide data and results of the research, we report the following.

The purpose of this paper is to explore the relationship between the peripheral blood neutrophil/lymphocyte ratio (NLR), platelet/lymphocyte ratio (PLR), systemic immune inflammatory index (SII), procalcitonin (PCT), C-reactive protein (CRP) and children's critical case score (PCIS) in children with community-acquired pneumonia (CAP), and to provide reference results for solutions.

## 2. Information and Methods

*2.1. General Information.* A total of 100 infants with CAP who were admitted to our hospital between January 2021 and December 2021 were selected as the infected group, and another 100 healthy infants who were examined at the same time in our child health department were selected as the control group.

*2.1.1. Inclusion Criteria.* Infants in the study group were required to meet both (1) the diagnostic criteria of the "Diagnosis of CAP in children (2019 edition)" in all cases [6]; (2) age 29 d to 1 week of age, all full-term singleton fetuses; and (3) positive sputum bacterial culture results; infants in the control group were required to meet both (1) the health check-up infants in our pediatric clinic; and (2) age 29 d to 1 week of age, all full-term singleton fetuses.

*2.1.2. Exclusion Criteria.* For both groups of infants, exclusion was based on any of the following: history of resuscitation by asphyxia at birth, the combination of congenital heart disease; renal disease; trauma; diabetes; hypertension; Kawasaki disease or connective tissue disease; immunodeficiency disorders; identification of extrapulmonary bacterial infections; and airway malformations. The study was approved by the hospital ethics committee; informed consent was signed by the parents of both groups of infants before enrollment. There were 55 males and 45 females in the infected group, with a mean age of (7.82 ± 2.65) months); 47 males and 53 females in the control group, with a mean age of (8.27 ± 2.30) months. The differences in basic information such as gender and age of infants in the two groups were not statistically significant (*P* > 0.05) and were comparable.

*2.2. Methods*

*2.2.1. Routine Blood Test.* After the infants in both groups were enrolled, 5 mL of fasting venous blood was collected in the early morning, and a fully automated blood cell analyzer was applied to perform routine blood tests (neutrophil count, lymphocyte count, monocyte count, platelet count) and calculate NLR, PLR, and SII.

*2.2.2. Detection of Serum CRP and PCT Levels.* The infants in the infected group had 4 mL of venous blood collected, and the supernatant was collected after centrifugation at 3000 r/min for 10 min at room temperature for 30 min and stored at −20°C. The serum samples were sent to Goldfield Medical Testing Center for CRP and PCT level testing.

*2.2.3. Severity Scores.* The severity of the infant's disease was assessed by the PCIS score based on the child's vital signs, blood analysis, blood gas analysis, electrolytes, and renal function test results at the time of admission, combined with the child's digestive system symptoms and signs, in which a score of >80 indicates noncritical, 71–80 indicates critical, and ≤70 indicates very critically [7].

*2.3. Statistical Analysis.* Spearman correlation analysis is applicable to judge the correlation between two continuous variables with non-normal distribution (or with abnormal values that cannot be eliminated). When using Spearman correlation analysis, two conditions need to be met: variables are continuous variables with non-normal distribution (or with abnormal values that cannot be eliminated); and there is a monotonic relationship between variables. The IBM SPSS Statistics 22.0 statistical software was used for statistical analysis of the data, and measures that conformed to a normal distribution with homogeneous variance were expressed as mean ± standard deviation ($\overline{x} \pm s$), and independent samples *t*-test was used for comparison between groups, while measures of non-normally distributed data were expressed as [*M* (*Q_R*)] and Mann–Whitney *U* test was used for comparison between groups. Count data were expressed as cases or percentages, using the chi-square test; Spearman correlation analysis was used to analyze the correlation between NLR, PLR, and SII and PCT, CRP, and PCIS indicators; The efficacy of NLR, PLR, and SII in the diagnosis of CAP and assessment of the extent of the condition in infants was assessed using the receiver operating characteristic curve (ROC), with *P* < 0.05 indicating a statistically significant difference.

## 3. Results

*3.1. Comparison of NLR, PLR, and SII Levels in Peripheral Blood of Infants in Two Groups.* The peripheral blood levels of NLR, PLR, and SII were higher in the infected children than in the control infants (*P* < 0.05). See Table 1.

*3.2. Correlation Analysis of Peripheral Blood NLR, PLR, and SII Levels with PCT, CRP, and PCIS Scores in Infants of the*

Table 1: Comparison of peripheral blood NLR, PLR, and SII levels between two groups of infants [$M$ ($Q_R$)].

| Groups | Number of cases | NLR | PLR | SII |
|---|---|---|---|---|
| Infection group | 100 | 1.96 (1.71) | 98.91 (33.60) | 739.04 (898.79) |
| Control group | 100 | 0.32 (0.21) | 69.39 (34.05) | 119.34 (99.43) |
| $Z$ | | 10.609 | 5.796 | 9.341 |
| $P$ | | <0.001 | <0.001 | <0.001 |

*Infected Group.* The results showed that PCT, CRP, and PCIS were non-normally distributed in the infected group of children, with median and interquartile distances of 0.82 (1.06), 16.90 (20.8), and 100.00 (8.00), respectively. Spearman analysis showed that NLR, PLR, and SII were positively correlated with PCT and CRP (all $P < 0.05$), and PCIS scores were negatively correlated (all $P < 0.05$). See Table 2.

### 3.3. ROC Analysis of Infants with CAP Diagnosed by Peripheral Blood NLR, PLR, and SII.

The ROC results showed that the AUCs of peripheral blood NLR, PLR, and SII for the diagnosis of infants with CAP were 0.934, 0.737, and 0.882, respectively. The best cut-off values based on the Jorden index were 0.54, 84.96, and 188.35, respectively. The sensitivity and specificity based on the best cut-off values were 91.00%, 84.00%, and 68.00%, and 74.00%, 86.00%, and 79.00%. See Figure 1, Table 3.

### 3.4. Comparison of Peripheral Blood Levels of NLR, PLR, and SII in Infants with Different Severity.

According to the PCIS score, 12 children with scores below 80 were in the severe group and the rest were in the mild group. The blood NLR, PLR, and SII levels of children in the mild group were lower than those in the severe group ($P < 0.05$). See Table 4.

The ROC results showed that the AUCs of peripheral blood NLR, PLR, and SII for predicting the extent of disease in infants with CAP were 0.815, 0.710, and 0.813, respectively. The sensitivity and specificity based on the best cut-off values were 91.67%, 62.50%, and 91.67%, 51.95%, 91.67%, and 64.77%. Based on the coefficients obtained from logistic regression to establish the joint detection index, the AUC of the joint detection was 0.862, and the sensitivity and specificity were 100% and 69.32%, respectively, which were higher than the prediction alone. See Table 5, Figure 2.

## 4. Discussion

Pneumonia is the leading cause of death in children under 5 years old in China, the vast majority of whom are CAP, and bacterial infection is the leading cause of CAP [7]. Once an infection occurs in infants and young children under 2 years old, it can easily develop into bronchitis or bronchopneumonia, or even severe pneumonia, posing a serious threat to the health of infants and toddlers [8]. The main clinical difficulties are the differentiation from noninfectious diseases and the clarification of the pathogenic diagnosis of infants who have failed empirical treatment. Although the sputum smear technique is faster, it requires high sputum samples, and even after the initial identification of pathogenic species, a further sputum culture is still needed to

Table 2: Correlation analysis of peripheral blood NLR, PLR, and SII levels with PCT, CRP, and PCIS scores.

| | NLR | | PLR | | SII | |
|---|---|---|---|---|---|---|
| | $r$ | $P$ | $r$ | $P$ | $r$ | $P$ |
| PCT (ng/mL) | 0.798 | <0.001 | 0.488 | <0.001 | 0.788 | <0.001 |
| CRP (mg/L) | 0.760 | <0.001 | 0.493 | <0.001 | 0.763 | <0.001 |
| PCIS (scores) | −0.568 | <0.001 | −0.348 | <0.001 | −0.595 | <0.001 |
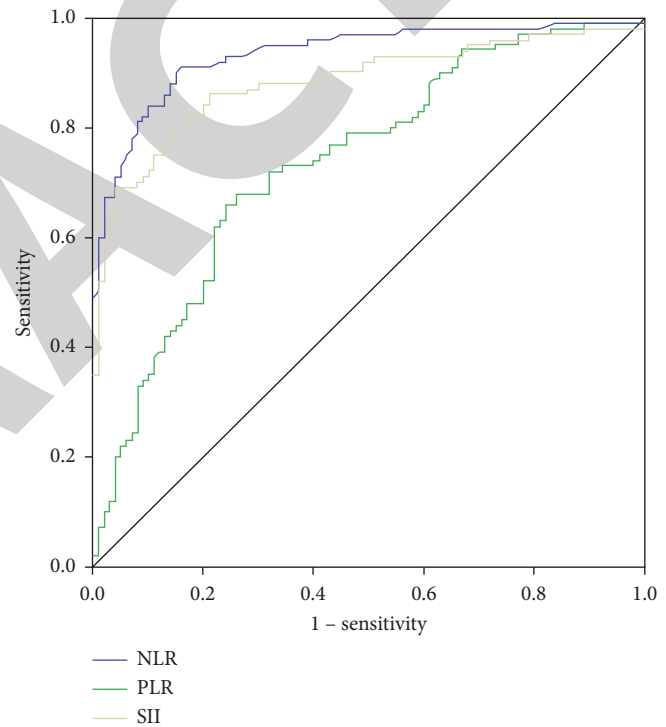


Figure 1: ROC curves of peripheral blood NLR, PLR, and SII for the diagnosis of infants with CAP.

clarify the pathogenic bacteria, while blood culture is only applicable to bacterial lung infections with bacteremia, and its clinical use is more limited, so it is clinically important to find some laboratory indicators for early diagnosis, disease assessment, and prognosis of bacterial pneumonia in infants.

The indicators currently included in the guidelines for CAP evaluation are leukocyte-to-neutrophil ratio, CRP, and PCT, but the sensitivity and specificity of these indicators for clinical application are still unsatisfactory [9]. Cellular immune dysfunction and disorders are the most studied pathogenesis of CAP in addition to the direct pathogen invasion theory [10]. Leukocytes and their subtypes (monocytes, lymphocytes, and macrophages), as important

Table 3: Efficacy of peripheral blood NLR, PLR, and SII in the diagnosis of infants with CAP.

| Index | AUC | Best cut-off values | 95% CI confidence interval | Sensitivity (%) | Specificity (%) |
|---|---|---|---|---|---|
| NLR | 0.934 | 0.54 | 0.890~0.964 | 91.00 | 84.00 |
| PLR | 0.737 | 84.96 | 0.670~0.797 | 68.00 | 74.00 |
| SII | 0.882 | 188.35 | 0.829~0.923 | 86.00 | 79.00 |

Table 4: Comparison of peripheral blood levels of NLR, PLR, and SII in infants with different severity $[M (Q_R)]$.

| Groups | Number of cases | NLR | PLR | SII |
|---|---|---|---|---|
| Severe group | 12 | 2.84 (1.60) | 126.76 (42.93) | 1249.78 (497.10) |
| Mild group | 88 | 1.72 (1.57) | 95.11 (30.50) | 624.43 (824.80) |
| Z | | 3.538 | 2.355 | 3.500 |
| P | | <0.001 | <0.05 | <0.001 |

2.5 ROC analysis of peripheral blood NLR, PLR, and SII to assess the extent of disease in infants with CAP.

Table 5: Efficacy of peripheral blood NLR, PLR, and SII in diagnosing the extent of disease in infants with CAP.

| Index | AUC | Best cut-off values | 95% CI confidence interval | Sensitivity (%) | Specificity (%) |
|---|---|---|---|---|---|
| NLR | 0.815 | 2.05 | 0.708~0.923 | 91.67 | 62.50 |
| PLR | 0.710 | 98.57 | 0.583~0.837 | 91.67 | 51.95 |
| SII | 0.813 | 823.41 | 0.715~0.910 | 91.67 | 64.77 |
| Joint forecast | 0.862 | | 0.782~0.942 | 100 | 69.32 |
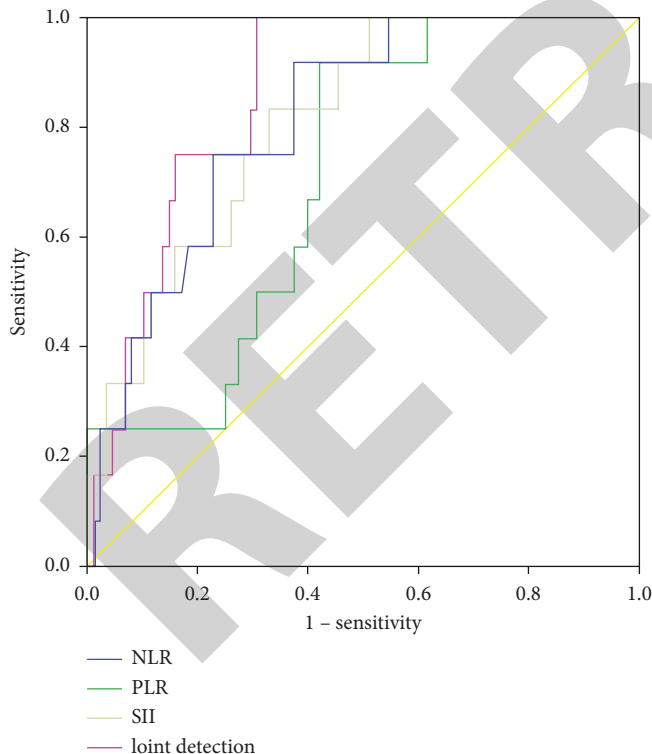


Figure 2: ROC curves of peripheral blood NLR, PLR, SII, and joint prediction of the extent of disease in infants with CAP.

immune cells involved in immune regulation, can cause changes in the level of relevant immune cells in the body when bacteria enter the body, and NLR, PLR, SII, and so on are important indicators reflecting the inflammatory response in the body obtained based on the level of immune cells [11–13]. In this study, 100 infants under 1 year of age diagnosed with bacterial CAP were selected as the infected group, and 100 healthy infants were selected as the control group during the same period. The levels of NLR, PLR, and SII in the peripheral blood of the two groups were compared, and it was found that the levels of NLR, PLR, and SII in the peripheral blood of the infected infants were significantly higher than those of the control infants. As an important indicator of the inflammatory response and immune homeostasis, the level of NLR in the peripheral blood of infants with bacterial CAP was significantly higher, which was consistent with the findings of Jiang et al. [14]; altered coagulation also plays an important role in the inflammatory response, but the body releases a variety of cytokines after infection, which activate the coagulation system and inhibits the fibrinolytic system. The PLR, as a ratio of platelet to lymphocyte levels, has higher stability compared to the two alone, and thus, PLR levels were significantly higher, in line with the findings of Lu and Zhu [15]; SII is an index that comprehensively reflects the inflammatory and immune homeostasis status of the body, calculated by platelet count, neutrophil, and lymphocyte levels, and the activation of immune function and inflammatory response caused by pathogen invasion can cause a significant increase in SII levels, in agreement with the findings of Acar et al. [16].

To further investigate the clinical application value of NLR, PLR, and SII, this study compared the correlation of NLR, PLR, and SII with the traditional inflammatory indexes CRP and PCT and the PCIS score, which reflects the degree of pediatric disease, using the Spearman's

correlation analysis. The results showed that NLR, PLR, and SII were positively correlated with CRP and PCT, and the correlation coefficients of NLR and SII were close to 0.8, suggesting that these three may have a high diagnostic value. The results of ROC analysis showed that the AUCs of NLR, PLR, and SII in the diagnosis of infants with bacterial CAP were 0.934, 0.737, and 0.882, respectively, indicating that both NLR and SII have high diagnostic value and are worthy of clinical reference. The PCIS score is an evaluation system used to reflect the systemic organ status of infants with pneumonia that is unique to our country [17]. The results of the present study showed that NLR, PLR, and SII were negatively correlated with PCIS scores, indicating that high levels of NLR, PLR, and SII may be related to the severity of disease and prognosis of an infant with CAP. By comparing the peripheral blood NLR, PLR, and SII levels of children in the severe and mild disease groups, we found that the NLR, PLR, and SII levels of children in the severe disease group were significantly higher than those in the mild disease group. The AUCs of NLR, PLR, and SII in the assessment of the severity of bacterial CAP children were found to be 0.815, 0.710, and 0.813, respectively, by ROC analysis. It indicated that NLR, PLR, and SII can differentiate the severity of CAP children, which is conducive to the timely adoption of appropriate therapeutic measures to improve the treatment effect, and the joint prediction of the three indicators is better.

## 5. Conclusions

NLR, PLR, and SII are significantly elevated in the peripheral blood of infants with CAP. As simple and easily accessible indicators for clinical work, these indicators help in the initial diagnosis and assessment of the condition of children with CAP, provide early warning information, guide active and effective clinical interventions, and play a positive role in avoiding the development of severe disease and reducing the death rate of infants and children. However, this study is a single-center, small-sample study limited to bacterial CAP, and its value in other pathogenic infection types of pneumonia requires a multicenter, larger sample randomized controlled study to further confirm the clinical credit value of the indicators in this study.

## Data Availability

The experimental data used to support the findings of this study are available from the corresponding author upon request.

## Conflicts of Interest

The authors declare that they have no conflicts of interest regarding this work.

## Authors' Contributions

Linwei Li and Hongyun Miao contributed equally to this work.

## References

[1] R. Izadnegahdar, A. L. Cohen, K. P. Klugman, and S. A. Qazi, "Childhood pneumonia in developing countries," *The Lancet Respiratory Medicine*, vol. 1, no. 7, pp. 574–584, 2013.

[2] J. T. Lai, X. X. Li, and F. Zheng, "Diagnostic value of chemiluminescence combined with quantitative PCR for cytomegalovirus infection combined with pneumonia in infants and children," *Guangdong Medical Journal*, vol. 40, no. 14, pp. 2104–2107, 2019.

[3] X. Xie, X. Pan, W. Zhang, and J. An, "A context hierarchical integrated network for medical image segmentation," *Computers and Electrical Engineering*, vol. 101, Article ID 108029, 2022.

[4] F. X. Ding, B. Liu, and X. H. Xie, "Analysis of the relationship between bacterial infections of the lower respiratory tract and persistent wheezing in infants and infants and the efficacy of antibiotics," *Chinese Journal of Practical Pediatrics*, vol. 31, no. 12, pp. 941–945, 2016.

[5] R. D. Ding and H. J. Zhang, "Effect of linezolid on serum PCT, ESR, and CRP in patients with pulmonary tuberculosis and pneumonia," *Medicine (Baltimore)*, vol. 97, no. 37, Article ID e12177, 2018.

[6] National Health Commission of the People's Republic of China State Administration of Traditional Chinese Medicine, "Guidelines for the management of community-acquired pneumonia in children," *Chinese Journal of Clinical Infectious Diseases*, vol. 12, pp. 6–13, 2019.

[7] X. Xie, X. Pan, F. Shao, W. Zhang, and J. An, "Mci-net: Multiscale context integrated network for liver ct image segmentation," *Computers and Electrical Engineering*, vol. 101, Article ID 108085, 2022.

[8] Y. W. Long, Y. F. Chen, and Y. Luo, "Pathogenetic characteristics and drug resistance analysis of 748 cases of severe community-acquired pneumonia in children in Chongqing," *Laboratory Medicine and Clinic*, vol. 18, no. 2, pp. 189–193, 2021.

[9] X. Xie, W. Zhang, H. Wang et al., "Dynamic adaptive residual network for liver CT image segmentation," *Computers and Electrical Engineering*, vol. 91, Article ID 107024, 2021.

[10] J. Zhu and W. W. Zhang, "Changes and significance of ultrasensitive C-reactive protein calcitoninogen and cellular immune indexes in peripheral blood of children with pneumonia," *Chinese Journal of Laboratory Diagnosis*, vol. 23, no. 10, pp. 1751–1753, 2019.

[11] Z. Huang, Z. Fu, W. Huang, and K. Huang, "Prognostic value of neutrophil-to-lymphocyte ratio in sepsis: A meta-analysis," *The American Journal of Emergency Medicine*, vol. 38, no. 3, pp. 641–647, 2020.

[12] J. Wang, F. Zhang, F. Jiang, L. Hu, J. Chen, and Y Wang, "Distribution and reference interval establishment of neutral-to-lymphocyte ratio (NLR), lymphocyte-to-monocyte ratio (LMR), and platelet-to-lymphocyte ratio (PLR) in Chinese healthy adults," *Journal of Clinical Laboratory Analysis*, vol. 35, no. 9, Article ID e23935, 2021.

[13] R. F. Chen, X. Y. Zhou, and G. F. He, "Clinical application value of neutrophil/lymphocyte ratio in evaluating the

*Research Article*

# Simvastatin Inhibits Endometrial Cancer Malignant Behaviors by Suppressing RAS/Mitogen-Activated Protein Kinase (MAPK) Pathway-Mediated Reactive Oxygen Species (ROS) and Ferroptosis

**Dan Zhou, Qiuhua Wu, Huajuan Qiu, Mi Li, and Yanqin Ji** [ID]

*Department of Gynaecology, Huizhou Central People's Hospital, Huizhou, Guangdong 516008, China*

Correspondence should be addressed to Yanqin Ji; yanqinjihzch@163.com

This paper was designed to explore the function of simvastatin as a chemotherapeutic drug on the endometrial cancer (EC) cell proliferation, invasion, and ferroptosis. Firstly, a number of *in vitro* experiments were conducted to determine the impact of different treatments of simvastatin on the Ishikawa cell invasion, proliferation, and colony formation. The concentration of DCFH-DA-labeled reactive oxygen species (ROS) in cells was assessed by flow cytometry. Enzyme-linked immunosorbent assay (ELISA) was performed to examine the intracellular contents of $Fe^{2+}$, malondialdehyde (MDA), and glutathione (GSH). Additionally, Western blot was utilized to measure the expression level of RAS/mitogen-activated protein kinase (MAPK)-related proteins and ferroptosis-related proteins in cells. The results showed that simvastatin at $10\,\mu M$ and $15\,\mu M$ apparently suppressed the proliferation of Ishikawa cells, colony formation, and invasion ability of Ishikawa cells, and upregulated the level of MDA and ROS, but downregulated the level of GSH. Besides, $10\,\mu M$ and $15\,\mu M$ of simvastatin promoted cell ferroptosis (up-regulation of $Fe^{2+}$ and TRF 1 protein level; down-regulation of SLC7A11 and FPN protein level) and lowered the RAS, p-MEK, and ERK protein level. Furthermore, experiments also revealed that the inhibitory effects of simvastatin on Ishikawa cell proliferation, colony formation, and invasion, as well as the promoting effects on oxidation and ferroptosis were reversed. All in all, simvastatin reduces the RAS/MAPK signaling pathway to inhibit Ishikawa cell proliferation, colony formation, and invasion, and promote cell oxidation and ferroptosis. This paper demonstrates the potential of simvastatin as a new anticancer drug for EC.

## 1. Introduction

As one of the three most prevalent malignancies of the female reproductive system, endometrial cancer (EC) is also the sixth most common malignant tumor in women. Recent years have witnessed the rapidly increased incidence of EC due to declined birth rate, climbed aging population, changed lifestyle changes, and other factors [1, 2]. In 2018, 382,000 new cases and 89,000 deaths were reported globally, with 12% of new cases reported in China [2]. Approximately one-fifth of EC cases are characterized by high risk and poor prognosis, for instance, the 5-year overall survival rate is less than 20% in EC patients with distant metastasis [3, 4]. The effectiveness of total hysterectomy for EC is unsatisfactory [5], and new therapies are needed to further improve the survival rate of patients.

Ferroptosis is known as a regulated type of iron-dependent cell death as a result of a buildup of lipid-based reactive oxygen species (ROS). As a recently identified type of regulated cell death, ferroptosis has new biological targets and pathophysiology features [6]. ROS buildup serves as one of the characteristics of ferroptosis. During ferroptosis, transferrin receptor 1 (TRF1) expression and ferritin degradation are both significantly regulated by ROS-induced autophagy. Some research studies have revealed that ferroptosis is linked to various diseases, such as ischemic organ damage, neuro-degeneration, liver and pulmonary fibrosis, autoimmune diseases, mycobacterium tuberculosis-induced tissue necrosis, smoking-related chronic obstructive pulmonary disease, and cancers [7, 8]. The female reproductive system has a special relationship with iron; iron disorders and iron-mediated cell deaths are

closely associated with a variety of endometrium-related diseases including endometrial hyperplasia, recurrent implantation failure, and endometriosis [9]. The research on ferroptosis in EC is, however, scant. Wang et al. stated that the down-regulation of PTPN18 could significantly stimulate the production of ROS and inhibit EC cell proliferation, and through the p-p38/GPX4/xCT axis, PTPN18 could induce ferroptosis [10]. Bioinformatics analysis by Yin et al. revealed that multiple ferroptosis-related genes could serve as predictors for the prognosis of EC patients [11].

Statins, as 3-hydroxy-3-methylglutaryl coenzyme A (HMG-CoA) reductase inhibitors, by lowering the level of low-density lipoprotein cholesterol (LDL-C), are commonly adopted to improve the morbidity and mortality of cardiovascular patients [12]. In addition, statins have anticancer effects, and their anticancer effects are associated with the regulation of growth factor receptors and cholesterol-dependent signaling in tumor cells [13]. Specifically, statins can suppress HMG-CoA reductase, deplete mevalonic acid and its downstream products, and ultimately induce tumor cell apoptosis [14]. Compared with the other statins, simvastatin shows the best lipophilicity and therapeutic effect [15]. Simvastatin can enter cells through the organic anion transporter (OATP1B1) to interrupt mevalonate pathway and inhibit LDL-C production [16]. In vitro experiments confirmed that simvastatin affected the migration, proliferation, and survival of various cancer cells [17]. Simvastatin has been shown in numerous in vitro experiments to slow the spread of cancer and lower mortality in individuals with pancreatic, stomach, breast, and lung cancers. [18].

The effects of simvastatin on the progression of EC remain unclear. Therefore, we investigated the molecular mechanism of simvastatin on Ishikawa cells and the effect of treating Ishikawa cells with RAS activator (ML-098) by in vitro experiments. The results showed that simvastatin exerted therapeutic effects on EC by reducing RAS/MAPK signaling pathway activity, suppressing the invasion, clone formation and proliferation of Ishikawa cells, and promoting cell oxidation and ferroptosis. Therefore, we hypothesized that simvastatin is a promising drug option for the therapy of EC. Our experiments confirmed this hypothesis.

## 2. Materials and Methods

*2.1. Cell Culture and Treatment.* EC cells (Ishikawa) were grown in a high-glucose DMEM medium that contained 10% fetal bovine serum (FBS) and 1% penicillin-streptomycin. And the medium was placed in an incubator with 5% of $CO_2$ at 37°C. Subsequently, Ishikawa cells were treated with simvastatin (5 $\mu$M, 10 $\mu$M, and 15 $\mu$M) for 72 h [19], or with simvastatin + RAS agonist (0.5 $\mu$M) for 72 h [20]; the cultured cells without treatment acted as a control.

*2.2. MTT Assay.* As previously mentioned, the MTT assay was carried out [9]. In brief, trypsin (Beyotime, China) was adopted to digest the cells in the logarithmic phase for the preparation of cell suspension. Then, a 96-well plate was introduced with 100 $\mu$L cell suspension at 3000 cells per well and then placed in an incubator at 37°C for cell adhesion. Subsequently, cells were then treated with different reagents for 72 hours following the experiment requirements. According to the MTT kit (Beyotime, China) instructions, the proliferation of cells before and after treatment was tested, respectively. To be specific, 10 $\mu$L (5 mg/ml) of cell suspensions was supplemented to the plate and incubated for 4 hours at 37°C. After adding 100 $\mu$L of Formazan dissolving solution, the incubation was continued until the precipitate was fully dissolved. Finally, we use a microplate reader (Thermo Fisher Scientific, Waltham, USA) to detect the absorbance value at 570 nm and calculate the cell viability, and we carried out the experiment three times independently.

*2.3. Colony Formation Assay.* The logarithmic growth expectation cells were trypsin digested and suspended in a DMEM medium containing 10% FBS. After cell counting, a six-well plate was inoculated with $1 \times 10^3$ cells per well and cultured in a cell incubator for 10–15 days. Before being stained with 0.5% crystal violet (sigma Aldrich, USA), they were fixed with 4% paraformaldehyde once the cells grew into clones visible to the naked eye. Under a microscope (Bethesda, MD, USA), colonies were counted and photographed. Each group is provided with 3 multiple holes.

*2.4. Transwell Assay.* A 24-well insert transwell assay and a Matrigel invasion assay (8.0 $\mu$m, Corning, NY, USA) were performed to investigate in vitro cell invasion. Transwell assay was conducted as directed by the manufacturer and as previously described [10]. Briefly stated, Matrigel (50 mg/L, BD, USA) was diluted in the ratio of 1 : 15 before being applied to the upper membrane surface in an amount of 100 L. Subsequently, Matrigel was solidified after 3 h of incubation at 37°C. After being digested and resuspended in a serum-free medium, the cells in the logarithmic phase were adjusted to have a concentration of $5 \times 10^5$ cells per milliliter. Then, the upper chamber in a 24-well Transwell plate was supplied with 100 $\mu$L suspension and the lower chamber with 600 $\mu$L of the 20% serum culture solution. For each well, three replicates were created. Incubation of the transwell inserts took place for 20 hours at a steady 37°C and 5% of $CO_2$ in an incubator. After that, the matrix and noninvasive cells were removed from the upper membrane surface using a cotton swab. Subsequently, 4% paraformaldehyde was utilized for fixture of the invasive cells and 0.5% of crystal violet solution (Sigma-Aldrich, USA) for cell staining. The cells were examined under a microscope after washing and drying and the images were collected.

*2.5. Determination of Reactive Oxygen Species.* ROS assay was conducted as instructed by the manufacturer. In brief, the cells were evenly inoculated into a 6-well plate at $1 \times 10^5$ cells/well, and different reagents were utilized to treat cells for 24 hours according to the experiment requirements. Then, 0.25% of trypsin without ethylenediaminetetraacetic acid (EDTA) was utilized to digest the treated cells. On completion of digestion, the cells were centrifuged and collected. After washing with PBS three times, $10 \mu M$ of dichloro-dihydro-fluorescein diacetate (DCFH-DA) was applied to the cells for incubation at 37°C following three rounds of PBS washing. After 20 min, the cells were resuspended in 500 l of PBS after being washed with serum-free media three times. Cell fluorescence was detected using flow cytometry at wavelengths of 525 nm for excitation and 485 nm for emission. With the results of three replicate wells, the average value was obtained and the specific formula was shown as follows: ROS = fluorescence intensity/(protein concentration × 0.19).

*2.6. Biochemical Kit-Based Assay.* Cells were lysed with RIPA lysis solution (Solarbio, China) on ice after being washed thrice with PBS. Following lysis, the cells were collected into EP tubes. The supernatant was collected for detection after centrifugation at 4°C and 12000 r/min for 30 min. According to the biochemical assay kit (Nanjing Jiancheng Bioengineering Institute, China), $Fe^{2+}$, glutathione (GSH), and malondialdehyde (MDA) levels in the cells were determined. Three independent replications of each experiment were performed.

*2.7. Western Blot.* With the help of RIPA lysis buffer (Solabio, China), the total protein was extracted from cells and tissues. The concentration of the extracted protein was determined with BCA kit (Beyotime, China), and $20 \mu g$ of protein was added to 5× loading buffer to boil for denaturation and denatured using SDS. By using 10% PAGE to separate the proteins, the resulting proteins were transferred to PVDF membranes by membrane transfer. The membranes were prepared by blocking them with 5% nonfat dry milk or 8% BSA (phosphorylated protein) for 2~3 h, and then mixed with the primary antibody anti-SLC7A11-antibody (1 : 1000, ab175186, Abcam), anti-TRF1-antibody (1 : 1000, ab129177, Abcam), anti-FPN-antibody (1 : 1000, ab235166, Abcam), anti-RAS-antibody (1 : 1000, ab235166, Abcam) 1000, ab52939, Abcam), anti-MEK-antibody (1 : 1000, ab32091, Abcam), anti-p-MEK-antibody (1 : 1000, Abcam-ab96379) anti-ERK-antibody (1 : 10000, M5670, Sigma), anti-pERK-antibody (Thr202/Tyr204) (1 : 1000, 9101S, Cell Signaling), and anti-$\beta$-actin-antibody (1 : 5000, ab8226, Abcam) were incubated overnight at 4°C. After three TBST washes the next day, the membrane was incubated with secondary antibodies, including goat antimouse IgG (1 : 5000, ab6789, Abcam), goat antirat IgG (1 : 5000, ab97057, Abcam) at ambient temperature, and goat antirabbit IgG (1 : 5000, ab6721, Abcam) for 2 h. ECL chemiluminescence reagent (Solebo, China) was used to display the protein bands, and Image J software to analyze the gray levels of the protein bands. Additionally, the relative protein expression was determined taking $\beta$-actin as an internal reference.

*2.8. Statistical Analysis.* With the use of SPSS 26.0, statistical analysis was carried out on all data results, which were presented as means with standard deviations (SD). One-way analysis of variance (ANOVA) was employed to determine the significant differences, followed by Dunnett's tests for multiple comparisons or unpaired Student's $t$-tests for two-group comparisons. $P < 0.05$ was deemed significantly different.

# 3. Results

This study sought to dig out the potential use of simvastatin as a chemotherapeutic drug. We hypothesized that simvastatin inhibits Ishikawa cell proliferation, colony formation, and invasion, and promotes cell oxidation and ferroptosis. Therefore, we performed Transwell assays, colony formation, and MTT to detect the effects of different treatments of simvastatin on the invasion, colony formation, and proliferation ability of Ishikawa cells, respectively. Flow cytometry was used to detect intracellular ROS levels; and enzyme linked immunosorbent assay (ELISA) to test intracellular $Fe^{2+}$, MDA, and GSH levels. In addition, the expression level of RAS/mitogen-activated protein kinase (MAPK)-related proteins and ferroptosis-related proteins were detected using Western blot. Our results suggested that simvastatin decreased RAS/MAPK signaling pathway activity and inhibited Ishikawa cell proliferation, colony formation, and invasion, and promoted cellular oxidation and iron ferroptosis. Collectedly, simvastatin has the potential to be a new anticancer drug for EC.

*3.1. Simvastatin Inhibits the Invasion, Colony Formation, and Proliferation of Ishikawa Cells.* To identify the effects of simvastatin on the invasion, proliferation, and other phenotypes of Ishikawa cells, colony formation, MTT, and transwell assays were performed. Relative to the control group, simvastatin treatment could lower the proliferation rate (Figure 1(a)), colony formation (Figures 1(b) and 1(c)), and invasion ability (Figures 1(d) and 1(e)) of Ishikawa cells. The inhibitory effect of simvastatin was dose-dependent; $10 \mu M$ and $15 \mu M$ groups exhibited more significant inhibitory effect. The above suggested that simvastatin could suppress the invasion, colony formation, and proliferation of Ishikawa cells.

*3.2. Simvastatin Increases the Oxidation Level of Ishikawa Cells.* To observe whether simvastatin affected the oxidation level of Ishikawa cells, flow cytometry and ELISA were utilized to analyze ROS, MDA, and GSH levels in Ishikawa cells receiving different concentrations of simvastatin ($5 \mu M$, $10 \mu M$, and $15 \mu M$). The outcome revealed that both $10 \mu M$
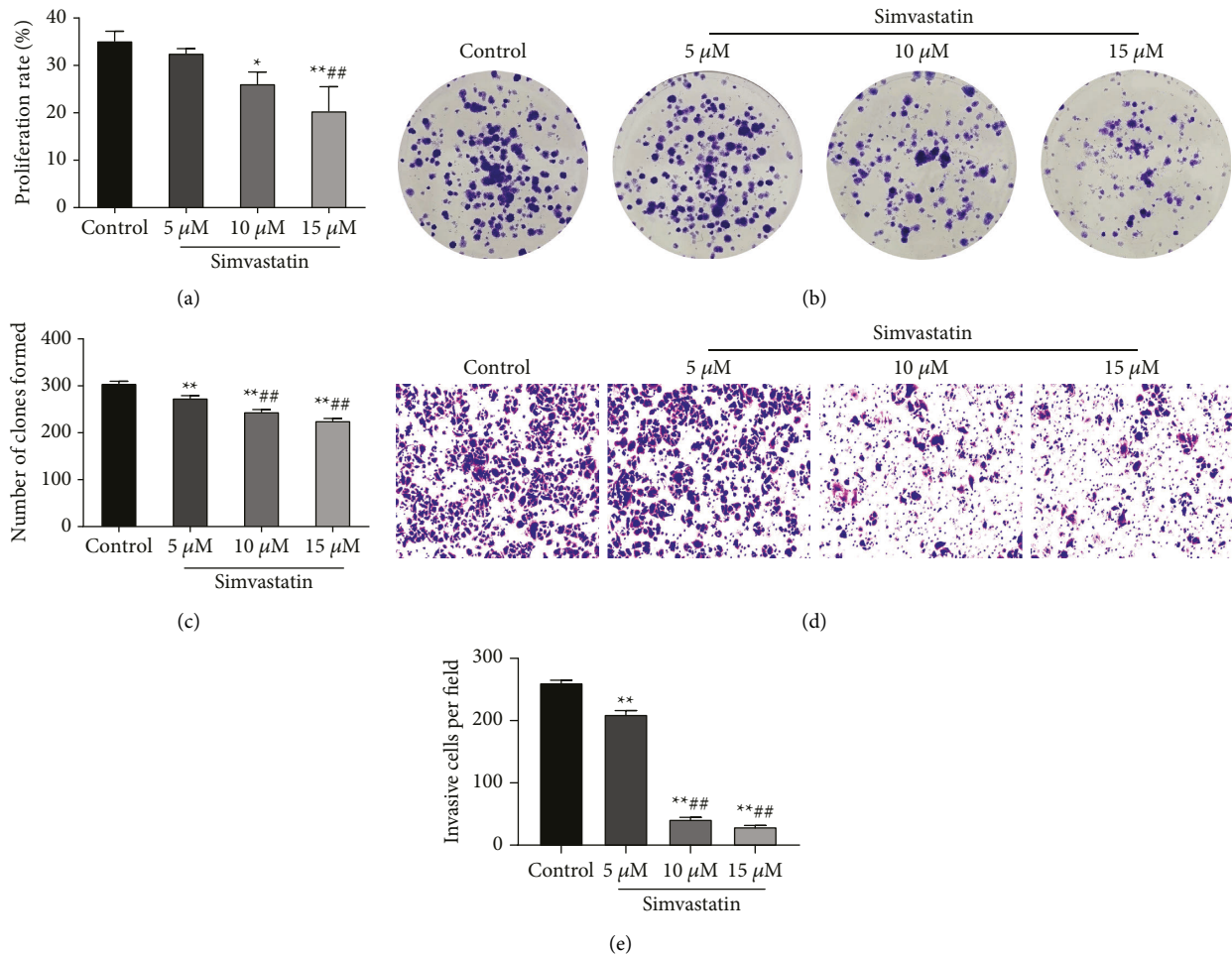
(a)



(b)



(c)



(d)



(e)

Figure 1: Simvastatin inhibits the proliferation, colony formation, and invasion of Ishikawa cells. (a): MTT to detect the proliferation of Ishikawa cells treated with simvastatin in different concentrations; (b–c): colony formation assay to measure the clone formation of Ishikawa cells treated with simvastatin in different concentrations; (d–e): transwell to detect the invasion of Ishikawa cells treated with simvastatin in different concentrations, $^*P < 0.01$ and $^{**}P < 0.01$ vs. control group; $^{##}P < 0.01$ vs. $5\,\mu M$ group.

and $15\,\mu M$ of simvastatin could increase the ROS level (Figures 2(a) and 2(b)) and MDA level (Figure 2(c)) ($P < 0.01$), but only the latter remarkably decreased the GSH level (Figure 2(d), $P < 0.01$). Additionally, although $5\,\mu M$ of simvastatin could also increase the level of ROS, MDA, and GSH in cells, no significant differences were observed compared with the control group. The above suggested that simvastatin with high concentration could significantly increase the oxidation level of Ishikawa cells.

3.3. Simvastatin Promotes Ferroptosis in Ishikawa Cells. An association between increased ROS levels and cellular ferroptosis has been reported in the literature [21]. Cystine/glutamate antiporter SLC7A11/xCT and ferroportin (FPN) serve as negative regulators of ferroptosis, while TRF1 protein acts as a positive regulator [22]. To clarify whether simvastatin caused ferroptosis in Ishikawa cells, we determined the Fe$^{2+}$ and ferroptosis-related proteins (SLC7A11, TRF 1 and FPN) levels in cells receiving different concentrations of simvastatin. Western blot results displayed that in contrast to the control group, simvastatin

could obviously decrease the SLC7A11 and FPN protein expression levels in Ishikawa cells ($P < 0.01$) and increase dose-dependently TRF1 expression ($P < 0.01$) (Figures 3(a)–3(d)). In addition, after treatment with $10\,\mu M$ and $15\,\mu M$ of simvastatin, a remarkably dose-dependently increase was observed in the level of Fe$^{2+}$ in cells (Figure 3(e)); while $5\,\mu M$ of simvastatin had no significant effect on Fe$^{2+}$ level. The above outcomes indicated that simvastatin could promote the ferroptosis in Ishikawa cells.

3.4. Simvastatin Inhibits the RAS/MAPK Signaling Pathway in Ishikawa Cells. The RAS/MAPK signaling pathway is responsible for the regulation of cancer initiation and progression, including cell proliferation, differentiation, and survival in a variety of solid and hematological cancers. The overexpression and overactivation of the members of Ras/MAPK cascade have been observed in tumors [23]. For investigating the function of the RAS/MAPK pathway in the Ishikawa cell growth and invasion, related proteins of this pathway (RAS, p-ERK, p-MEK, MEK, and ERK) were detected using Western blot. The results revealed that,
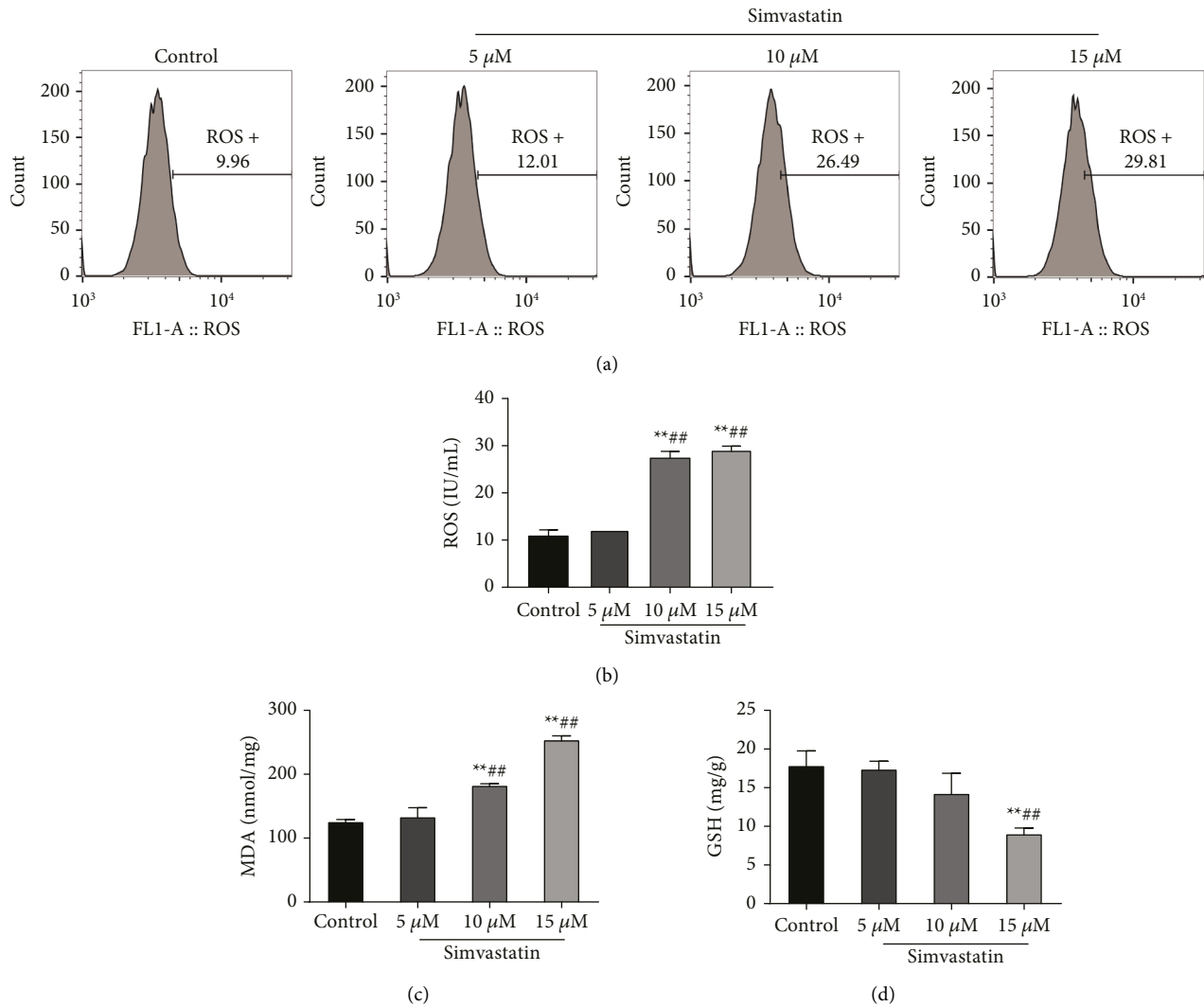
(a)



(b)



(c)



(d)

FIGURE 2: Simvastatin increases the oxidation level of Ishikawa cells. (a–b): flow cytometry to detect ROS level in Ishikawa cells treated with simvastatin in different concentrations; (c–d): ELISA to detect MDA (c) and GSH (d) levels in Ishikawa cells treated with simvastatin in different concentrations, $**P < 0.01$ vs. control group; $^{\#\#}P < 0.01$ vs. $5\,\mu$M group. ROS, reactive oxygen species; MDA, malondialdehyde; GSH, glutathione.

simvastatin treatment ($10\,\mu$M and $15\,\mu$M) significantly re-duced the RAS, p-MEK, and p-ERK levels, and the ratios of p-MEK/MEK and p-ERK/ERK in a dose-dependent manner (Figures 4(a)–4(d)). Therefore, simvastatin may inhibit the Ishikawa cell proliferation and invasion through the RAS/MAPK signaling pathway.

### 3.5. RAS Agonist Reverses the Inhibitory Effects of Simvastatin on Ishikawa Cell Invasion, Colony Formation, and Proliferation.

To further clarify whether simvastatin exerted its inhibitory effect on the Ishikawa cell growth by inhibiting the RAS/MAPK signaling pathway, the invasion, colony formation, and proliferation ability of the cells were detected after treatment with RAS agonist (ML-098) and $15\,\mu$M of simvastatin simultaneously. The above malignant behaviors of the cells were significantly promoted in the simvastatin + ML-098 group relative to the simvastatin

group (Figures 5(a)–5(e)). Taken together, simvastatin's inhibitory effect on Ishikawa cell invasion, colony formation, and proliferation may be reversed by ML-098 when used in combination.

### 3.6. ML-098 Reverses the Promoting Effects of Simvastatin on Oxidation and Ferroptosis in Ishikawa Cells.

Further, we researched the effects of simultaneous ML-098 and sim-vastatin treatment on oxidative substances (ROS, GSH, and MDA), $Fe^{2+}$ and ferroptosis-related proteins (SLC7A11, TRF 1, and FPN) levels in Ishikawa cells. The investigation results indicated that in contrast to the simvastatin group, the ROS, MDA, and $Fe^{2+}$ levels in cells of simvastatin + ML-098 group were decreased, while GSH level was remarkably increased ($P < 0.01$, Figures 6(a)–6(e)). In addition, Western blot results suggested that the SLC7A11 and FPN protein levels in the cells of simvastatin + ML-098 group were
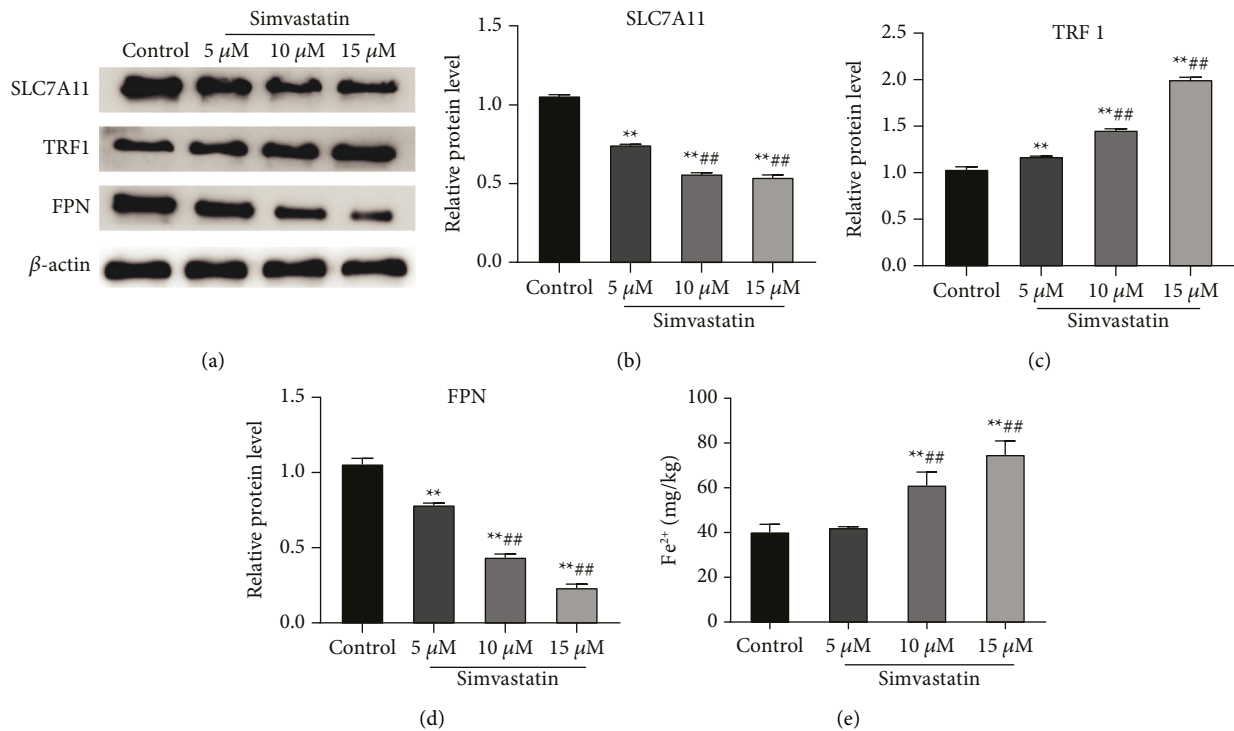
Figure 3: Simvastatin promotes ferroptosis in Ishikawa cells. (a–d): Western blot for detection of the effect of simvastatin on the expression of ferroptosis-related proteins (SLC7A11, FPN, and TRF 1) (a) and quantitative analysis based on Image J (b–d); (e): ELISA for detection the effect of simvastatin on $Fe^{2+}$ level in Ishikawa cells, $**P < 0.01$ vs. control group; $##P < 0.01$ vs. $5 \mu M$ group. SLC7A11, solute carrier family 7 member 11; TRF1, transferrin receptor 1; FPN, ferroportin.

significantly higher than those in the simvastatin group, while the protein expression level of TRF1 was remarkably lower (Figures (f)6-6(g)). The above suggested that ML-098 could reverse the antitumor effect of simvastatin.

## 4. Discussion

Statins, in addition to lowering cholesterol, can also exert various anticancer effects in liver, colon, and breast cancers, such as antiproliferation, pro-apoptosis, antiangiogenesis, immunoregulation, and anti-invasion [24, 25]. As one of the statins, simvastatin may have potential to treat and prevent cancers. Jin et al. discovered that simvastatin could reduce the viability of EC cells (RL-95-2, Ishikawa and HEC-1B) and induce cell apoptosis [26]. MTOR inhibition may be a mechanism for the antiproliferative actions of simvastatin and metformin, as evidenced by the upregulation of phosphorylated AMPK and the down-regulation of downstream phosphorylated S6 following their treatment [26]. We also found that $10 \mu M$ and $15 \mu M$ of simvastatin could significantly dose-dependently reduce cell proliferation rate, colony formation, and invasive ability. Long-term exposure to simvastatin can more effectively inhibit the growth of poorly differentiated cells derived from the lung (Calu-3 and Calu6), skin (SCC-M7 and SCC-P9), colon (Caco-2 and HCT-116), prostate (LNCaP and PC-3), breast (MCF7 and SKBr-3) and other tissues [27]. Moreover, simvastatin also has a more significant effect on cells of highly metastatic malignant tumors than it does on cells of benign tumors with

the same origin; and this may be related to the need of metastatic tumor cells for more isoprene and mevalonate to improve cell survival [28].

One of the most significant factors contributing to the initiation, metastasis, and progression of cancer is the disruption of redox equilibrium [29]. It is reported that the imbalance of redox homeostasis is caused by increased free radicals (mainly ROS) [21]. Several studies have revealed that a variety of anticancer drugs induce apoptosis and autophagy by generating ROS. For example, resveratrol, a natural polyphenol, regulates antioxidant enzymes to induce mitochondrial $H_2O_2$ accumulation, and then to induce apoptosis of prostate cancer cells PC-3, breast cancer cells MCF-7, and liver cancer cells HepG2 [30]. Existing studies have proved the promotion of simvastatin to ROS production. For instance, Buranrat et al. claimed that simvastatin could significantly promote the accumulation of ROS in MCF-7 cells, so that doxorubicin had a greater effect [31]. Wang et al. pointed out that simvastatin caused an increase of ROS level and then induced apoptosis in OCM-1 cells [32]. In this study, $10 \mu M$ and $15 \mu M$ of simvastatin could increase the ROS level in Ishikawa cells. Collectively, simvastatin-induced cancer cell death is associated with ROS accumulation.

Ferroptosis is thought to be characterized by lipid peroxidation [33], and ROS-induced lipid peroxidation is a key factor in ferroptosis [21]. At present, cancer treatment regimens based on ferroptosis-induction are effective in reducing the amount of cancer cells. For example, the Food
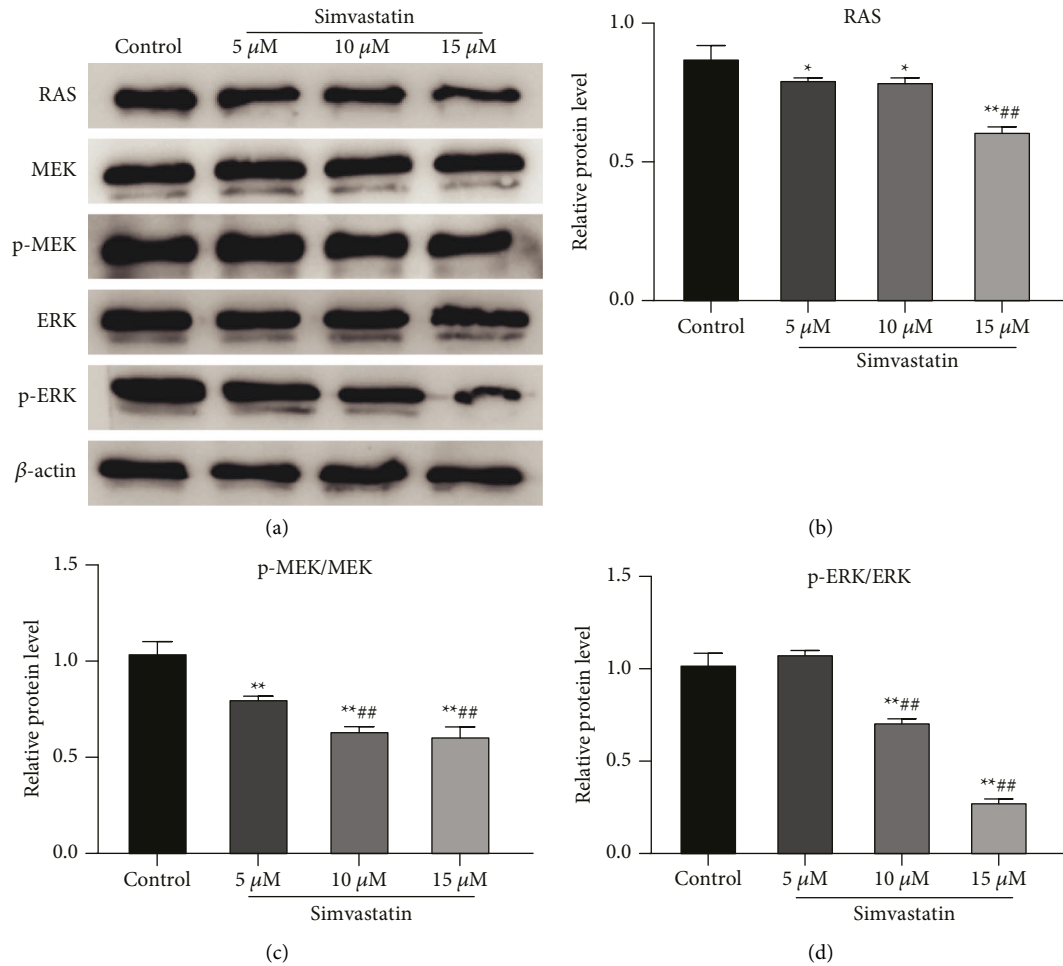
FIGURE 4: Simvastatin inhibits the RAS/MAPK signaling pathway in Ishikawa cells. (a–d): Western blot to detect the effect of simvastatin with different concentrations on the expression of RAS/MAPK pathway-related proteins (RAS, p-MEK, MEK, p-ERK, and ERK) in Ishikawa cells (a), and quantitative analysis based on Image J (b–d), $^*P < 0.05$ vs. control group; $^{##}P < 0.01$ vs. $5 \mu M$ group.

and Drug Administration (FDA) has authorized sorafenib, a medication for the induction of ferroptosis, for the treatment of hepatocellular carcinoma [34]. In this paper, simvastatin could significantly increase the $Fe^{2+}$ level and MDA level, decrease the level of GSH, downregulated the SLC7A11 and FPN levels, and upregulated the TRF1 level. SLC7A11/xCT can promote cystine uptake and glutathione biosynthesis, thereby preventing oxidation and ferroptosis [35, 36]. All in all, simvastatin can exert an anticancer effect by inducing ferroptosis in cells.

Simvastatin suppresses the proliferation of cancer cells by triggering apoptosis and slowing the progression of the cell cycle via a variety of cell signaling pathways, as shown by several in vitro studies. In the measurement of ferroptosis-related proteins, we discovered that simvastatin could greatly promote the TRF1 expression, and some research studies also revealed the correlation of TRF1 expression with the RAS/MAPK pathway activation [37]. Furthermore, the stimulation of the RAS/MAPK pathway can restore the sensitivity of tumor cells to anticancer drugs, which has been presented in many articles [38]. Besides, some other scholars have stated that the sensitivity of ferroptosis in individual

cell lines can be determined by the RAS/MAPK pathway [39]. Briefly, one important signaling pathway that controls ferroptosis in cancer cells is the RAS/MAPK pathway. Interestingly, Afrin et al. pointed out that simvastatin could reduce the protein level of RAS and affect the activity of the RAS/MAPK pathway [40]. In this paper, we also discovered that simvastatin inhibited RAS/MAPK pathway activity in Ishikawa cells. For further confirmation, cells were treated with ML-098 (an agonist of the RAS/MAPK pathway) and simvastatin simultaneously, and the outcomes suggest that ML-098 significantly weakened the effects of simvastatin. It could be concluded that simvastatin inhibited the RAS/MAPK signaling pathway to suppress the proliferation, clone formation, invasion of EC cells, and induce ferroptosis.

This study has certain restrictions as well. Firstly, only Ishikawa cells were selected to explore the function and mechanism of simvastatin. However, a study by Kim et al. revealed that simvastatin consistently had an impact on three EC cells (RL-95-2, HEC-1B, and Ishikawa) [26]. So we suspected similar effects of simvastatin in other EC cells as in Ishikawa cells. Besides, Kim et al. also revealed a stronger anticancer effect of the combination of simvastatin and met
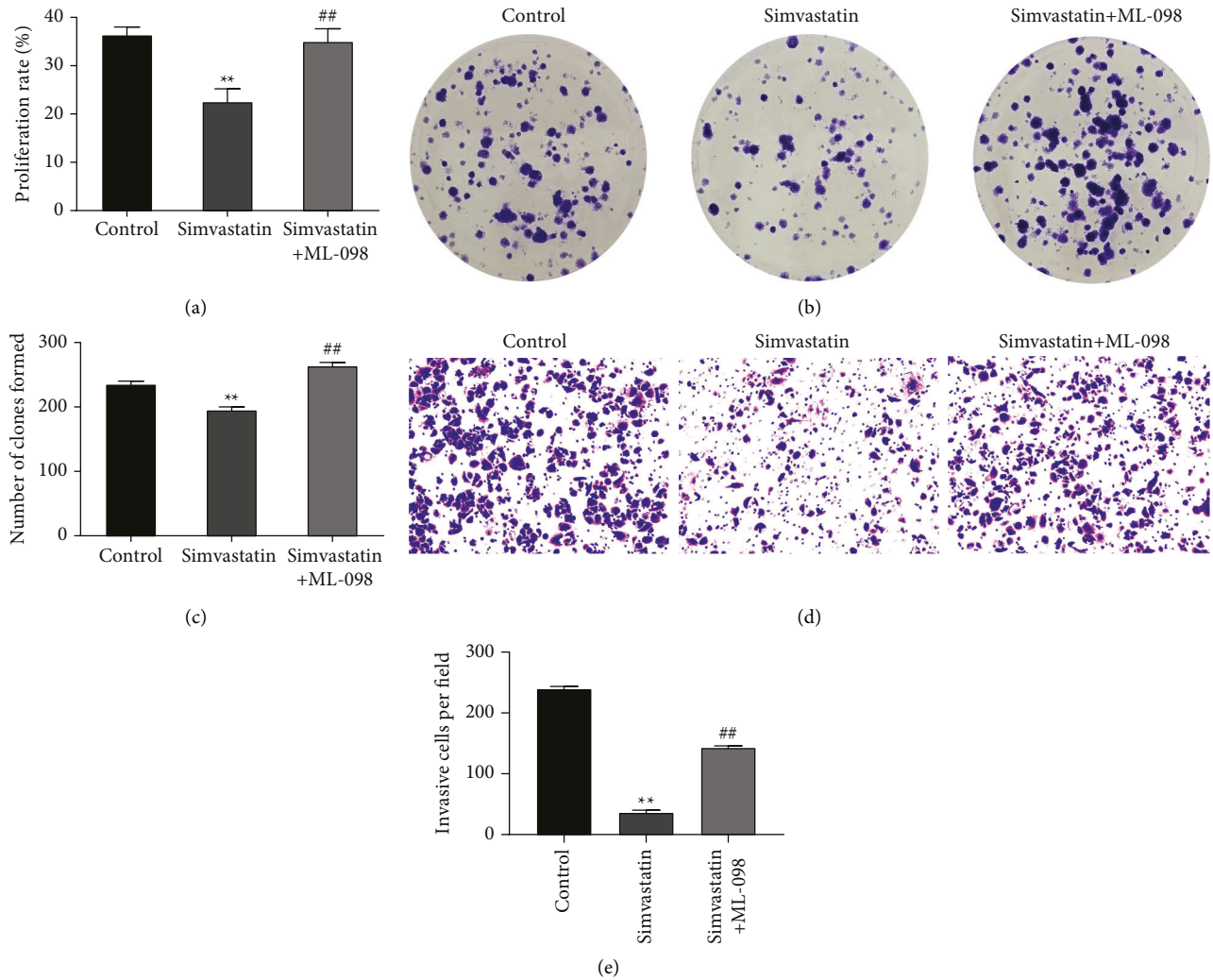
FIGURE 5: RAS agonist reverses the inhibitory effects of simvastatin on Ishikawa cell proliferation, colony formation, and invasion. (a): MTT assay to detect the effect of simultaneous treatment of ML-098 and simvastatin on the proliferation of Ishikawa cells; (b–c): colony formation assay to explore the effect of simultaneous treatment of ML-098 and simvastatin on the colony formation ability of Ishikawa cells; (d–e): transwell assay to detect the effect of simultaneous treatment of ML-098 and simvastatin on the invasion ability of Ishikawa cells, $^{**}P < 0.01$ vs. control group; $^{##}P < 0.01$ vs. simvastatin group.

form than a single drug in their study [26], so further investigation on combined drugs can be performed to obtain better clinical efficacy. Furthermore, only *in vitro*

experiments were conducted in our paper, and more comprehensive experimental data are expected to be obtained by further *in vitro* experimental validation.

(a)

(b)

(c)

(d)

(e)

(f)

(g)
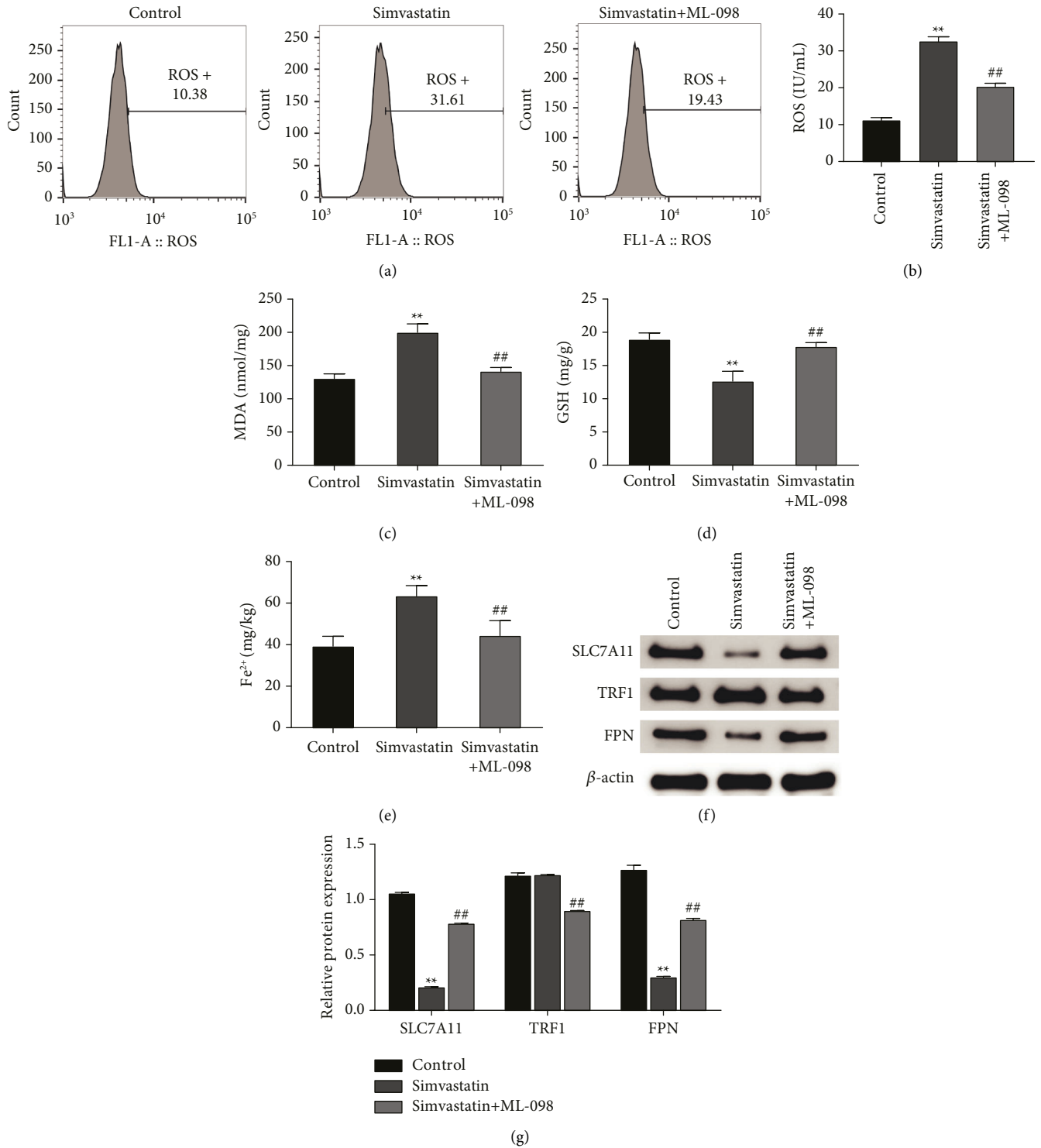
FIGURE 6: RAS agonist reverses the promoting effects of simvastatin on ROS level and ferroptosis in Ishikawa cells. (a–b): flow cytometry detected the effects of simultaneous treatment of ML-098 and simvastatin on DCFH-DA-labeled ROS level in Ishikawa cells; (c–d): ELISA detected the effects of simultaneous treatment of ML-098 and simvastatin on the level of MDA (c) and GSH (d) in Ishikawa cells; (e): ELISA to detect the effect of simultaneous treatment of ML-098 and simvastatin on the Fe$^{2+}$ level in Ishikawa cells; (f-g): Western blot to determine the effect of simultaneous treatment of ML-098 and simvastatin on the expression of ferroptosis-related proteins (SLC7A11, TRF1, and FPN) in Ishikawa cells, $^{**}P < 0.01$ vs. control group; $^{##}P < 0.01$ vs. simvastatin group. ROS, reactive oxygen species; MDA, malondialdehyde; GSH, glutathione; solute carrier family 7 member 11; TRF1, transferrin receptor 1; FPN, ferroportin.

## 5. Conclusion

To sum up, simvastatin inhibits cell colony formation, invasion, and proliferation in EC Ishikawa cells by suppressing the RAS/MAPK signaling pathway. Besides, the inhibition to the RAS/MAPK signaling pathway allows simvastatin to induce ferroptosis through up-regulating the level of ROS, MDA, $Fe^{2+}$, and TRF1 and reducing the level of GSH, SLC7A11, and FPN in cells. In a word, simvastatin has the potential to be a targeted drug for EC treatment.

## Data Availability

The data used to support the findings of this study are available from the corresponding author upon request.

## Ethical Approval

This article does not contain any studies with human participants or animals performed by any of the authors.

## Conflicts of Interest

The authors declare that they have no conflicts of interest.

## References

[1] C. M. Nagle, E. J. Crosbie, A. Brand et al., "The association between diabetes, comorbidities, body mass index and all-cause and cause-specific mortality among women with endometrial cancer," *Gynecologic Oncology*, vol. 150, no. 1, pp. 99–105, 2018.

[2] F. Bray, J. Ferlay, I. Soerjomataram, R. L. Siegel, L. A. Torre, and A. Jemal, "Global cancer statistics 2018: GLOBOCAN estimates of incidence and mortality worldwide for 36 cancers in 185 countries," *CA: A Cancer Journal for Clinicians*, vol. 68, no. 6, pp. 394–424, 2018.

[3] A. L. Beavis, T. T. Yen, R. L. Stone et al., "Adjuvant therapy for early stage, endometrial cancer with lymphovascular space invasion: is there a role for chemotherapy?" *Gynecologic Oncology*, vol. 156, no. 3, pp. 568–574, 2020.

[4] J. Perera and P. Hoskin, "Adjuvant therapy for high-risk endometrial carcinoma," *Clinical Oncology*, vol. 33, no. 9, pp. 560–566, 2021.

[5] M. Arnold, N. Pandeya, G. Byrnes et al., "Global burden of cancer attributable to high body-mass index in 2012: a population-based study," *The Lancet Oncology*, vol. 16, no. 1, pp. 36–46, 2015.

[6] B. R. Stockwell, J. P. Friedmann Angeli, H. Bayir et al., "Ferroptosis: a regulated cell death nexus linking metabolism, redox biology, and disease," *Cell*, vol. 171, no. 2, pp. 273–285, 2017.

[7] Z. Guan, J. Chen, X. Li, and N. Dong, "Tanshinone IIA induces ferroptosis in gastric cancer cells through p53-mediated SLC7A11 down-regulation," *Bioscience Reports*, vol. 40, no. 8, Article ID BSR20201807, 2020.

[8] X. Jiang, B. R. Stockwell, and M. Conrad, "Ferroptosis: mechanisms, biology and role in disease," *Nature Reviews Molecular Cell Biology*, vol. 22, no. 4, pp. 266–282, 2021.

[9] M. Zhang, T. Zhang, C. Song et al., "Guizhi fuling capsule ameliorates endometrial hyperplasia through promoting p62-Keap1-NRF2-mediated ferroptosis," *Journal of Ethnopharmacology*, vol. 274, Article ID 114064, 2021.

[10] H. Wang, S. Peng, J. Cai, and S. Bao, "Silencing of PTPN18 induced ferroptosis in endometrial cancer cells through p-P38-mediated GPX4/xCT down-regulation," *Cancer Management and Research*, vol. 13, pp. 1757–1765, 2021.

[11] M. Ge, J. Niu, P. Hu et al., "A ferroptosis-related signature robustly predicts clinical outcomes and associates with immune microenvironment for thyroid cancer," *Frontiers of Medicine*, vol. 8, Article ID 637743, 2021.

[12] T. R. Pedersen and J. A. Tobert, "Simvastatin: a review," *Expert Opinion on Pharmacotherapy*, vol. 5, no. 12, pp. 2583–2596, 2004.

[13] J. P. Kitzmiller, D. M. Sullivan, M. A. Phelps, D. Wang, and W. Sadee, "CYP3A4/5 combined genotype analysis for predicting statin dose requirement for optimal lipid control," *Drug Metabolism and Drug Interactions*, vol. 28, no. 1, pp. 59–63, 2013.

[14] D. K. Xia, Z. G. Hu, Y. F. Tian, and F. J. Zeng, "Statin use and prognosis of lung cancer: a systematic review and meta-analysis of observational studies and randomized controlled trials," *Drug Design, Development and Therapy*, vol. 13, pp. 405–422, 2019.

[15] C. R. Cardwell, U. Mc Menamin, C. M. Hughes, and L. J. Murray, "Statin use and survival from lung cancer: a population-based cohort study," *Cancer Epidemiology, Biomarkers & Prevention*, vol. 24, no. 5, pp. 833–841, 2015.

[16] R. A. Schnoll, T. A. Johnson, and C. Lerman, "Genetics and smoking behavior," *Current Psychiatry Reports*, vol. 9, no. 5, pp. 349–357, 2007.

[17] R. Tate, E. Zona, R. De Cicco et al., "Simvastatin inhibits the expression of stemnessrelated genes and the metastatic invasion of human cancer cells via destruction of the cytoskeleton," *International Journal of Oncology*, vol. 51, no. 6, pp. 1851–1859, 2017.

[18] K. Matsuo, M. S. Hom, A. Yabuno et al., "Association of statins, aspirin, and venous thromboembolism in women with endometrial cancer," *Gynecologic Oncology*, vol. 152, no. 3, pp. 605–611, 2019.

[19] M. N. Schointuch, T. P. Gilliam, J. E. Stine et al., "Simvastatin, an HMG-CoA reductase inhibitor, exhibits anti-metastatic and anti-tumorigenic effects in endometrial cancer," *Gynecologic Oncology*, vol. 134, no. 2, pp. 346–355, 2014.

[20] H. L. Li, X. M. Fei, Y. Tang, Y. L. Yang, L. X. Wang, and J. W. Geng, "Effect of doxycycline on intrinsic apoptosis of myeloma cell line H929 and its mechanism," *Zhongguo Shi Yan Xue Ye Xue Za Zhi*, vol. 30, no. 2, pp. 441–448, 2022.

[21] L. J. Su, J. H. Zhang, H. Gomez et al., "Reactive oxygen species-induced lipid peroxidation in apoptosis, autophagy, and ferroptosis," *Oxidative Medicine and Cellular Longevity*, vol. 2019, Article ID 5080843, 13 pages, 2019.

[22] L. Galluzzi, I. Vitale, S. A. Aaronson et al., "Molecular mechanisms of cell death: recommendations of the nomenclature committee on cell death 2018," *Cell Death & Differentiation*, vol. 25, no. 3, pp. 486–541, 2018.

[23] M. Dillon, A. Lopez, E. Lin, D. Sales, R. Perets, and P. Jain, "Progress on Ras/MAPK signaling research and targeting in blood and solid cancers," *Cancers*, vol. 13, no. 20, p. 5059, 2021.

[24] N. G. Vallianou, A. Kostantinou, M. Kougias, and C. Kazazis, "Statins and cancer," *Anti-Cancer Agents in Medicinal Chemistry*, vol. 14, no. 5, pp. 706–712, 2014.

[25] L. Chushi, W. Wei, X. Kangkang, F. Yongzeng, X. Ning, and C. Xiaolei, "HMGCR is up-regulated in gastric cancer and promotes the growth and migration of the cancer cells," *Gene*, vol. 587, no. 1, pp. 42–47, 2016.

[26] J. S. Kim, J. Turbov, R. Rosales, L. G. Thaete, and G. C. Rodriguez, "Combination simvastatin and metformin synergistically inhibits endometrial cancer cell growth," *Gynecologic Oncology*, vol. 154, no. 2, pp. 432–440, 2019.

[27] D. G. Menter, V. P. Ramsauer, S. Harirforoosh et al., "Differential effects of pravastatin and simvastatin on the growth of tumor cells from different organ sites," *PLoS One*, vol. 6, no. 12, Article ID e28813, 2011.

[28] L. Matusewicz, J. Meissner, M. Toporkiewicz, and A. F. Sikorski, "The effect of statins on cancer cells--review," *Tumor Biology*, vol. 36, no. 7, pp. 4889–4904, 2015.

[29] S. Saikolappan, B. Kumar, G. Shishodia, S. Koul, and H. K. Koul, "Reactive oxygen species and cancer: a complex interaction," *Cancer Letters*, vol. 452, pp. 132–143, 2019.

[30] M. A. Khan, H. C. Chen, X. X. Wan et al., "Regulatory effects of resveratrol on antioxidant enzymes: a mechanism of growth inhibition and apoptosis induction in cancer cells," *Molecular Cell*, vol. 35, no. 3, pp. 219–225, 2013.

[31] B. Buranrat, W. Suwannaloet, and J. Naowaboot, "Simvastatin potentiates doxorubicin activity against MCF-7 breast cancer cells," *Oncology Letters*, vol. 14, no. 5, pp. 6243–6250, 2017.

[32] Y. Wang, S. L. Xu, Y. Z. Wu et al., "Simvastatin induces caspase-dependent apoptosis and activates P53 in OCM-1 cells," *Experimental Eye Research*, vol. 113, pp. 128–134, 2013.

[33] R. Tang, J. Xu, B. Zhang et al., "Ferroptosis, necroptosis, and pyroptosis in anticancer immunity," *Journal of Hematology & Oncology*, vol. 13, no. 1, p. 110, 2020.

[34] X. Sun, Z. Ou, R. Chen et al., "Activation of the p62-Keap1-NRF2 pathway protects against ferroptosis in hepatocellular carcinoma cells," *Hepatology*, vol. 63, no. 1, pp. 173–184, 2016.

[35] J. He, H. Ding, H. Li, Z. Pan, and Q. Chen, "Intra-tumoral expression of SLC7A11 is associated with immune microenvironment, drug resistance, and prognosis in cancers: a pan-cancer analysis," *Frontiers in Genetics*, vol. 12, Article ID 770857, 2021.

[36] T. Sehm, M. Rauh, K. Wiendieck, M. Buchfelder, I. Y. Eyupoglu, and N. E. Savaskan, "Temozolomide toxicity operates in a xCT/SLC7a11 dependent manner and is fostered by ferroptosis," *Oncotarget*, vol. 7, no. 46, p. 74630, Article ID 74647, 2016.

[37] W. S. Yang and B. R. Stockwell, "Synthetic lethal screening identifies compounds activating iron-dependent, non-apoptotic cell death in oncogenic-RAS-harboring cancer cells," *Chemistry & Biology*, vol. 15, no. 3, pp. 234–245, 2008.

[38] N. Eling, L. Reuter, J. Hazin, A. Hamacher-Brady, and N. R. Brady, "Identification of artesunate as a specific activator of ferroptosis in pancreatic cancer cells," *Oncoscience*, vol. 2, no. 5, pp. 517–532, 2015.

[39] F. Ye, W. Chai, M. Xie et al., "HMGB1 regulates erastin-induced ferroptosis via RAS-JNK/p38 signaling in HL-60/NRAS(Q61L) cells," *American Journal of Cancer Research*, vol. 9, no. 4, pp. 730–739, 2019.

[40] S. Afrin, M. S. Islam, K. Patzkowsky et al., "Simvastatin ameliorates altered mechanotransduction in uterine leiomyoma cells," *American Journal of Obstetrics and Gynecology*, vol. 223, no. 5, p. 733.e1, Article ID 733.e14, 2020.

*Retraction*

# Retracted: Meta-Analysis of Different Acupuncture Points in the Treatment of Ankylosing Spondylitis with Supervised Moxibustion

**Evidence-Based Complementary and Alternative Medicine**

This article has been retracted by Hindawi following an investigation undertaken by the publisher [1]. This investigation has uncovered evidence of one or more of the following indicators of systematic manipulation of the publication process:

(1) Discrepancies in scope

(2) Discrepancies in the description of the research reported

(3) Discrepancies between the availability of data and the research described

(4) Inappropriate citations

(5) Incoherent, meaningless and/or irrelevant content included in the article

(6) Peer-review manipulation

The presence of these indicators undermines our confidence in the integrity of the article's content and we cannot, therefore, vouch for its reliability. Please note that this notice is intended solely to alert readers that the content of this article is unreliable. We have not investigated whether authors were aware of or involved in the systematic manipulation of the publication process.

In addition, our investigation has also shown that one or more of the following human-subject reporting requirements has not been met in this article: ethical approval by an Institutional Review Board (IRB) committee or equivalent, patient/participant consent to participate, and/or agreement to publish patient/participant details (where relevant).

Wiley and Hindawi regrets that the usual quality checks did not identify these issues before publication and have since put additional measures in place to safeguard research integrity.

We wish to credit our own Research Integrity and Research Publishing teams and anonymous and named external researchers and research integrity experts for contributing to this investigation.

The corresponding author, as the representative of all authors, has been given the opportunity to register their agreement or disagreement to this retraction. We have kept a record of any response received.

## References

[1] J. Cheng, X. Wang, L. Wang et al., "Meta-Analysis of Different Acupuncture Points in the Treatment of Ankylosing Spondylitis with Supervised Moxibustion," *Evidence-Based Complementary and Alternative Medicine*, vol. 2022, Article ID 4688689, 7 pages, 2022.

Hindawi

*Research Article*

# Meta-Analysis of Different Acupuncture Points in the Treatment of Ankylosing Spondylitis with Supervised Moxibustion

**Jie Cheng,[1] Xinyi Wang,[2] Leisheng Wang,[2] Yufei Zhang,[2] Yu Gu,[1] Dan Mao,[1] Xingyu Zhou,[1] Xiaolong Wang,[1] and Yuansheng Tian [2]**

[1]*College of Henan Traditional Chinese Medicine, Zhengzhou 450000, Henan, China*
[2]*The Affiliated Hospital of Henan Academy of Traditional Chinese Medicine, Zhengzhou 450000, Henan, China*

Correspondence should be addressed to Yuansheng Tian; 100234@yzpc.edu.cn

*Objective*. To investigate the clinical efficacy of different acupuncture points in the treatment of ankylosing spondylitis with supervised moxibustion. *Methods*. Retrospective analysis of 61 AS patients (diagnosed as ankylosing spondylitis of kidney-yang deficiency type by Chinese medicine) admitted to our hospital from January 2020 to February 2021, randomly divided into 30 cases in the experimental group (Du moxibustion + basic western medicine treatment) and 31 cases in the control group (basic western medicine treatment alone). The changes in quantitative scores of the main symptoms and major signs (thoracic mobility, occipital-wall distance, finger-ground distance, and laboratory index (ESR)) were analyzed before and after treatment. *Results*. Of the 30 cases in the experimental group, 2 were clinically cured, 3 were apparently effective, 21 were effective, and 4 were ineffective, with an overall effective rate of 86.7%; of the 31 cases in the control group, 1 was clinically cured, 1 was apparently effective, 1 was effective. 24 were effective, and 5 were ineffective, with an overall effective rate of 83.9%. Comparing the efficacy by $t$-test, $P < 0.05$, indicating that the effect of Du moxibustion + Western medicine treatment was better. *Conclusion*. The treatment of ankylosing spondylitis with kidney-yang deficiency by moxibustion + western medicine can improve the efficacy, alleviate the inflammatory response and improve the patient's symptoms and signs, and immune indexes.

## 1. Introduction

Ankylosing spondylitis (AS) is a chronic progressive immune inflammatory disease with undetermined pathogenesis. It mainly affects the medial and peripheral joints of the human body, manifesting mainly as synovial inflammatory lesions of the joints, followed by deformation and destruction of the cartilage, and eventually developing into bony ankylosis and vertebral joint-like changes, as well as involving the eyes, heart, lungs, and kidneys. It may also involve the eyes, heart, lungs, kidneys, and other organs. The early manifestations are mainly pain in the sacroiliac joints, and the onset of the disease is relatively insidious, but because of the late start of rheumatological research in China and the lack of attention to rheumatic diseases, the diagnosis is often unknown or late. Epidemiological surveys have shown that there are significant ethnic and regional differences in the disease, with a prevalence of 0.3% in China and a predominantly adolescent population with a male to female ratio of 2 : 1. In China, 60% of patients with ankylosing spondylitis have hip involvement, and 15–20% have bony ankylosis of the hip joint, or even lifelong disability [1, 2], which causes great pain to the patient's work and life, and is a serious burden to the family and society, so research into this disease is of great significance.

Ankylosing spondylitis is not known as a disease in traditional Chinese medicine, but there are many records relating to it. It can also be classified as "paralysis" or "lumbago." From the perspective of Chinese medicine, the causes are internal and external. The internal cause is mainly a deficiency in the kidney [2], which is responsible for the production of bone and marrow. The kidney is the innate essence of the human body, and all physiological functions of the human body depend on the fullness of kidney qi. The

Kidney is also the innate essence of the human body and all physiological functions of the body depend on the fullness of Kidney Qi. The Governor's Vessel oversees the Yang Qi of the body and is the sea of Yang Qi. The main external causes of the disease are closely related to "cold and dampness." In Su Wen's Theory of Paralysis, the three gases of wind, cold, and damp come together and become paralysis.

The insidious onset of ankylosing spondylitis and the atypical early symptoms make it easy to confuse the disease with other diseases, presenting a significant obstacle to early diagnosis and treatment. The treatment of AS has not yet been found to be curative, and the goal of treatment remains to control the disease, reduce pain and mobility restrictions to the greatest extent possible, prevent bone damage to the joints and restore mobility to the spinal joints. The first-line drugs used in Western medicine to treat AS are still mainly NSAIDs, antirheumatic drugs, anti-TNF antagonists, and glucocorticoids, with the rest being thalidomide and leflunomide, which are not as effective as the first-line drugs, while hip replacement surgery is less acceptable to patients because of the greater risk of postoperative heterotopic ossification. Moreover, the long-term application of NSAIDs is extremely damaging to patients' gastrointestinal tract and liver and kidney functions. The treatment of AS in Chinese medicine is based on the principle of evidence-based treatment and is classified according to the causes and symptoms of the disease, which are mostly classified into cold-damp paralysis and obstruction, damp-heat paralysis, stasis-blood paralysis, and obstruction. The internal treatment method is based on traditional Chinese medicine soup or Chinese medicine pills processed according to the Chinese medicine formula, which are effective in reducing joint pain and improving joint function in AS. The external treatment of ankylosing spondylitis is based on a variety of methods, such as acupuncture, moxibustion, acupuncture, Gua Sha, compressing, fumigation, and Tui Na, which are fast acting, effective, and reduce the side effects of oral medication.

The insidious onset of ankylosing spondylitis and the atypical early symptoms make it easy to confuse the disease with other diseases, presenting a significant obstacle to early diagnosis and treatment. The treatment of AS has not yet been found to be curative, and the goal of treatment remains to control the disease, reduce pain and mobility restrictions to the greatest extent possible, prevent bone damage to the joints and restore mobility to the spinal joints. The first-line drugs for the treatment of AS in Western medicine are still mainly NSAIDs, antirheumatic drugs, anti-TNF antagonists, and glucocorticoids, and the rest are thalidomide and leflunomide, which are not ideal for first-line drug effects, while hip arthroplasty is less acceptable to patients due to the greater risk of postoperative heterotopic ossification [3, 4]. Moreover, the long-term application of NSAIDs is extremely damaging to patients' gastrointestinal tract and liver and kidney functions. The treatment of AS in TCM is based on the principle of evidence-based treatment, is classified according to the etiology and symptoms of the disease, and is mostly divided into evidence types such as cold-damp paralysis and obstruction, damp-heat paralysis, stasis-blood

paralysis, and obstruction. The internal treatment method is based on traditional Chinese medicine soup or Chinese medicine pills processed according to the Chinese medicine formula, which are effective in reducing joint pain and improving joint function in AS. There are many external treatments for ankylosing spondylitis, such as acupuncture, moxibustion, acupuncture, Gua Sha, compressing, fumigation, and Tui Na, which are fast acting and effective and reduce the side effects of oral medication.

Chinese medicine treatment is mainly based on the identification and treatment of positive deficiency, evil actuality, and mixed deficiency and actuality, using Chinese medicine's internal and external treatment methods, but the efficacy is limited [5, 6]. If the kidney yang is deficient, the fire of the vital gate is insufficient, the source of the Governor's Vessel is depleted, and the warming power is weak; if the Governor's Vessel is blocked, the circulation of Qi and blood is poor, and the ability to resist external evil is reduced. In recent years, studies have found that the treatment of ankylosing spondylitis with moxibustion is effective, improving clinical symptoms and relieving fatigue [7, 8]. However, there are shortcomings in the treatment of ankylosing spondylitis, such as uneven heat distribution, low drug utilization rate, and easy-to-burn patients. The moxibustion box is a kind of warm moxibustion apparatus that can effectively use the smoke and heat produced by burning moxa, and by fumigating or warming certain parts of the body surface, it can adjust the function of meridians and internal organs, thus playing a role in disease prevention and treatment. In this study, moxibustion was applied to patients with ankylosing spondylitis with a deficiency of kidney yang in order to provide a basis and new ideas for the adjunctive treatment of ankylosing spondylitis.

## 2. Materials and Methods

*2.1. Source of Cases.* Patients with AS who were admitted to our hospital from January 2020 to February 2021 (with a TCM diagnosis of renal yang deficiency building) were selected. A total of 63 cases met inclusion criteria, 2 cases dropped out during the treatment period, and 61 cases completed the course of treatment. The gender ratio was 43 males and 18 females; age ranged from 19 to 65 years old, with an average age of 40 years old; income cases The course of disease ranges from 1 to 10 years, with an average of 5 years. According to the random number table, patients were randomly divided into two groups: experimental and control.

*2.2. Diagnostic Criteria of Western Medicine.* Western medicine diagnosis is based on the AS criteria in China's 2002 Guidelines for Clinical Studies of New Western Medicines. The main symptoms are lumbosacral pain, back pain, restricted spinal movement, joint swelling not exceeding the surrounding bony signs, and morning stiffness; the main signs are tenderness at the attachment point, Schober test (+), positive occipital wall, finger test, positive, or normal thoracic range of motion; X-ray film shows mild

Inflammatory infiltrate with indistinct contours, dense shadows around the joint, and a slightly smaller interarticular space.

*2.3. Chinese Medicine Syndrome Differentiation Criteria.* The TCM typology of ankylosing spondylitis is based on the Guidelines for Clinical Research on New Chinese Medicines. Kidney-yang deficiency syndrome's primary symptoms are as follows: back pain, back pain, restricted lumbar spine movement, morning stiffness, local cold pain, aversion to cold and warmth, lack of warmth in the hands and feet, heel pain, and soreness and weakness of the waist and knees. Secondary symptoms are as follows: lack of energy, pale complexion, soreness and weakness of the waist and knees, impotence, and excessive nocturia. Tongue and pulse: pale tongue with white fur and deep and thin pulse.

*2.4. Quantitative Scoring Criteria for Major Symptoms.* The quantitative scoring standard of main symptoms in this experiment is based on my country's "Trial Implementation of Principles for Guiding Clinical Research on New Chinese Medicines" and is prepared according to specific clinical manifestations of clinically collected patients.

*2.5. Inclusion Criteria.* The inclusion criteria were set as follows:

(1) Previously diagnosed with ankylosing spondylitis, with a history of more than 1 year and no more than 10 years

(2) Conform to TCM syndrome differentiation of ankylosing spondylitis with kidney-yang deficiency syndrome

(3) Aged between 19 and 65 years old

(4) After informing the patient of a specific treatment plan, he is still willing to accept 2 courses of treatment, and cooperates with a relevant examination, as evidenced by signing "informed consent"

*2.6. Exclusion Criteria.* The exclusion criteria were set as follows:

(1) Ankylosing spondylitis is not clearly diagnosed; those who do not meet TCM classification criteria for kidney-yang deficiency

(2) Age < 19 or > 65 years old; female patients during menstruation, pregnancy or lactation

(3) Patients with other joint diseases coexisting with negative rheumatoid factor accompanied by more serious chronic primary underlying diseases such as hypertension, disease, coronary heart disease, diabetes, blood with coagulation, hematopoietic, and other disorders; patients with systemic diseases; patients with mental or unconscious problems

(4) Patients with severe joint deformities or even disabilities;

(5) Those who refuse to cooperate with researchers, or have incomplete clinical data, which may affect the statistics of research results

*2.7. Rejection Criteria.* The rejection criteria were set as follows:

(1) After inclusion, it was found that patient concealed their condition but did not actually meet the inclusion criteria to be selected

(2) Those who have poor compliance, do not follow doctor's orders for a course of treatment, and refuse to cooperate with treatment and inspection

(3) Other conditions that may affect the results of this treatment occur during the study period

*2.8. Falling off Standard.* The following cases are regarded as dropout cases: those who drop out of an incomplete course of treatment due to the patient's own reasons (work or personal reasons); those who drop out of an incomplete course of treatment due to serious discomfort with Du moxibustion during the course of treatment.

*2.9. Research Content.* Based on the principle of randomized control, clinical treatment of Du moxibustion in the treatment of ankylosing spondylitis (kidney-yang deficiency type) was observed. A total of 63 cases meeting inclusion criteria were collected in Min 2.2 grouping, and they were randomly divided into an order of hospitalization time and random number (table. 2) groups: experimental (the Governor's moxibustion + western medicine basic treatment), control (simple western medicine basic treatment). During the course of treatment, 1 case dropped out in experimental and control, respectively, so a total of 30 cases were completed in experimental and 31 cases in control.

*2.10. Treatment Methods.* Experimental: Governor's moxibustion + basic western medicine treatment.

*Specific Operations.* Acupuncture: the patient is placed in a prone position, and Hua Lun Jiaji acupoint is selected, that is, under a spinous process of 1st thoracic vertebra to 5th lumbar vertebra, 0.5 cun on the left and right sides, 17 acupoints on each side, a total of 34 acupoints. Disposable sterile governor moxibustion needles were punctured obliquely at 45° in direction of the spine, needles were inserted 15 mm, and needles were retained for 30 min. For 6 consecutive days, once a day, and on the 7th day, Du moxibustion was performed. On the 7th day, supervisor moxibustion: take an appropriate amount of small turmeric, wash it, crush it with a juicer, then take out the crushed ginger paste, wrap it in gauze, squeeze out a little ginger juice, and instruct the patient to lie on the bed, fully expose spine, use iodine disinfect local skin of T, ~Ls, lay a layer of gauze, and then lay ginger mud, about 5 cm wide and 1.5 cm thick, and place moxa columns (diameter 1.5 cm) on it, with an interval of about 2 cm between each column. After burning, the next column was

replaced, and a total of 3 columns were continuously applied for moxibustion, as shown in Figure 1. For 1 month after moxibustion, do not take cold water baths and fast food. Acupuncture treatment was continued after Governor's moxibustion, and this cycle of treatment, every 2 weeks was a course of treatment, a total of 4 courses of treatment, and a total of 2 months of treatment.

Western medicine basic treatment: oral celecoxib capsules (produced by China Pfizer Pharmaceutical Co., Ltd.), 1 tablet (0.2 g) each time, once a day. 1 week is a course of treatment, and a total of 2 courses of treatment are taken. Control: only received basic western medicine treatment. 1 week is a course of treatment, and a total of 2 courses of treatment are taken. Care measures: advise patients to eat a diet high in nutrients and vitamins, light and easy to digest; advise patients with noncardiopulmonary insufficiency to take appropriate spinal and joint function-based exercises; and advise patients to sleep on a hard bed.

*2.11. General Observation Indicators.* The evaluation of the efficacy of ankylosing spondylitis was carried out according to the assessment of ankylosing spondylitis (ASAS) [9], and the thoracic mobility, finger-to-floor distance, occipital-wall distance, and Schober test were evaluated before and after treatment in both groups.

Laboratory parameters: early morning fasting venous blood was collected from both groups before and after treatment by the same nursing staff and sent to the hospital's laboratory department for testing. The interleukin-17 (IL-17) and interleukin-1$\beta$ (IL-1) samples were sent to the laboratory department of the hospital. The erythrocyte sedimentation rate (ESR) of all samples was measured by a fully automatic dynamic sedimentation analyzer (purchased from Shenzhen Yafei Long Biotechnology Co. protein (CRP) levels were measured with a fully automated hematology analyzer (purchased from Shenzhen Meizu Biomedical Electronics Co.

*2.12. Main Symptoms.* Based on my country's 2002 "Principles for Guiding Clinical Research on New Chinese Medicines," based on self-made scoring standards based on the main symptoms of clinical patients, patients' lumbosacral, back pain, spinal activity, and other symptoms were evaluated. Finally, the total score was used to compare the improvement of the main symptoms.

*2.13. Main Signs.* The thoracic activity, occipital-wall distance, and finger-ground distance (cm) of patients were measured and recorded for comparison.

*2.14. Laboratory Indicators.* After admission, patients underwent serum ESR detection in our hospital, and changes in erythrocyte sedimentation rate (mm/h) were compared.

*2.15. Criteria for Determining Clinical Efficacy.* After the clinical rash, symptoms of lumbosacral and back pain disappeared or basically disappeared, and the range of motion



Figure 1: Schematic diagram of supervisor moxibustion method.

of spinal joints was basically normal. The activity of the chest seat increased by > 2.5 cm, the pillow-to-wall distance decreased by > 10 cm, and the finger-to-ground distance decreased by >10 cm. ESR reduction > 10 mm/h. The symptoms of lumbosacral and back pain were relieved, and the range of motion of spinal joints was improved. Thoracic range of motion > 1 cm and < 2.5 cm, pillow-to-wall distance decreased by > 5 cm and < 10 cm, and finger-to-ground distance decreased by >5 cm and <10 cm. ESR > 5 mm/ho improved, lumbosacral and back pain symptoms were relieved, spinal joint mobility improved, chest gallery mobility slightly improved, the occipital-wall distance decreased by > 10 cm, and finger-ground distance by > 10 cm. The ESR results were slightly improved. There was no change in ineffective symptoms compared with those before treatment. Effective rate = cure + marked effect + improvement.

*2.16. Criteria for Judging Efficacy of Syndromes.* The clinical symptoms related to TCM basically disappeared, and the quantitative score of symptoms decreased by >90%. The symptoms related to TCM with marked effect were improved, and the symptom quantitative score decreased by >70%. Effective TCM-related symptoms were improved, and the symptom quantitative score decreased by > 30%.

*2.17. Quality Control*

(1) Design the experiment rigorously and reasonably, and comprehensively collect theoretical data supporting the experiment

(2) A clinician who did not participate in the treatment operation of this experiment measured and recorded various clinical indicators, and evaluated TCM symptoms strictly according to self-made scoring standards

(3) Provide professional training to experimental operators, formulate clear operating specifications and experimental procedures, and conduct experiments in accordance with standardized operations during treatment;

(4) The final data are statistically analyzed with professional software

(5) The experimental operation is always carried out by one person to prevent experimental results from being affected by deviation of acupoint selection method or irregular operation

*2.18. Statistical Methods.* SPSS 21.0 statistical software was used for statistical analysis and processing of the data. The mean ± standard deviation ($\overline{x} \pm s$) was used for measurement data. $\alpha = 0.05$, $P < 0.05$ is considered a statistically significant difference.

## 3. Results

Among 63 AS patients, there were 45 males and 18 females; random serial numbers were obtained from a random number table, and cases were randomly divided into two groups by the remainder method. There were 30 cases and 31 cases in control. The age, gender, and duration of disease were compared. See Table 1.

A nonparametric test was used for curative effect, indicating that the total effective rate of experimental was better. See Table 2.

The $t$ test was used to analyze quantitative scores of the main symptoms of patients. The curative effect of the experiment was better; a comparison of each was performed by $t$-test, and results showed that scores after treatment were lower than those before treatment. See Table 3.

By comparing changes in a thoracic range of motion, occipital-wall distance, and finger-to-ground distance of patients, results were statistically analyzed, and $t$-test was used to compare. The curative effect of the experiment was better; see Tables 4–6.

The $t$-test was used to analyze ESR changes. The results showed that there was a difference in ESR after treatment ($F = 9.611$, $P < 0.05$), and the curative effect of the experiment was better. See Table 7.

## 4. Discussion

The results of this study showed that the moxibustion intervention in the moxibustion box of the Governor's Vessel was effective in improving the TCM symptoms and signs of patients with ankylosing spondylitis. The basic pathogenesis of ankylosing spondylitis is that the patient has congenital deficiencies and deficiencies in the Governor's Vessel and kidney channels. In modern Chinese medicine, clinical trials suggest that the kidneys and the Governor's Vessel are the basis of ankylosing spondylitis, with the Governor's Vessel running through the entire spine and connecting to the kidneys, and the Governor's Vessel unifying the Yang of the body. If the disease is not treated for a long period of time, it will become a condition where "the jib takes the place of the heel and the spine takes the place of the head" (Su Wen-Theory of Paralysis). "Kidney deficiency and stagnation of the Governor's Vessel are the main causes of this condition. A deficiency of kidney yang leads to insufficient fire in the vital gate, depletion of the source of the Governor's Vessel, and weakness in warming power. Moxibustion interventions in the moxibustion box of the Governor's Vessel can tonify the kidneys and open up the channels and meridians, stimulating and strengthening the warmth of Yang, which in turn promotes the flow of Qi and blood, ultimately achieving the purpose of unblocking the Qi flow, harmonizing Qi and blood, and restoring physiological functions [10, 11]. By warming the yang of the body, the warming effect of kidney qi is used to nourish the kidney essence, which in turn enriches the bone marrow, thereby improving the local and general symptoms of ankylosing spondylitis, and its clinical effects have been confirmed.

The results of this study showed that after treatment, the thoracic mobility and Schober's test scores were higher in the observation group than in the control group, and the finger-ground and occipital-wall distances were lower than in the control group ($P < 0.05$). Sacroiliitis is a hallmark of ankylosing spondylitis, which can be characterized by bone and articular cartilage defects in the early stages and spinal deformities and ankylosis in the later stages, with severe limitations in functional activity. The moxibustion box is a warm moxibustion apparatus, when moxibustion is ignited in the box, it allows the moxa to burn fully to produce smoke and heat, which can burn or warm the patient's body surface, thus playing a role in regulating the function of the meridians and organs and playing a curative role. A study [12] used supervised moxibustion combined with oral salazapyridine tablets to treat ankylosing spondylitis and showed that compared with acupuncture combined with oral salazapyridine tablets, supervised moxibustion combined with oral salazapyridine tablets treatment could significantly improve the symptoms and signs of patients with ankylosing spondylitis with deficiency of kidney yang. Some studies have shown that ginger-garlic supervision and moxibustion can significantly improve the signs and bone metabolic indexes of patients with ankylosing spondylitis with a deficiency of kidney yang [13, 14]. The results of this study showed that the signs improved in both groups after treatment, but the observation group was better than the control group. It may be that the warm stimulation of the moxibustion box moxibustion therapy of the Governor's vein can better stimulate the body's ability to resist disease.

Moxibustion can remove blood stasis and activate blood, improve blood rheology, correct free radical metabolism disorders, and can inhibit the release of inflammatory cytokines, and enhance the body's immune function [15, 16]. The results of this study suggest that the levels of IL-1, IL-17, CRP, and ESR in the observation group were lower than

TABLE 1: Comparison of general conditions of patients.

| Grouping | Number of cases | Age ($\overline{x} \pm s$, years) | Gender | | The course of disease ($\overline{X} \pm S$, year) |
| --- | --- | --- | --- | --- | --- |
| | | | Male | Female | |
| Treatment | 30 | 39.93 ± 10.52 | 20 | 10 | 4.77 ± 3.06 |
| Control | 31 | 40.06 ± 10.64 | 23 | 8 | 6.16 ± 2.88 |

TABLE 2: Comparison of curative effects of patients (cases).

| Group | $n$ | Recovery | Remarkable effect | Valid | Invalid | Efficiency (%) |
| --- | --- | --- | --- | --- | --- | --- |
| Treatment | 30 | 2 | 3 | 21 | 4 | 86.7 |
| Control | 31 | 1 | 1 | 24 | 5 | 83.9 |

TABLE 3: Comparison of quantitative scores of main symptoms of patients ($\overline{x} \pm s$).

| Group | $n$ | Before treatment | After treatment |
| --- | --- | --- | --- |
| Treatment | 30 | 26.95 ± 3.90 | 11.2 ± 4.21 |
| Control | 31 | 25.05 ± 3.37 | 13.62 ± 3.68 |
| $F$-value | | 1.085 | 2.593 |
| $P$-value | | 0.304 | 0.02 |

TABLE 4: Comparison of thoracic range of motion ($\overline{x} \pm s$).

| Group | $N$ | Before treatment | After treatment |
| --- | --- | --- | --- |
| Treatment | 30 | 2.48 ± 0.86 | 4.18 ± 1.51 |
| Control | 31 | 1.95 ± 0.79 | 2.5 ± 0.96 |
| $F$-value | | 1.162 | 5.821 |
| $P$-value | | 0.285 | 0.019 |

TABLE 5: Comparison of occipital-wall distance ($\overline{x} \pm s$).

| Group | $N$ | Before treatment | After treatment |
| --- | --- | --- | --- |
| Treatment | 30 | 6.886.27 | 3.09 ± 4.67 |
| Control | 31 | 5.27 ± 4.13 | 4.02 ± 3.94 |
| $F$ value | | 1.483 | 1.982 |
| $P$ value | | 0.226 | 0.049 |

TABLE 6: Comparison of the finger-ground distance ($\overline{x} \pm s$).

| Group | $N$ | Before treatment | After treatment |
| --- | --- | --- | --- |
| Treatment | 30 | 23.44 ± 10.86 | 15.95 ± 8.44 |
| Control | 31 | 24.92 ± 14.02 | 19.18 ± 12.35 |
| $F$ value | | 1.482 | 5.765 |
| $P$ value | | 0.227 | 0.022 |

TABLE 7: Comparison of ESR ($\overline{x} \pm s$).

| Group | $n$ | Before treatment | After treatment |
| --- | --- | --- | --- |
| Treatment | 30 | 14.05 ± 10.53 | 8.79 ± 7.68 |
| Control | 31 | 20.86 ± 20.32 | 12.86 ± 16.05 |
| $F$ value | | 0.754 | 9.613 |
| $P$ value | | 0.454 | 0.005 |

those in the control group after treatment ($P < 0.05$). IL-1, IL-17, CRP, and ESR are common indicators of the inflammatory response. IL-17 can further induce pro-inflammatory cytokine expression, causing and exacerbating inflammatory cell infiltration and tissue damage [17, 18]. Studies have shown that moxibustion can effectively reduce inflammatory indicators such as CRP and ESR, which is consistent with the results of this study [19, 20]. The moxibustion box can regulate the body's immune response and endocrine, effectively controlling the inflammatory response and improving the therapeutic effect of ankylosing spondylitis [21].

The combination of moxibustion and moxibustion box moxibustion can stimulate and strengthen the Yang energy to warm the body and then promote the flow of Qi and blood, ultimately achieving the purpose of clearing the Qi flow, harmonizing Qi and blood, and restoring physiological functions, thus effectively improving the therapeutic effect, relieving the inflammatory response and improving clinical symptoms. There are still shortcomings in this study, such as the small sample size, the short duration of the study design, and the single type of evidence. There is a need to further expand the sample size and conduct in-depth studies on different types of patients.

## Data Availability

The experimental data used to support the findings of this study are available from the corresponding author upon request.

## Conflicts of Interest

The authors declared that they have no conflicts of interest regarding this work.

## Acknowledgments

## References

[1] Y. C. Xuan, J. Liu, Y. Y. Huang et al., "Therapeutic effect of long-snake moxibustion combined with western medication on diarrhea type irritable bowel syndrome of spleen and kidney yang deficiency," *Zhongguo Zhen Jiu = Chinese Acupuncture & Moxibustion*, vol. 41, no. 2, pp. 133–136, 2021.